

Review of timing measurements with Silicon Photo-multipliers

G.Collazuol, Scuola Normale Superiore and INFN - Pisa
on behalf of the DASIPM collaboration

Overview

- Introduction
- Review of intrinsic SiPM timing
- Qualitative comparison with RPL model
- Examples of electronics for timing and of timing applications
- Conclusions
- Appendix: SiPM properties at different temperatures

Operation principle of a GM-APD

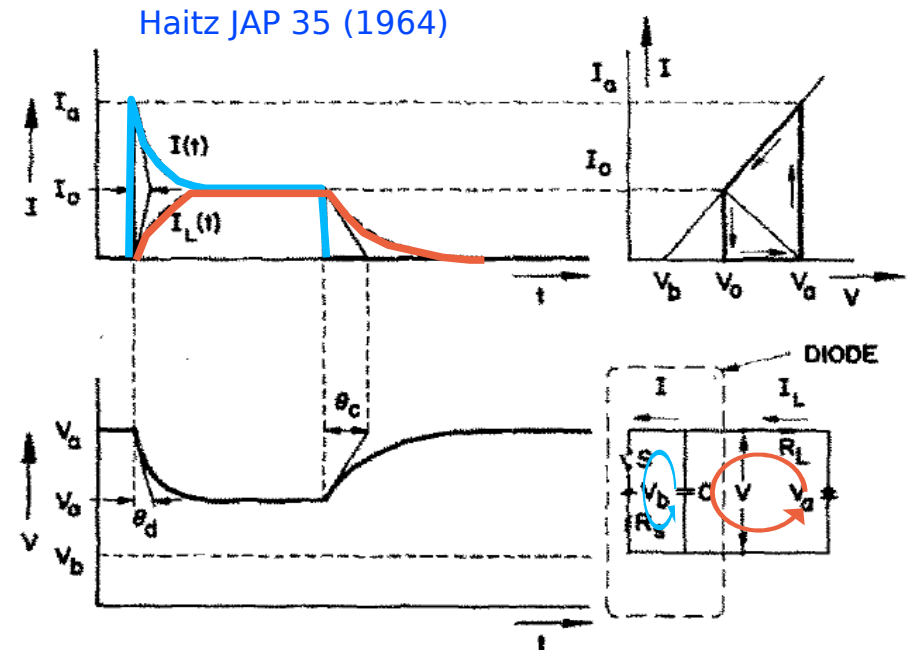
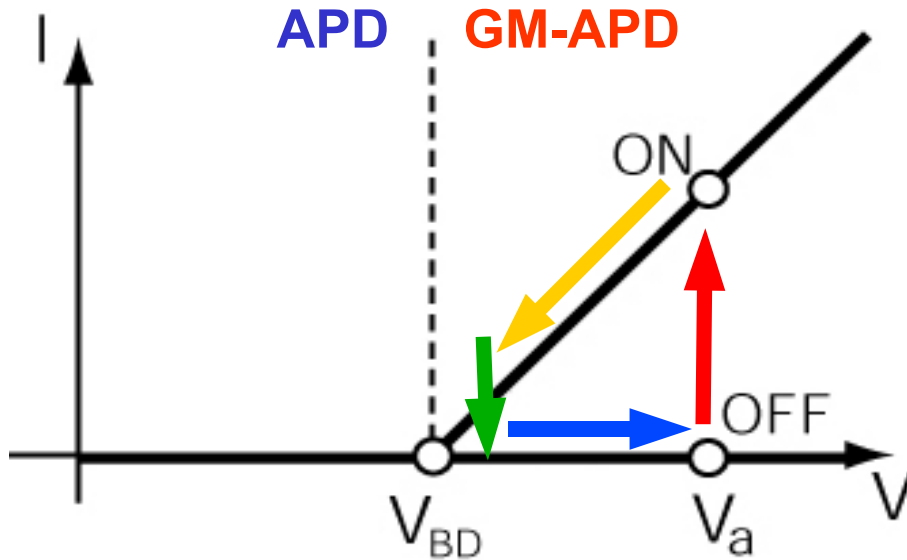


FIG. 3. Shape of current pulse for $\theta_d \ll \tau_1(I_0)$.

OFF condition: avalanche quenched, switch open, capacitance charged until no current flowing from V_{BD} to V_{BIAS} with time constant $R_q \times C_D = \tau_{Quenching}$ (\rightarrow recovery time)

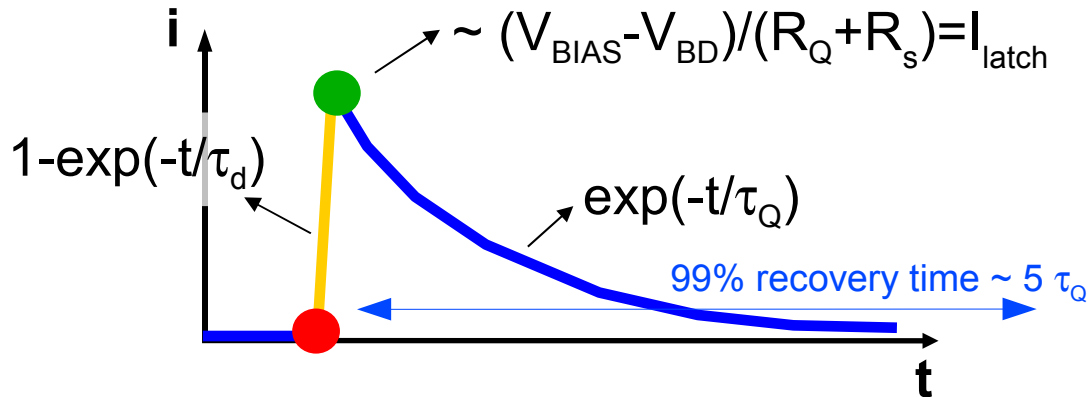
P_{01} = turn-on probability
probability that a carrier traversing the high-field region triggers the avalanche

P_{10} = turn-off probability
probability that the number of carriers traversing the high-field region fluctuates to 0

ON condition: avalanche triggered, switch closed
 C_D discharges to V_{BD} with a time constant $R_S \times C_D = \tau_{discharge}$,
at the same time the external current asymptotic grows to $(V_{BIAS} - V_{BD}) / (R_Q + R_S)$

Operation principle of a GM-APD

If R_Q is high enough the internal current is so low that statistical fluctuations may quench the avalanche



The leading edge of the signal is much faster than trailing edge:

1. $\tau_d = R_s \cdot C_D \ll R_Q \cdot C_D = \tau_Q$
2. turn-off mean time is very short
(if R_Q is sufficiently high, $I_{\text{latch}} \sim 10 \mu\text{A}$)

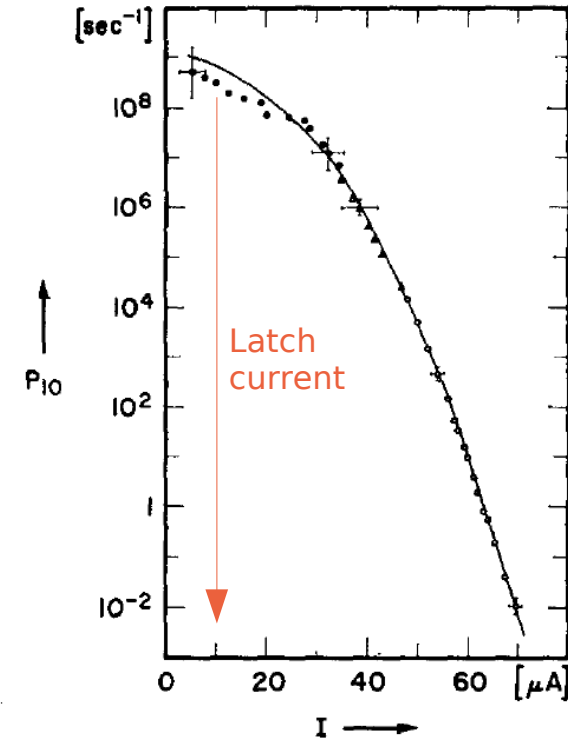


FIG. 2. Turnoff probability per second as function of pulse current.

Haitz JAP 35 (1964)

The charge collected per event is the **area under the exponential** which is determined by circuital elements and bias.

➡ It is possible to define a GAIN (discharge of a capacitor !!!)

$$G = \frac{I_{\text{max}} \cdot \tau_Q}{q_e} = \frac{(V_{\text{bias}} - V_{\text{BD}}) \cdot \tau_Q}{(R_Q + R_s) \cdot q_e} = \frac{(V_{\text{bias}} - V_{\text{BD}}) \cdot C_D}{q_e}$$

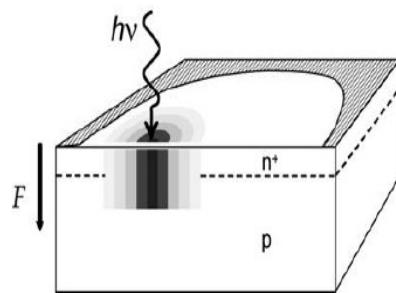
➡ Gain fluctuations in GM-APD are smaller than in APD because electrons and holes give the same signal !!!

GM-APD timing: fast and slow components

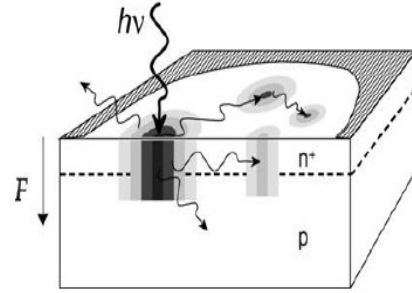
1) Fast component: gaussian with time scale $O(10\text{ps})$

Statistical fluctuations in the avalanche:

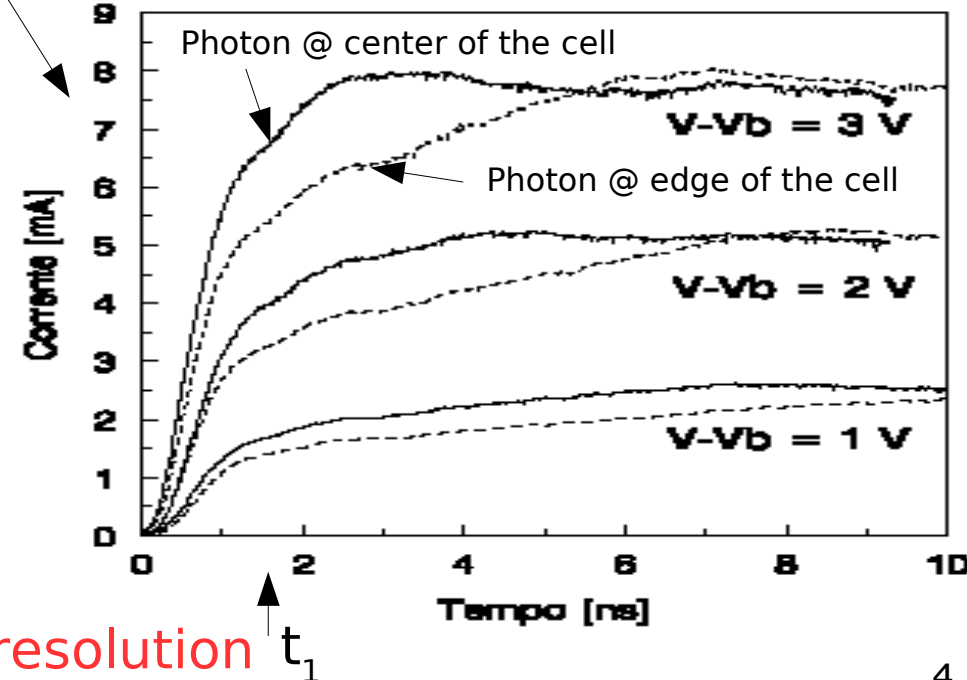
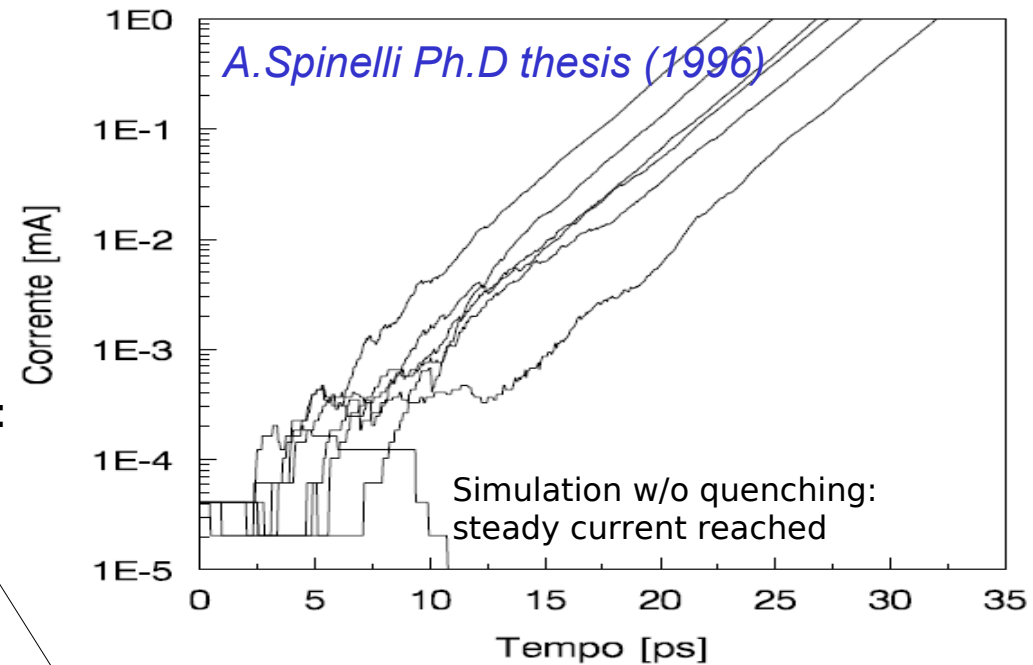
- Longitudinal build-up (minor contribution)
- Transversal propagation (main contribution):
 - via Multiplication assisted diffusion (dominating)
A.Lacaita et al. APL and El.Lett. 1990
 - via Photon assisted propagation
PP.Webb, R.J. McIntyre RCA Eng. 1982
A.Lacaita et al. APL 1992



Multiplication assisted diffusion



Photon assisted propagation



Dependence of avalanche build-up rate on the impact position (\rightarrow cell size)

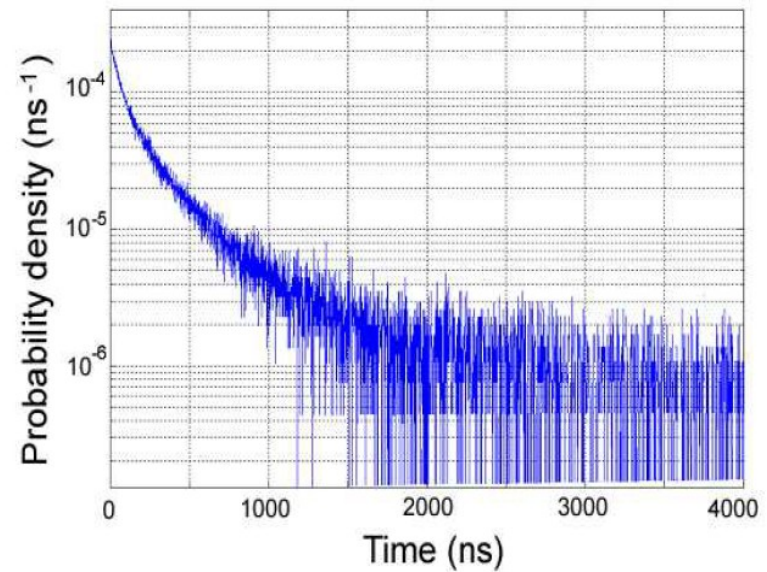
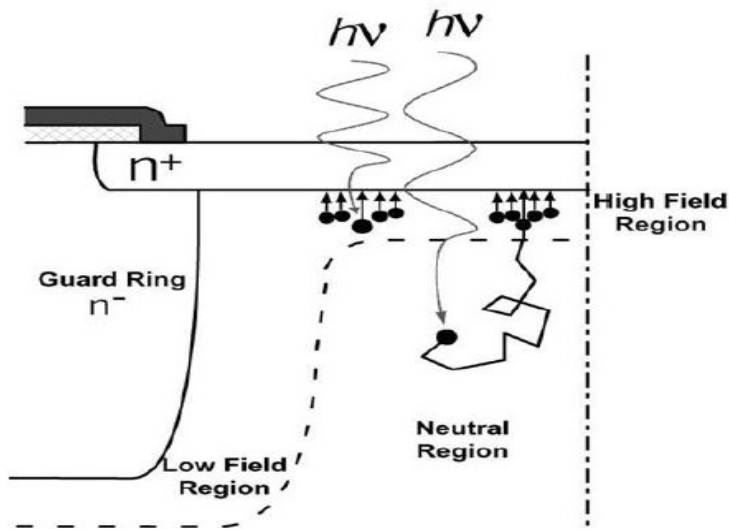
Higher overvoltage \rightarrow improved time resolution t_1

GM-APD timing: fast and slow components

2) Slow component: minor non gaussian tails with time scale $O(ns)$

Carriers photogenerated in the neutral regions beneath the junction and reaching the electric field region by diffusion

G.Ripamonti, S.Cova Sol.State Electronics (1985)



tail lifetime: $\tau \sim L^2 / \pi^2 D$

L = effective neutral layer thickness

D = diffusion coefficient

S.Cova et al. NIST Workshop on SPD (2003)

Shorter wavelengths → higher resolution (less tails)

Single photon time resolution: measurement

Experimental Method

- SiPM exposed to **pulsed femto-second laser** in low light intensity conditions (single photon)
- SiPM signal is sampled at high rate and the time of the pulses measured by **waveform analysis**
- Time resolution measured by studying the distribution of **time differences between successive pulses** (from the same SiPM)
- Samples: FBK-IRST, Hamamatsu (HPK), CPTA/Photonique

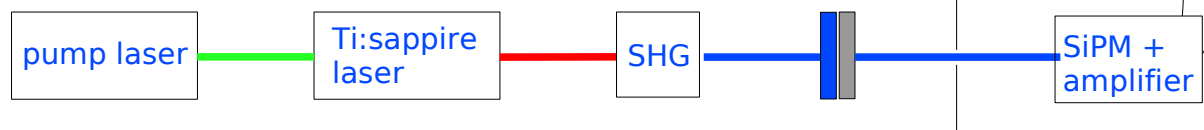
Experimental Setup

Pump Laser

Millenia V (Spectra-physics)
solid state CW visible laser

Crystal for Second Harmonic Generation (SHG)

conversion $800\text{ nm} \rightarrow 400\text{ nm}$
efficiency at % level



Low noise LV suppliers

Dark box

LeCroy SDA 6020

Analog bandwidth: 6GHz
Sampling rate: 20GS/s
Vertical resolution: 8 bits

(Acknowledgments:
E.Marcon, LeCroy)

Mode-locked Ti:sapphire Laser

Tsunami (Spectra-physics)
femtosecond pulsed laser

Filters

blue + neutral
for rejecting IR light
and tune intensity

External trigger from
Ti:sapphire laser
signal

wavelength: tuned at $800 \pm 15\text{ nm}$
pulse width: $\sim 60\text{ fs}$ FWHM
pulse period: $\sim 12\text{ ns}$
pulse timing jitter $< 100\text{ fs}$

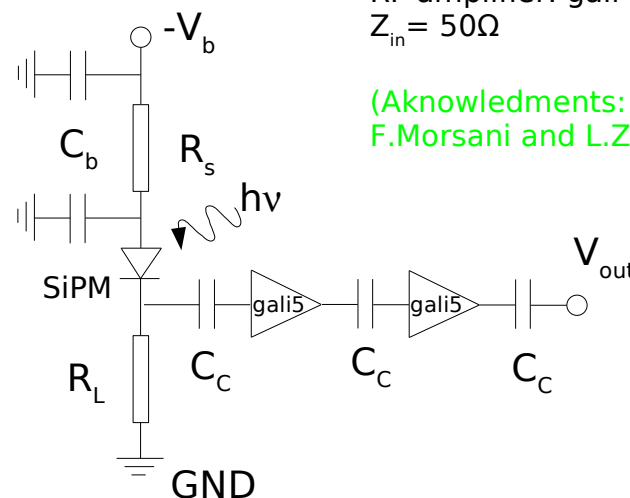
Electronics

$I \rightarrow V$ conversion via R_L (500Ω)
Two stage voltage amplification ($= \times 50$)
based on high-bandwidth low-noise
RF amplifier: gali-5 (MiniCircuit)
 $Z_{in} = 50\Omega$

(Acknowledgments:
F.Morsani and L.Zaccarelli, INFN-Pisa)

Data taking conditions:

- different V_{bias}
- both at 800 nm and 400 nm
- with different light intensities
(counting rates
in the range $10 \div 20\text{ MHz}$
ie $15 \div 30\text{ KHz}$ per single cell)



Waveform analysis: method

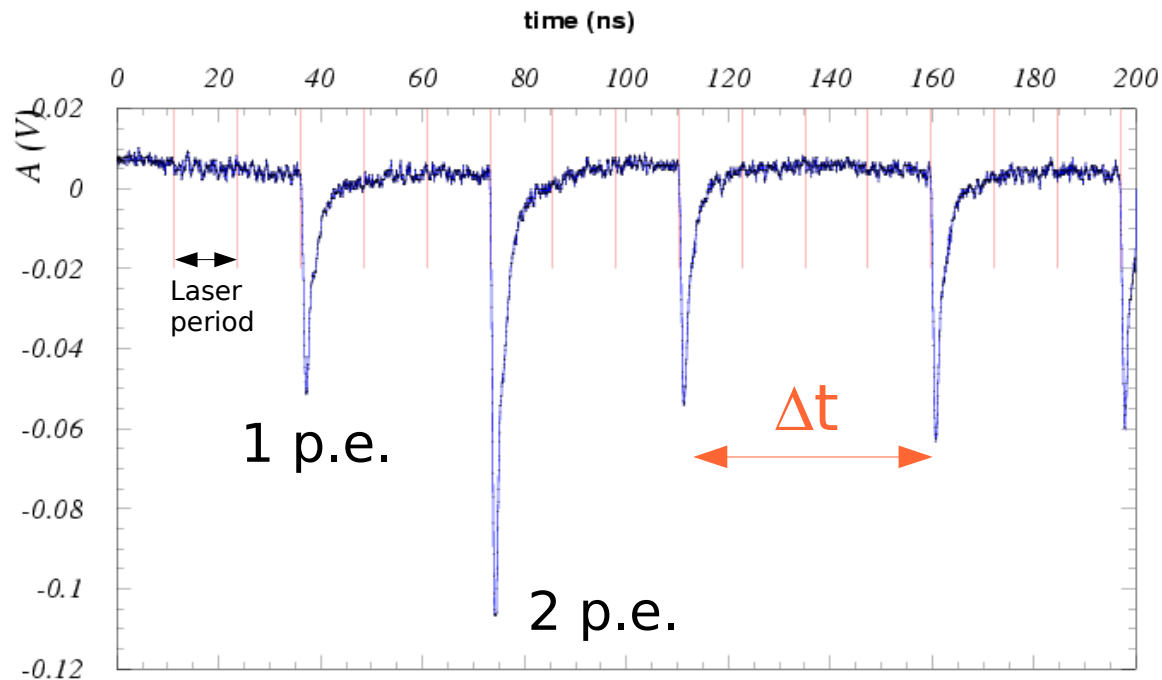
(1) Selection of candidate peaks:

- single photon peaks
- proper signal shape
- **low instantaneous intensity**
(no activity before/after within 50ns)
- **low noise** during the previous 10 ns
(typical noise $\sim 1\text{mV rms}$)

(2) Peak reconstruction

- **optimum time reconstruction**
- amplitude and width (baseline shift correction)

(3) Time difference Δt between consecutive peaks

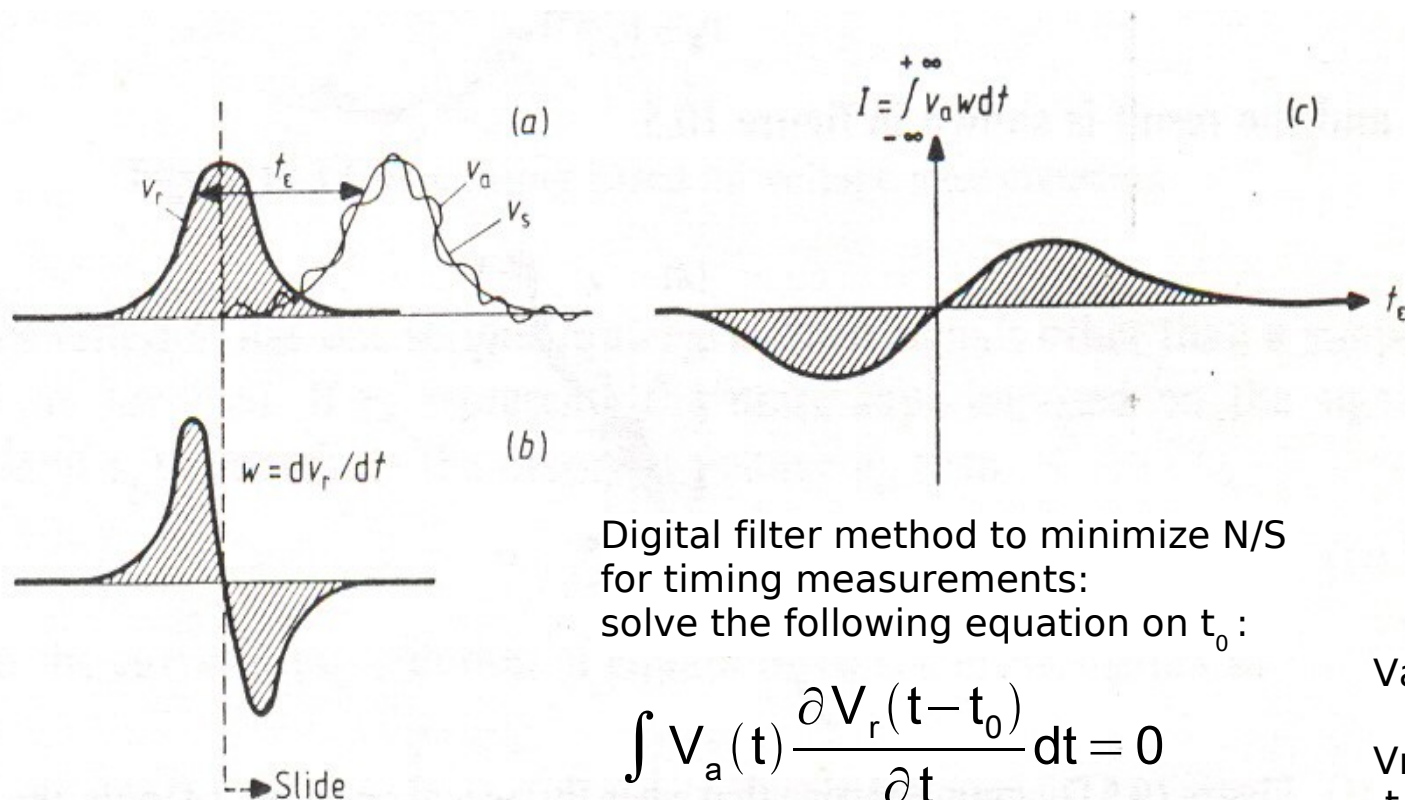


NOTE: working fine at 20MHz counting rate

Waveform analysis: time reconstruction

Different methods to reconstruct the time of a peak:

- ✗ parabolic fit to find the peak maximum
- ✗ average of time samples weighted by the waveform derivative
- ✓ digital filter: weighting by the derivative of a reference signal
→ best against noise (signal shape known)



Digital filter method to minimize N/S
for timing measurements:
solve the following equation on t_0 :

$$\int V_a(t) \frac{\partial V_r(t-t_0)}{\partial t} dt = 0$$

V_a = measured signal
(includes noise)
 V_r = reference signal
 t_0 = reference time

Single Photon Timing Resolution (SPTR)

Analysis of the distributions of the t difference between successive peaks
(modulo the laser period $T_{\text{laser}} = 12.367\text{ns}$)

Data at $\lambda = 400\text{nm}$
fit gives reasonable χ^2
with gaussian (σ_t^{fit}) +
constant term (dark noise contribution)

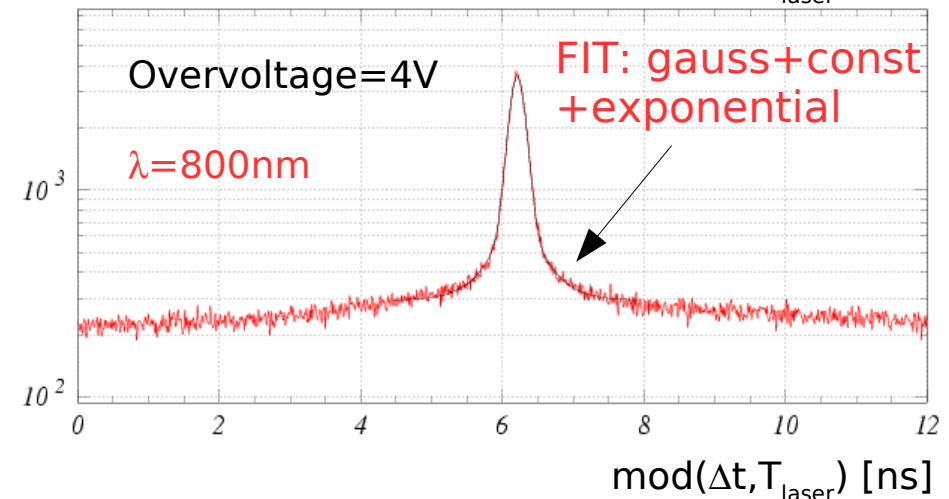
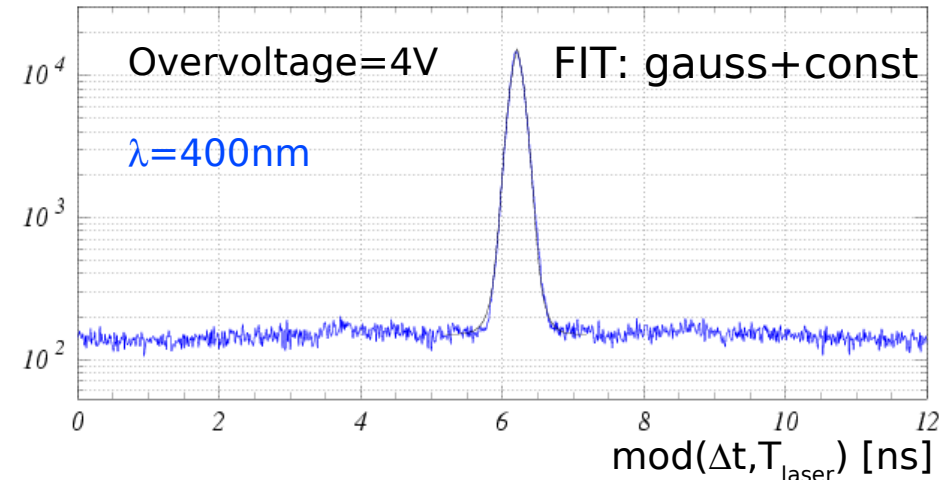
The detector resolution is obtained by
 $\sigma_t^{\text{fit}}/\sqrt{2}$

Data at $\lambda = 800\text{nm}$
fit gives reasonable χ^2 with an
additional **exponential term** $\exp(-\Delta t/\tau)$

- $\tau \sim 0.2 \div 0.8\text{ns}$ in rough agreement with diffusion tail lifetime: $\tau \sim L^2 / \pi^2 D$ if L is taken to be the diffusion length
- Contribution from the tails $\sim 10 \div 30\%$ of the resolution function area

Gaussian
rms $\sim 50\text{-}100\text{ ps}$

+ Tails (long λ)
 $\sim \exp(-t / O(\text{ns}))$
contrib. several %
for long wavelengths



Distributions of the difference in time between successive peaks (modulo the measured laser period $T_{\text{laser}} = 12.367\text{ns}$)

Systematics

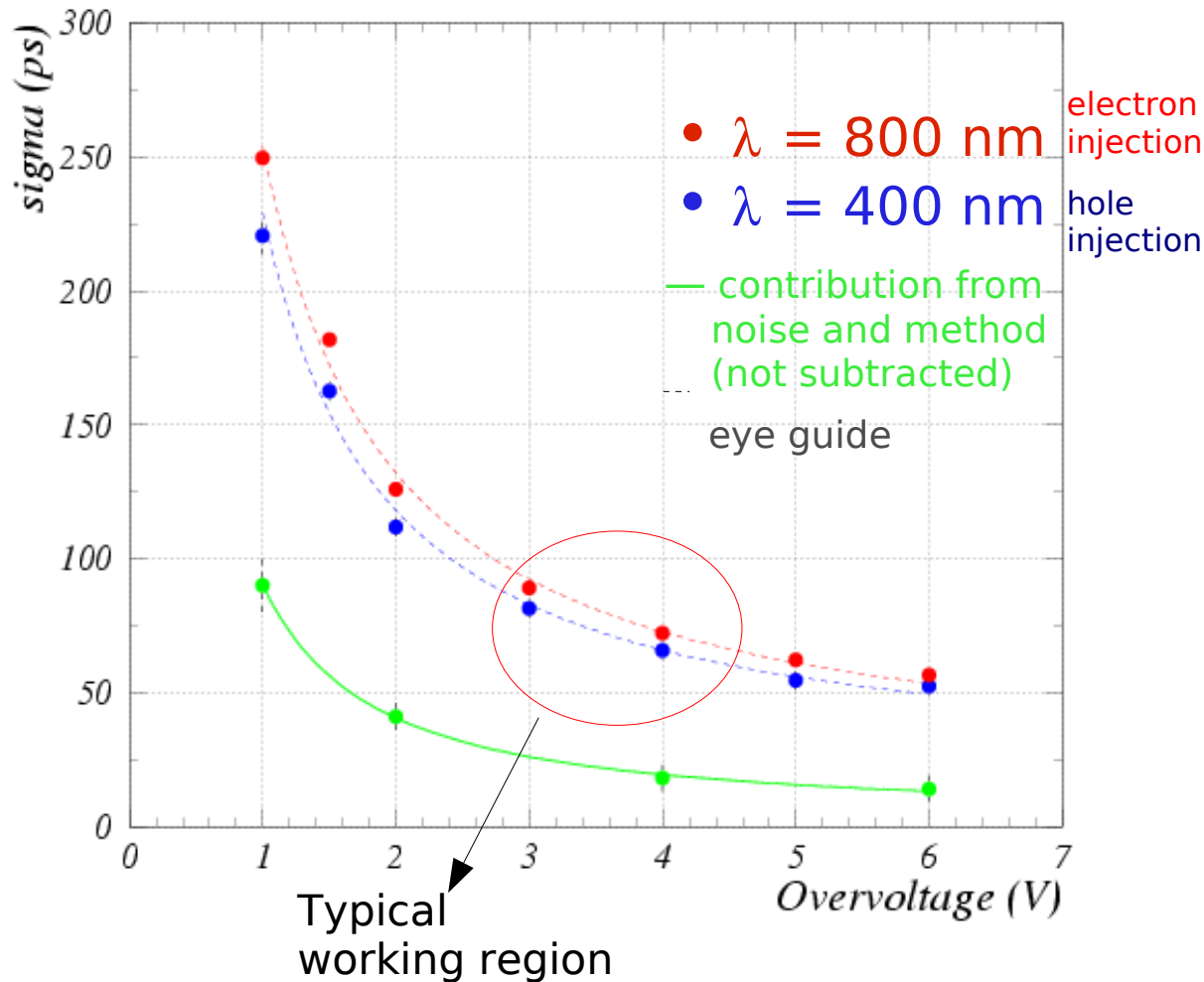
- Contribution (main) from the electronic noise:

- (1) directly measured by splitting in two the signal of the SiPM, delaying one and recombine the two signals again. Measure the (fixed) time difference.
- (2) cross-check by doubling the noise and measuring the effect on the resolution

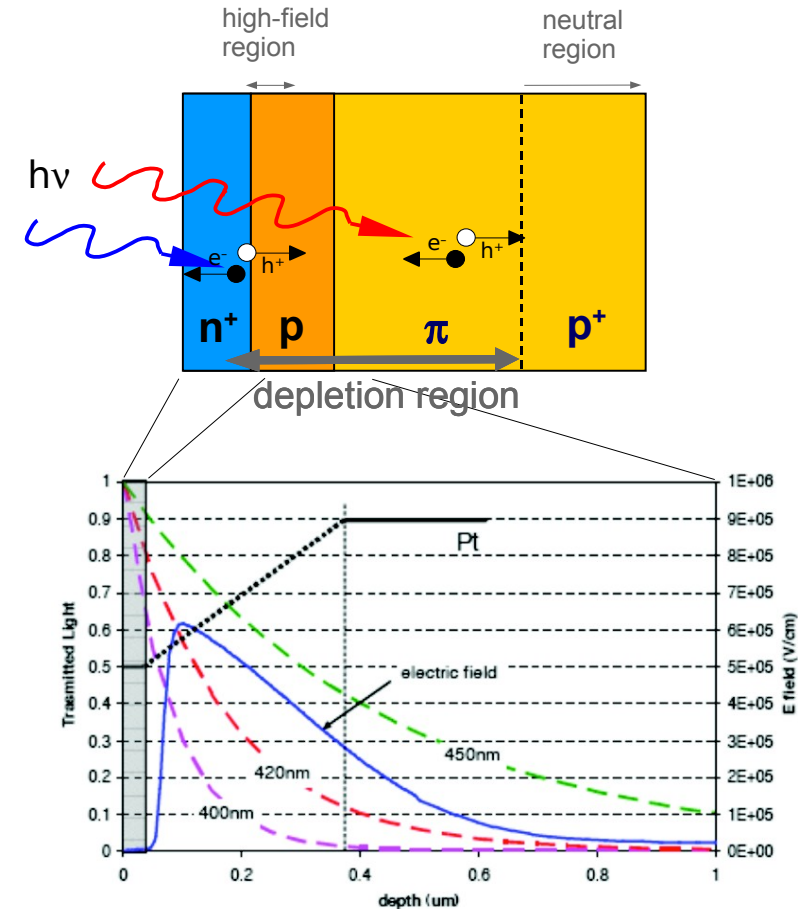
This contribution includes also the systematics related to the method of time reconstruction by waveform analysis

- Contribution from sampling hardware (clock jitter, ...) $< 5\text{ps}$
- Sensitivity to the shape of the reference waveform $< 5\text{ps}$
- Systematics from fit procedure $< 5\text{ps}$
- Systematics from intensity dependence $\sim 5\text{ps}$

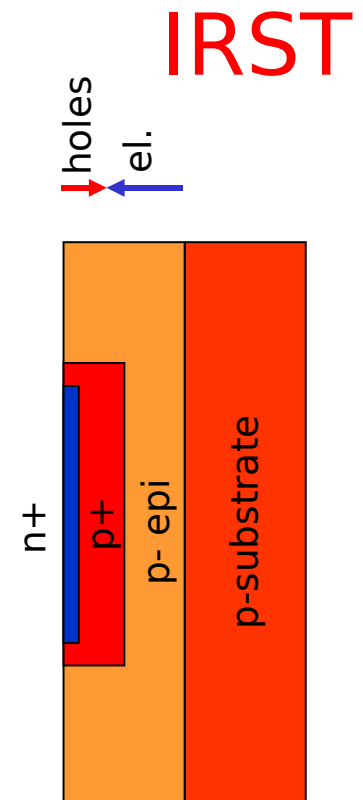
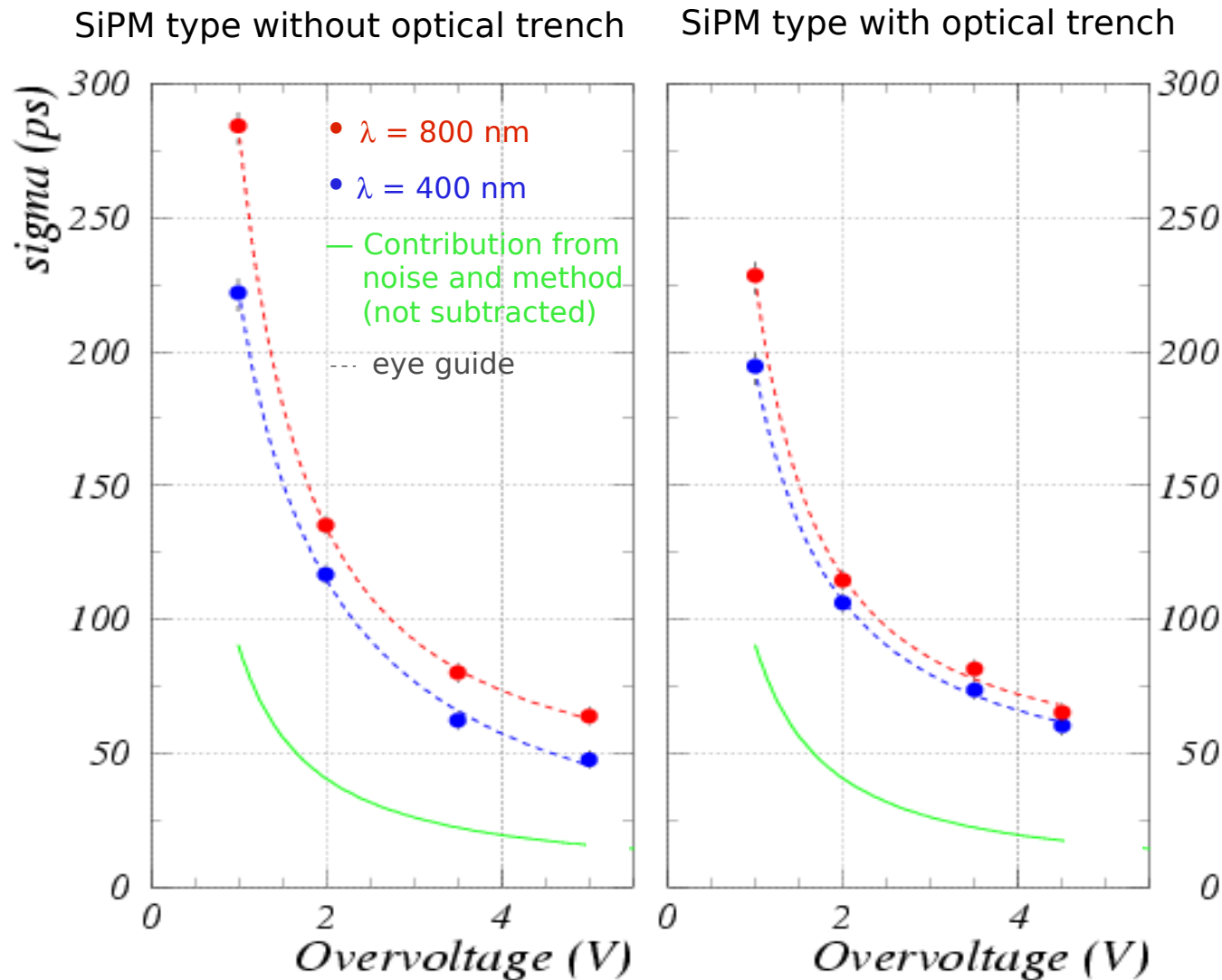
IRST - single photon timing res. (SPTR)



Better resolution for short wavelengths: carriers generated next to the peak of high E field ...

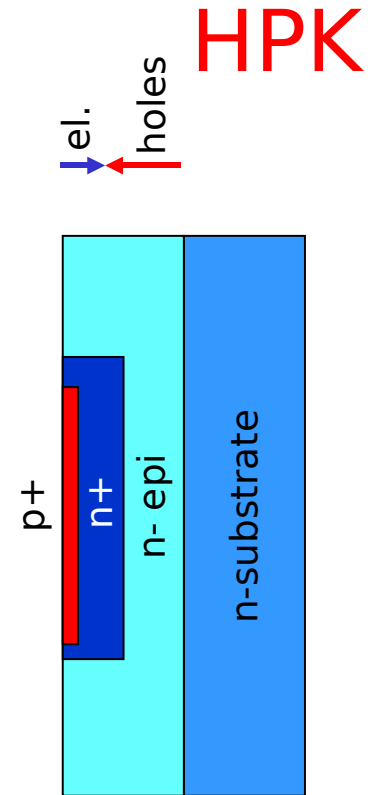
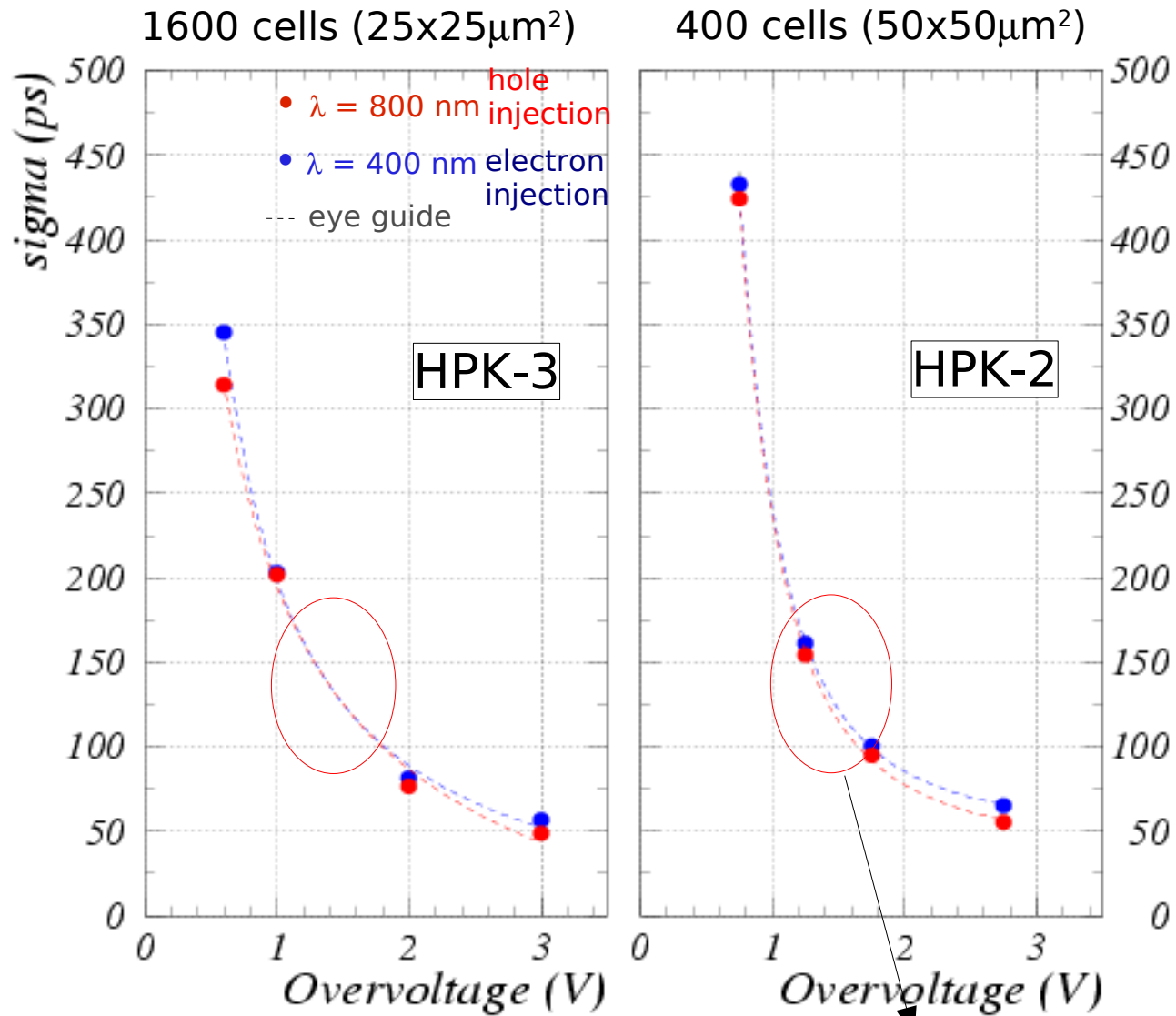


IRST devices (different types)



Results in fair agreement for devices with the same structure

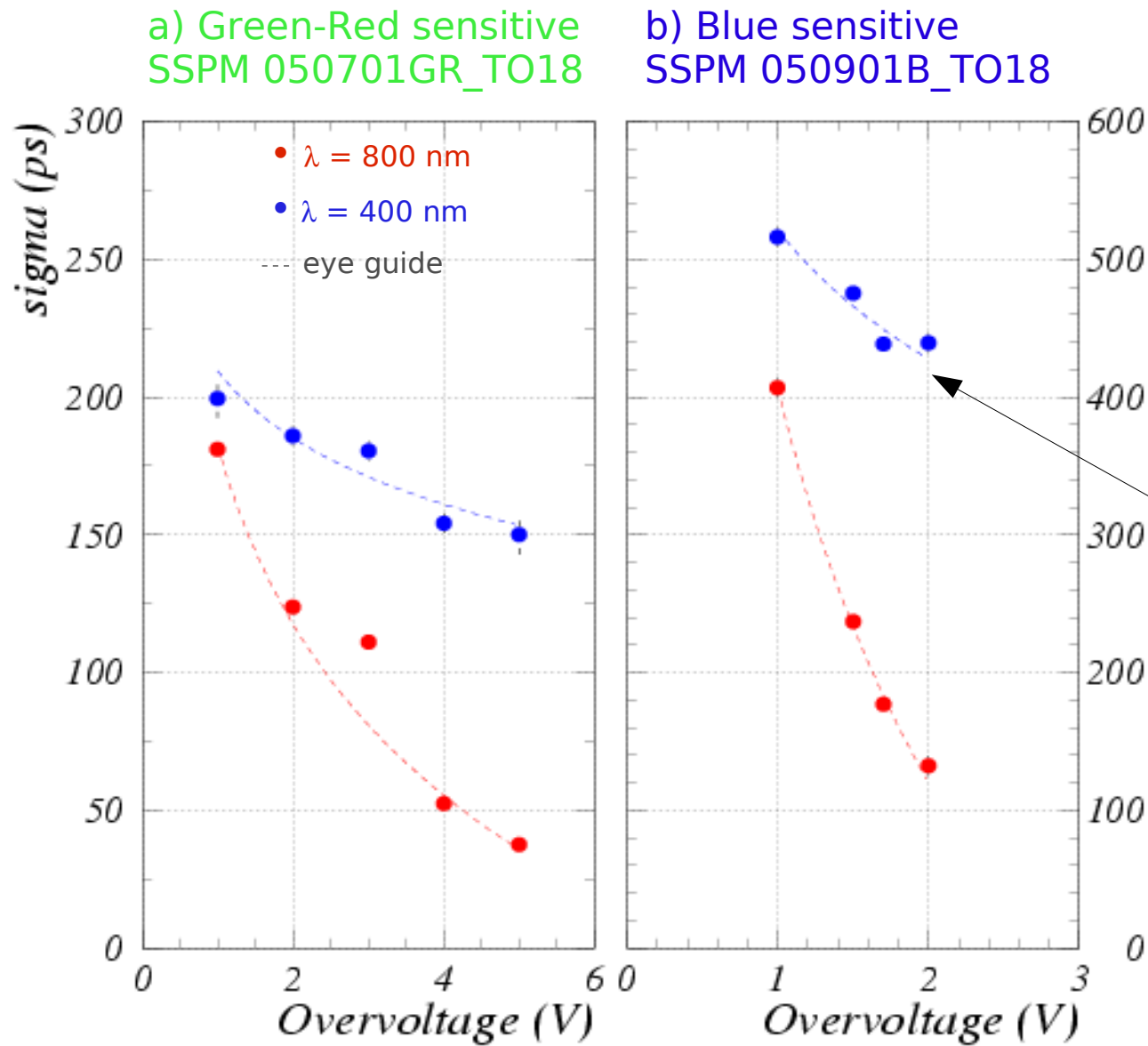
Hamamatsu - single photon timing res.



G.Collazuol et al (unpublished)

Suggested
Operating range

CPTA/Photonique – single photon timing res.



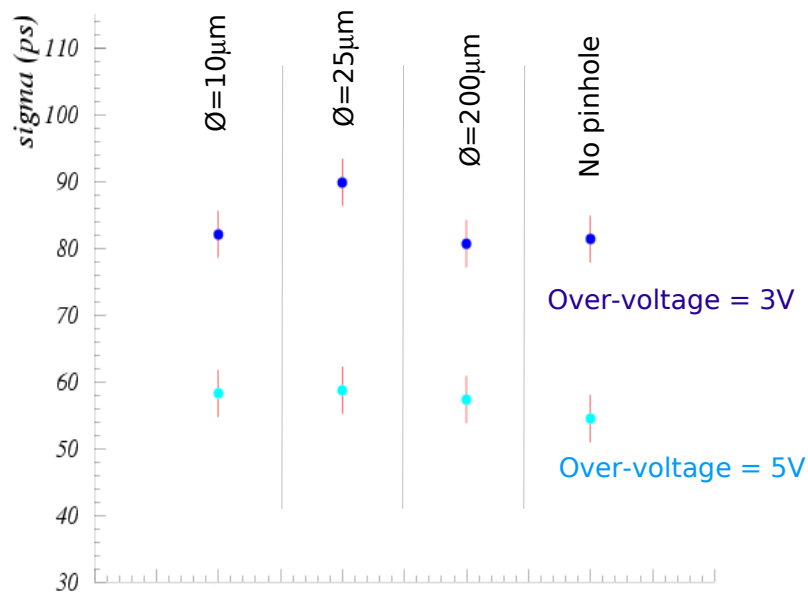
Two different structures:
a) thick n+/p
b) p+/n deep junction

Carrier trapping ?

G.Collazuol et al (unpublished)

Timing studies (IRST devices)

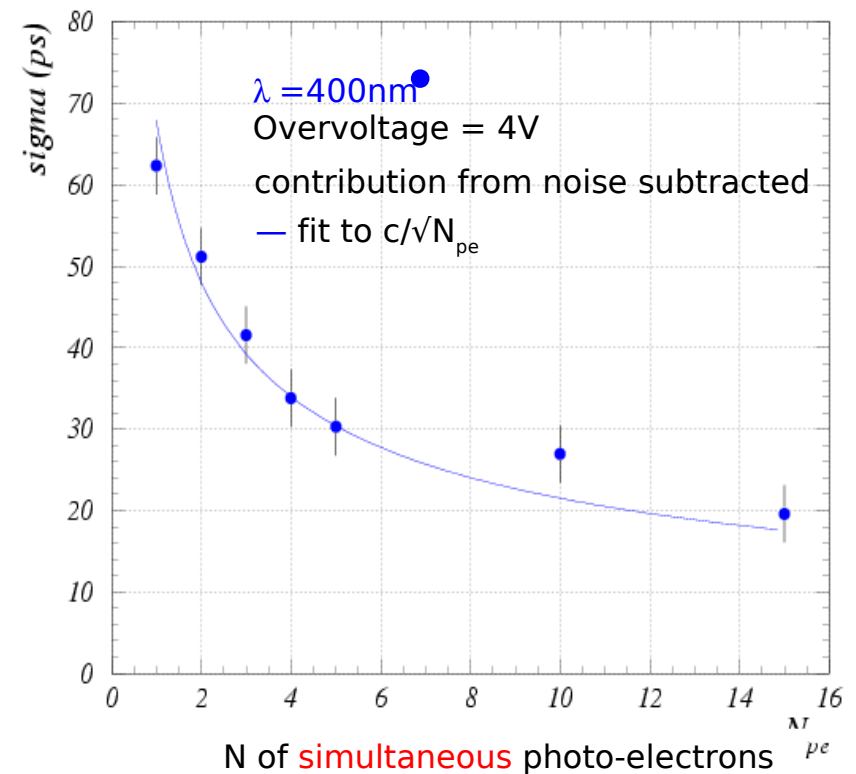
Dependence of SiPM timing on the
light spot size and position
(By using pinhole in front of the SiPM)



No relevant spread
→ Uniformity of rise-time
among different cells

Dependence of SiPM timing on the
number of simultaneous photons

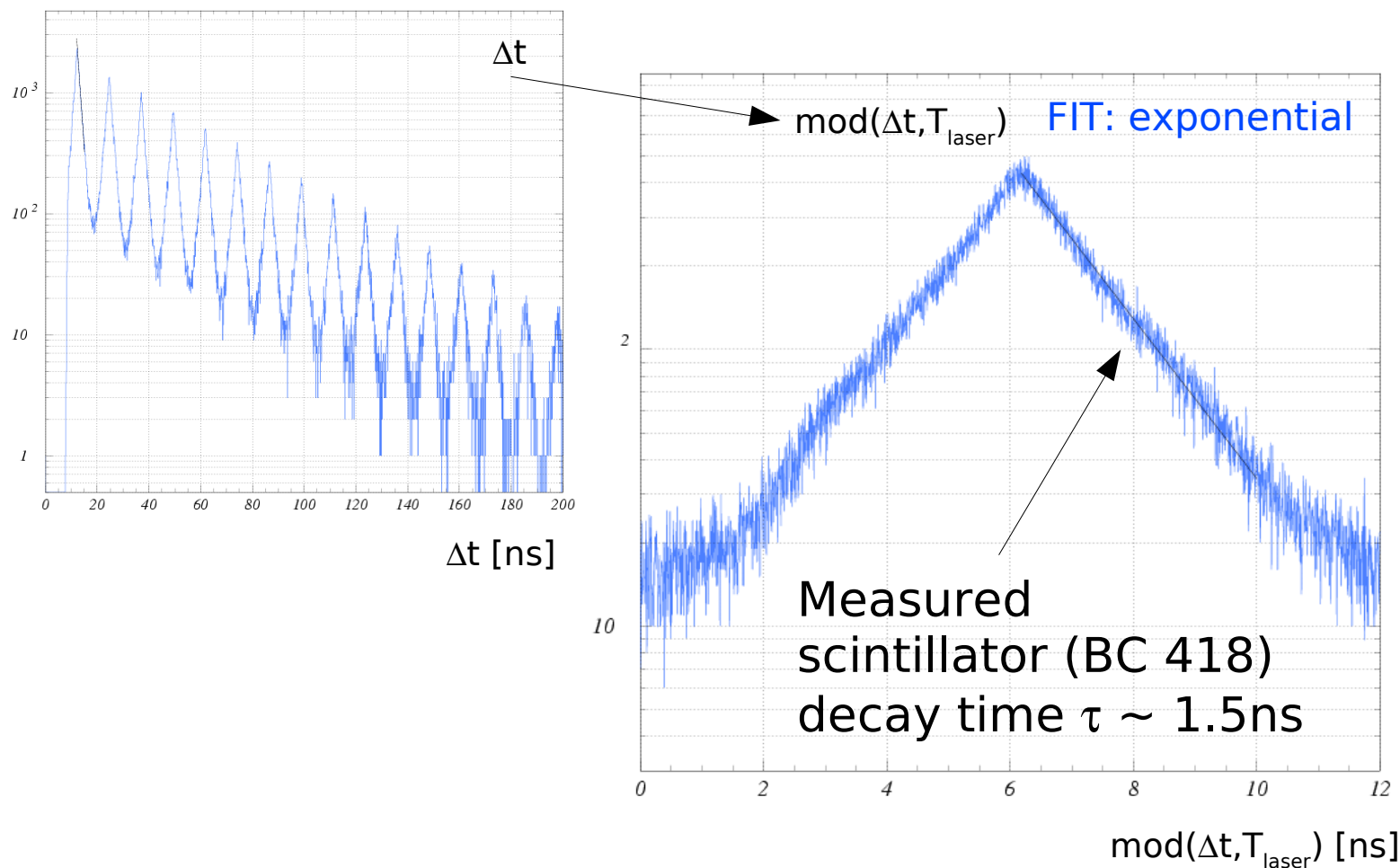
Poisson statistics: $\sigma_t \propto 1/\sqrt{N_{pe}}$



Scintillator decay time

Cross check: SiPM coupled to a fast plastic scintillator $2 \times 2 \times 15\text{mm}^3$
Only the scintillator excited by the laser **blue light** $\lambda=400\text{nm}$.
No direct laser light to the SiPM

→ measurement of the **scintillator decay tail**





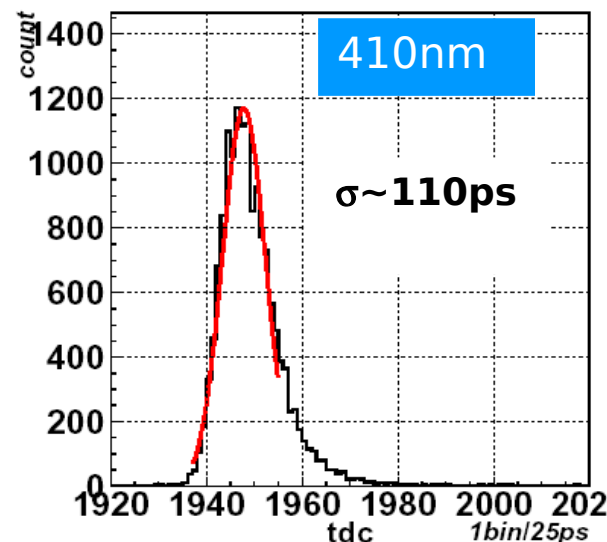
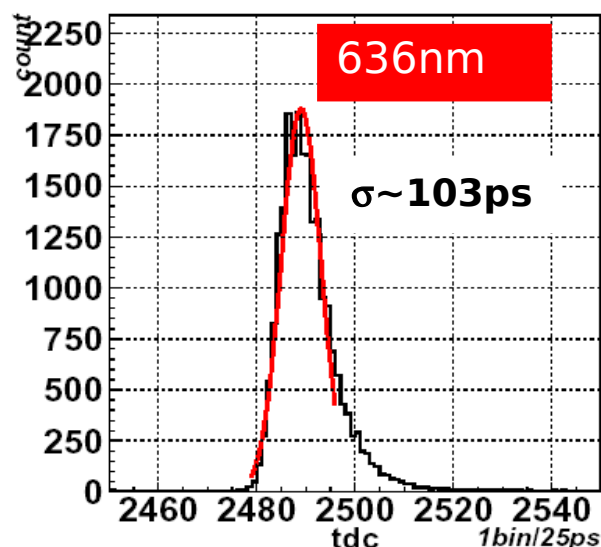
Other studies of intrinsic Single Photon Timing Resolution (SPTR)

SPTR: HPK/CPTA comparison

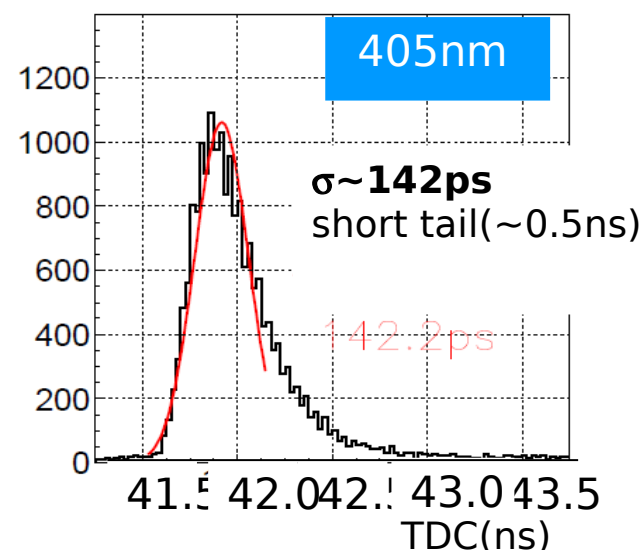
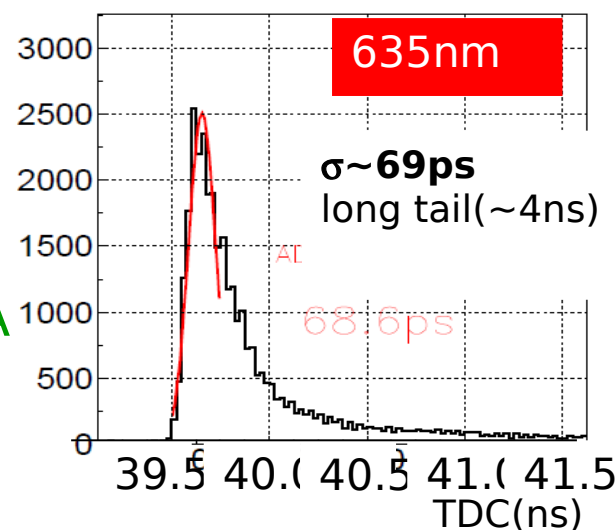
T.Iijima - PD07

Nagoya and Lubiana groups

SiPM - HPK
(MPPC)



SiPM - CPTA
(MRS-APD)

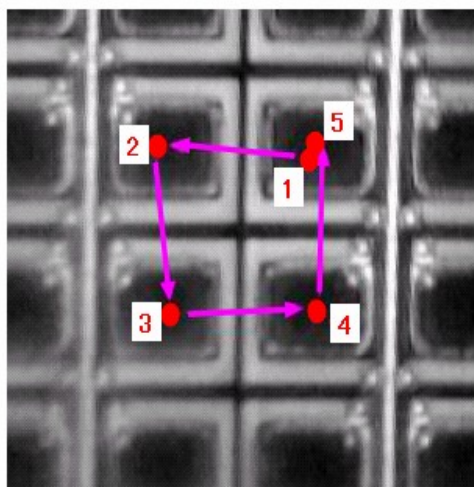


Method: CFD + TDC + Time walk corrections

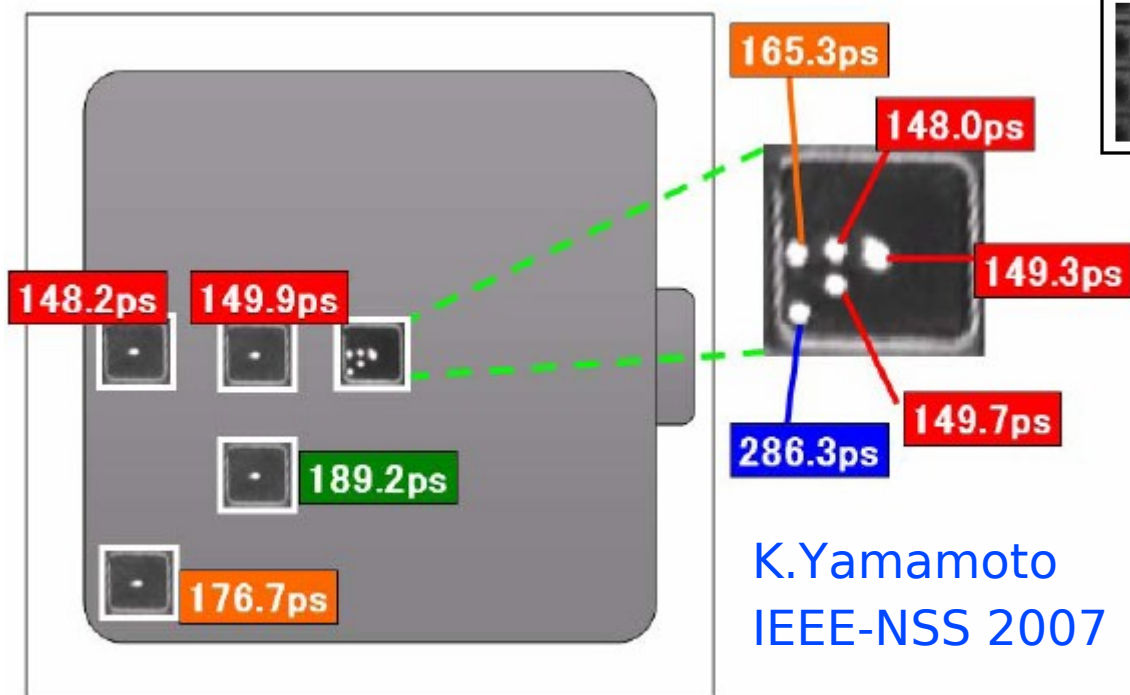
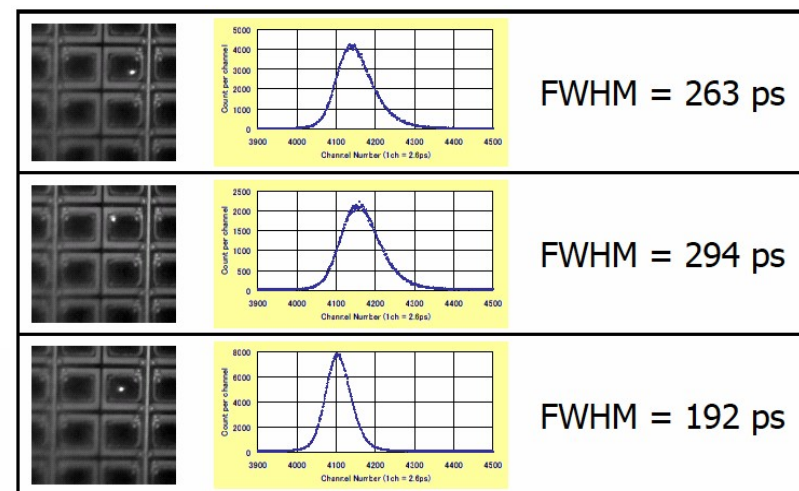
Compatible with DASIPM measurements

SPTR: position dependence

Yamamoto et al
(Hamamatsu)



	FWHM (ps)	FWTM (ps)
1	199	393
2	197	389
3	209	409
4	201	393
5	195	383



K.Yamamoto
IEEE-NSS 2007

K.Yamamoto PD07

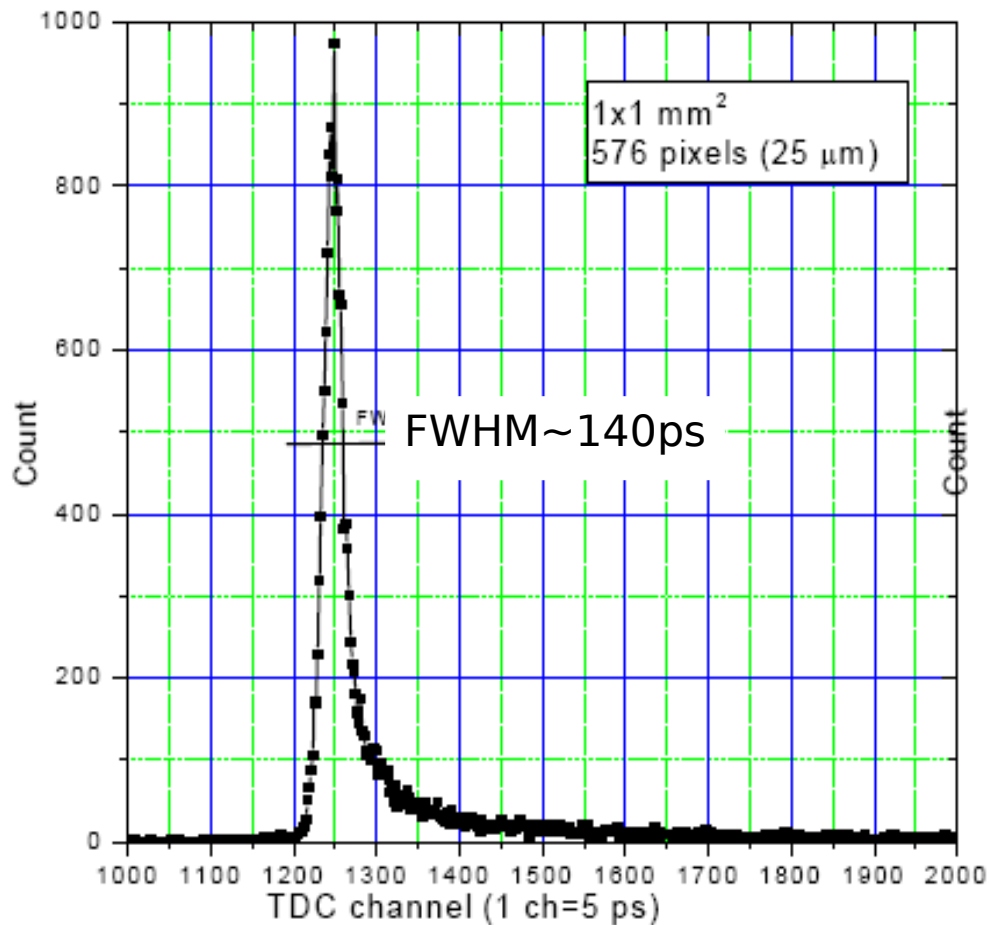
Lower jitter if photoproduction
at the center of the cell

Data include the system jitter (common offset, not subtracted)

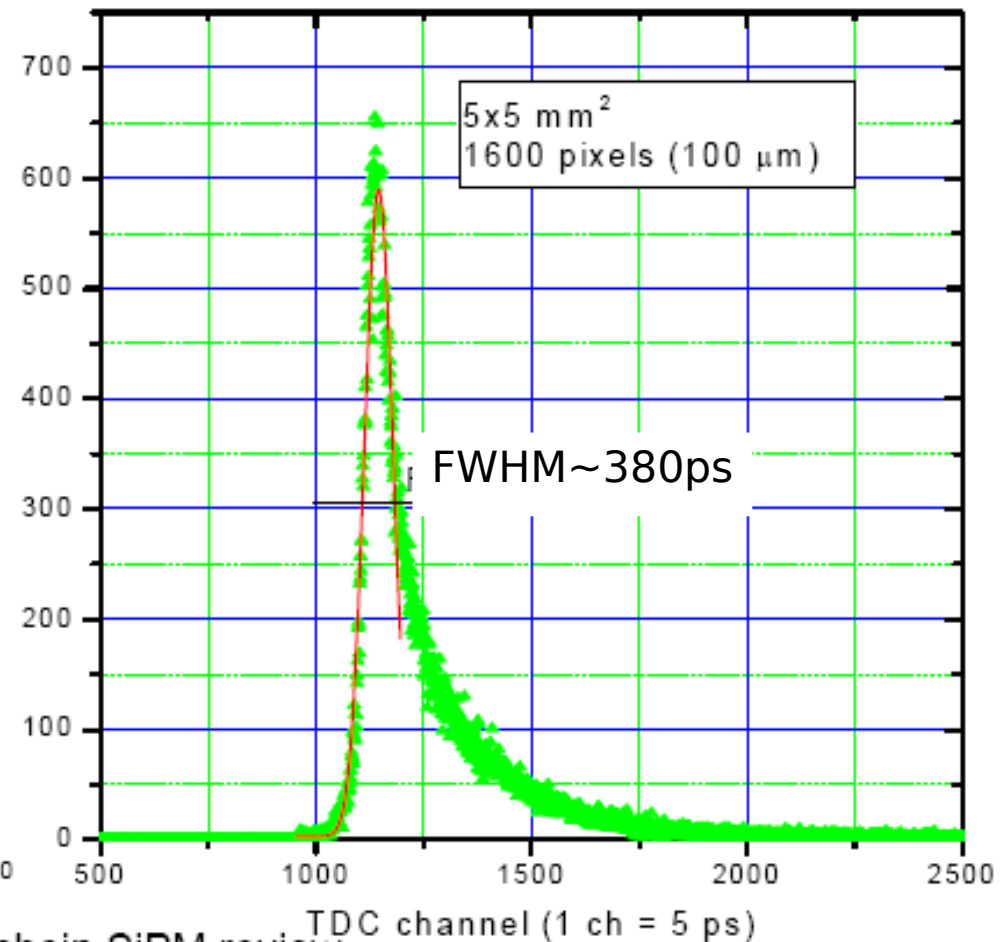
SPTR: cell and sipm size dependence

B.Dolgoshein - LIGHT07

SiPM - MePhI/Pulsar:
576 cells ($25 \times 25 \mu\text{m}^2$)
Area = $1 \times 1 \text{ mm}^2$



SiPM - MePhI/Pulsar:
1600 cells ($100 \times 100 \mu\text{m}^2$)
Area = $5 \times 5 \text{ mm}^2$



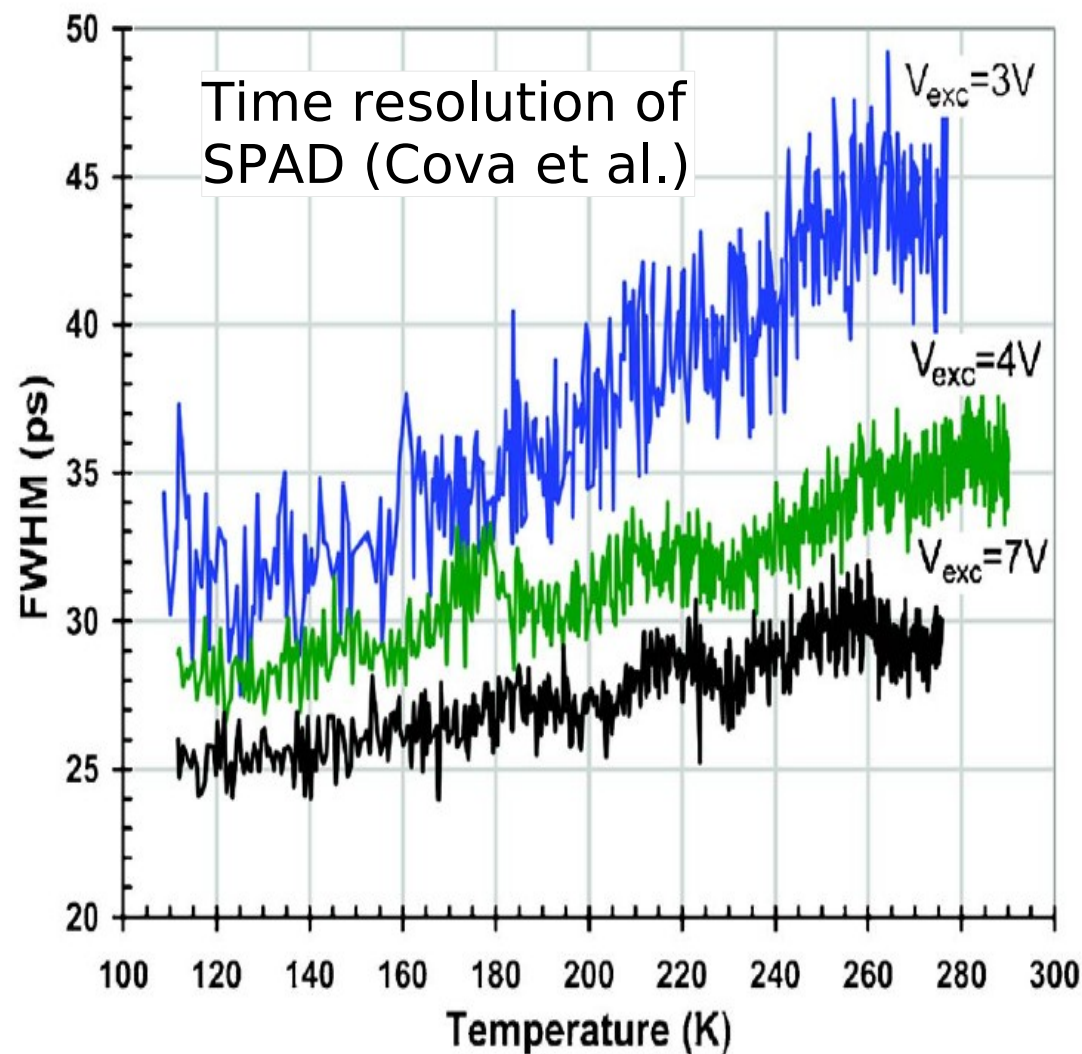
B.Dolgoshein, SiPM review

SPTR: T dependence for SPAD devices


Timing: better at low T

Lower jitter at low T due to higher mobility

(Over-voltage fixed)



I.Rech et al, Rev.Sci.Instr. 78 (2007)



Qualitative understanding of the
timing and PDE characteristics...

...in view of a quantitative comparison
with different models

RPL model: fast simulation

“Statistics of Avalanche Current Buildup Time in Single-Photon Avalanche diodes”

C.H.Tan, J.S.Ng, G.J.Rees, J.P.R.David (Sheffield U.)

IEEE J.Quantum Electronics 13 (4) (2007) 906

Numerical model (MC): **Random distribution of impact ionization Path Length (RPL)**

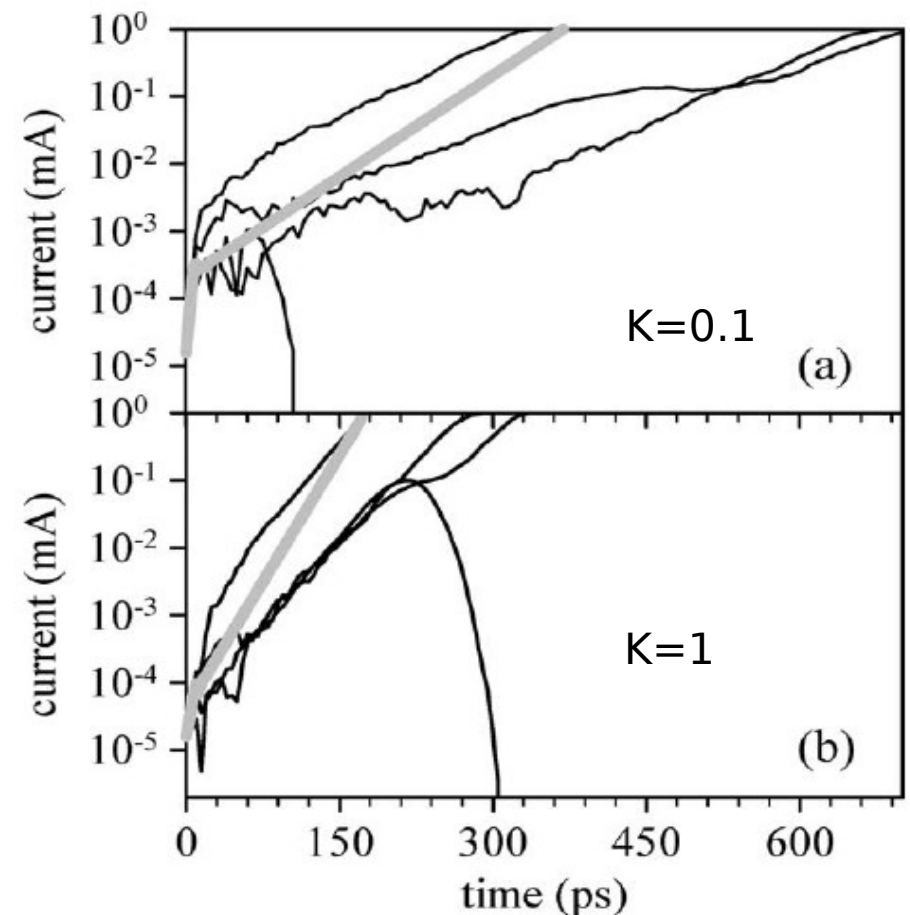
Analysis of **breakdown probability**, **breakdown time** and **timing jitter** as functions of avalanche region width (w), ionization coefficient ratio ($k = \beta_{\text{hole}} / \alpha_{\text{electron}}$) and dead space parameter (d) (uniform E field, constant carrier velocity)

1) **increasing k :**

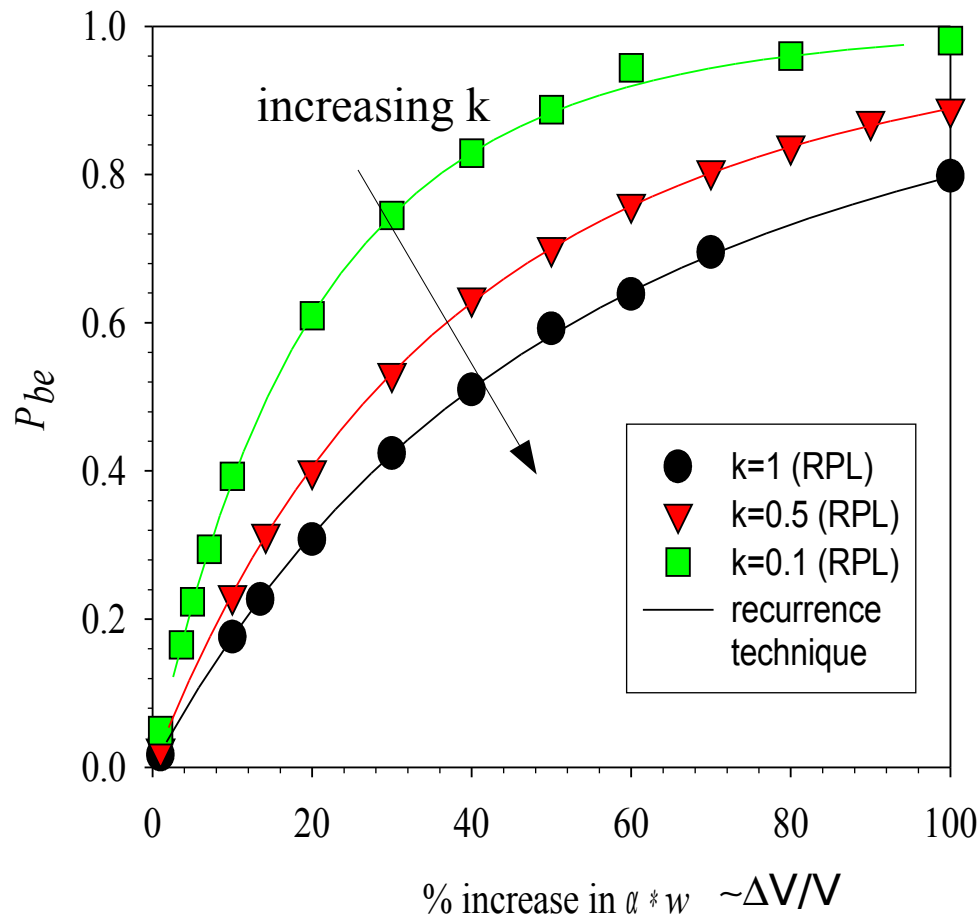
- **improves timing** performances
- but breakdown probability P_{br} **increases slowly** with overvoltage

1a) hole injection results in better timing than electron injection (in Si devices)

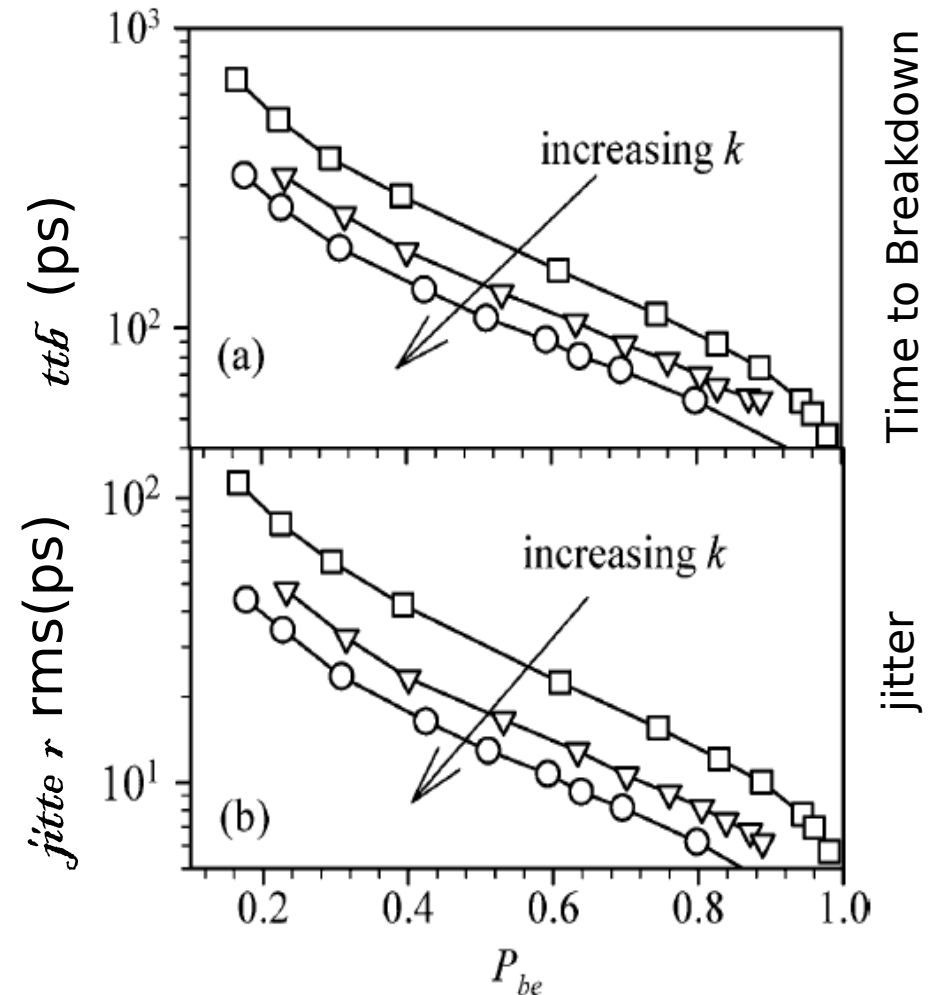
2) **dead space effects** worsen timing performances (the more at small k)
Important for devices with **small w**



Increasing k
 → slower slope P_{br} vs ΔV



Increasing k
 → optimized timing



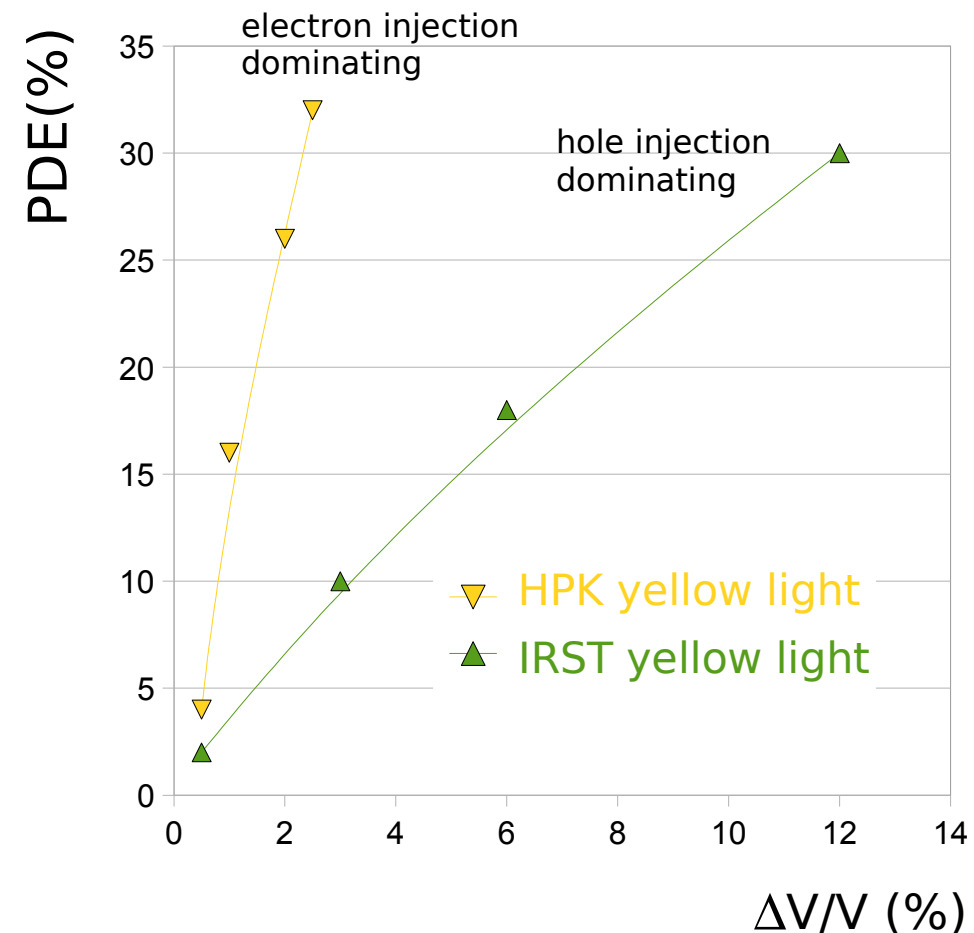
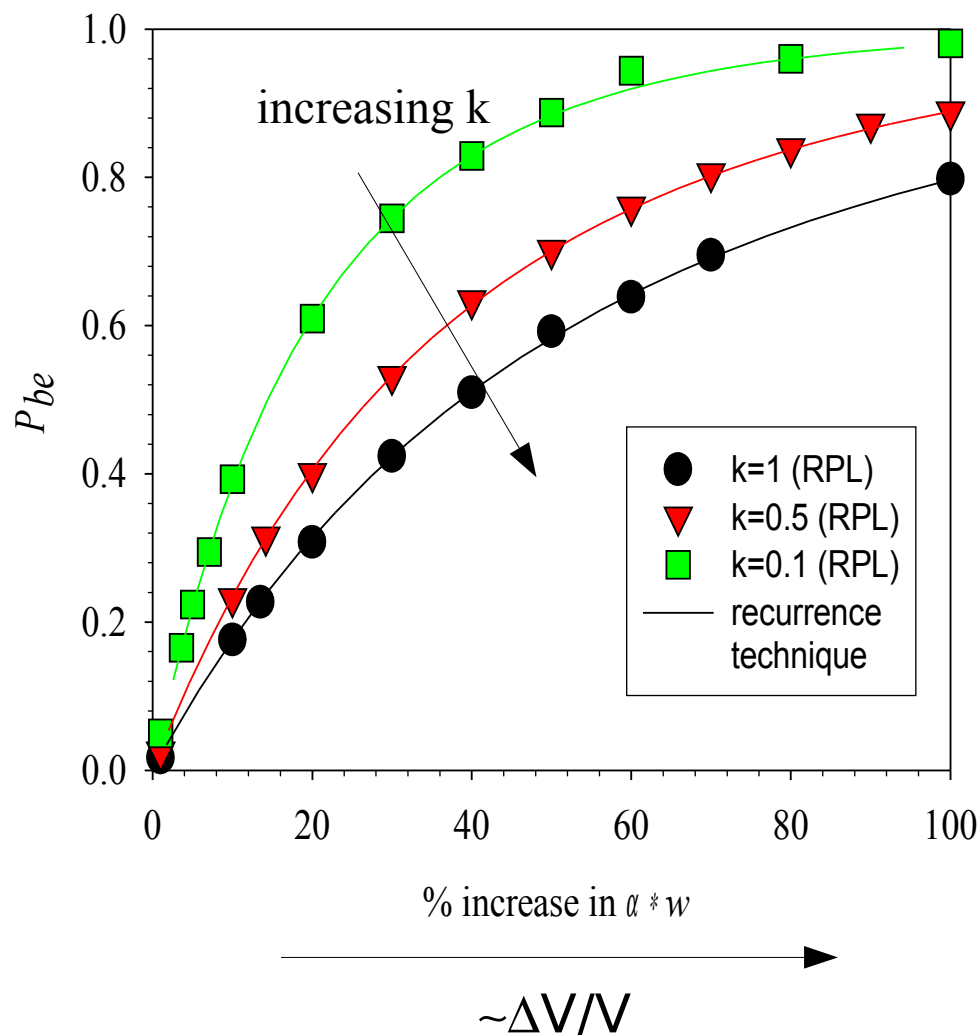
Courtesy of C.H.Tan

The conditions to optimize the device timing (high impact ionization ratio β/α) are **opposite** of those to optimal (fast) rise PDE vs ΔV

Comparison with data ... not yet

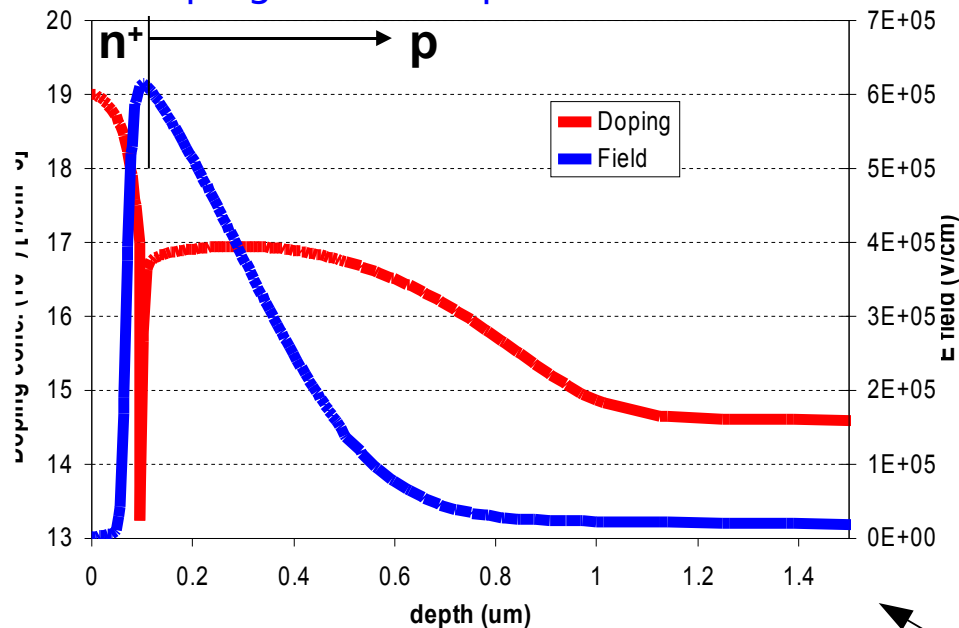
In order to compare model with data detailed modelization will be done (ongoing work) accounting based on:

- E field profile, carrier injection profile and saturated velocities e-h
- Check with PDE and Gain

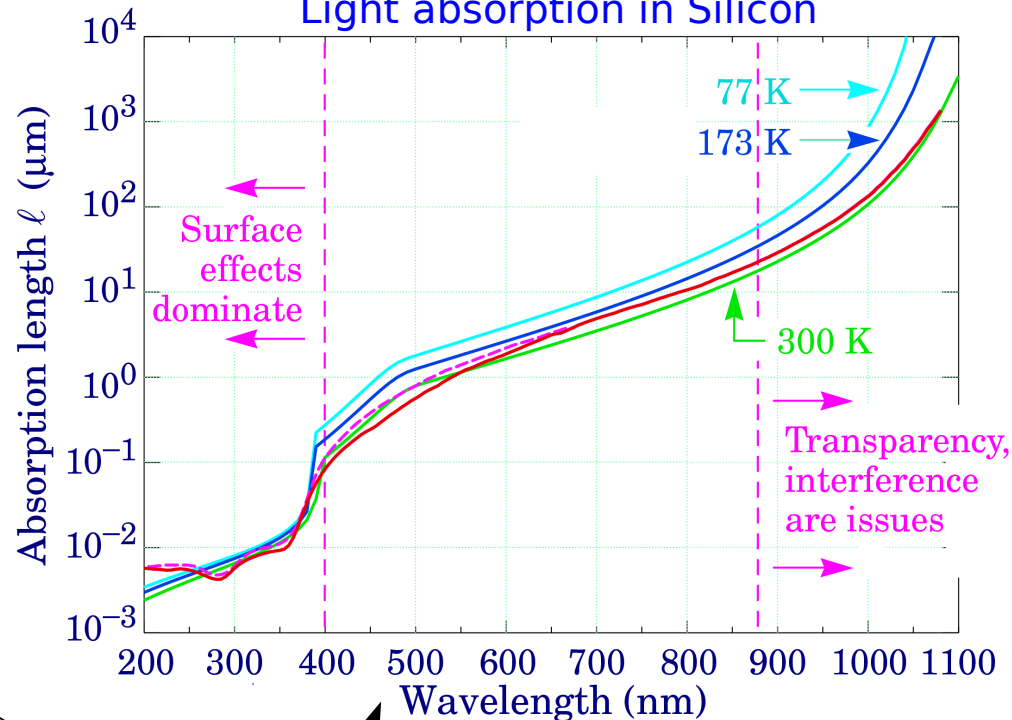


Close up of a cell (IRST)

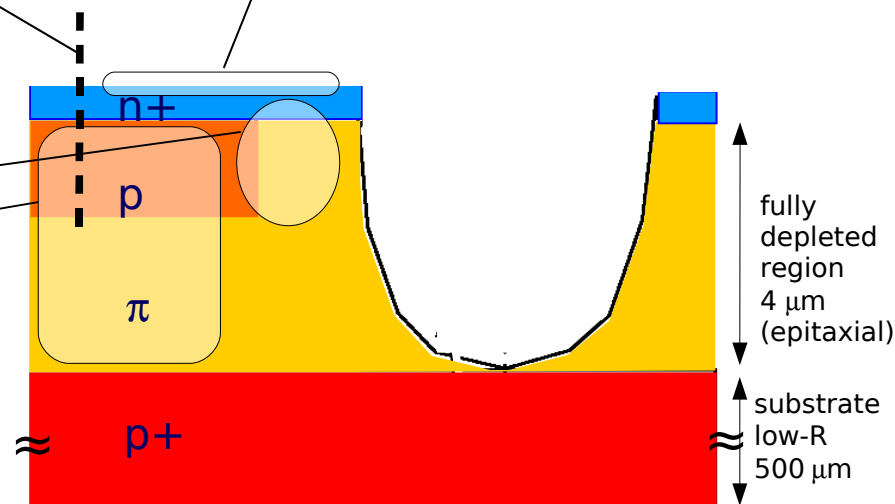
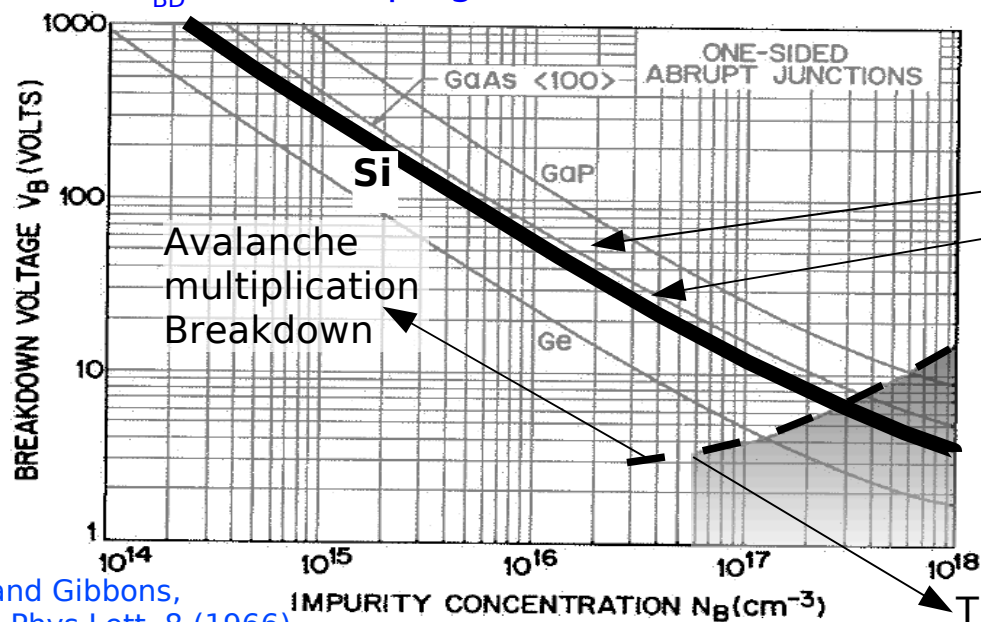
Doping and Field profiles



Light absorption in Silicon



V_{BD} versus doping concentration

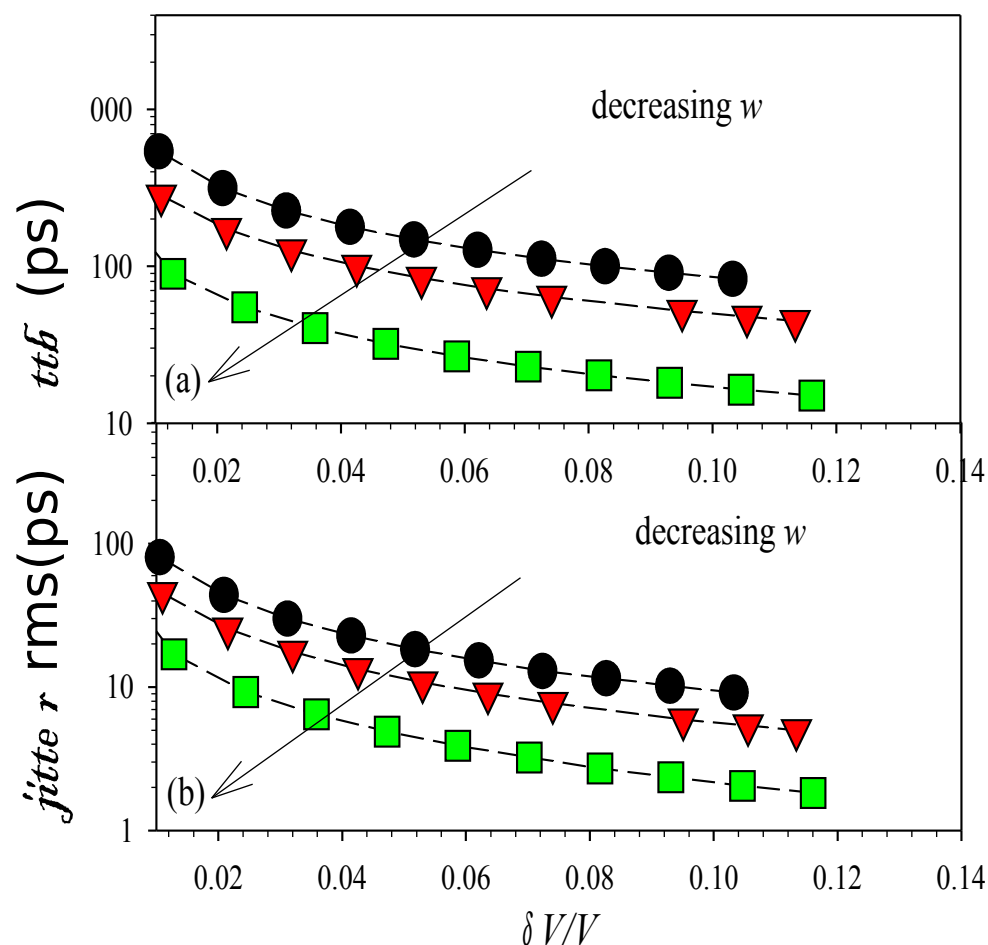


Tunneling effect Breakdown

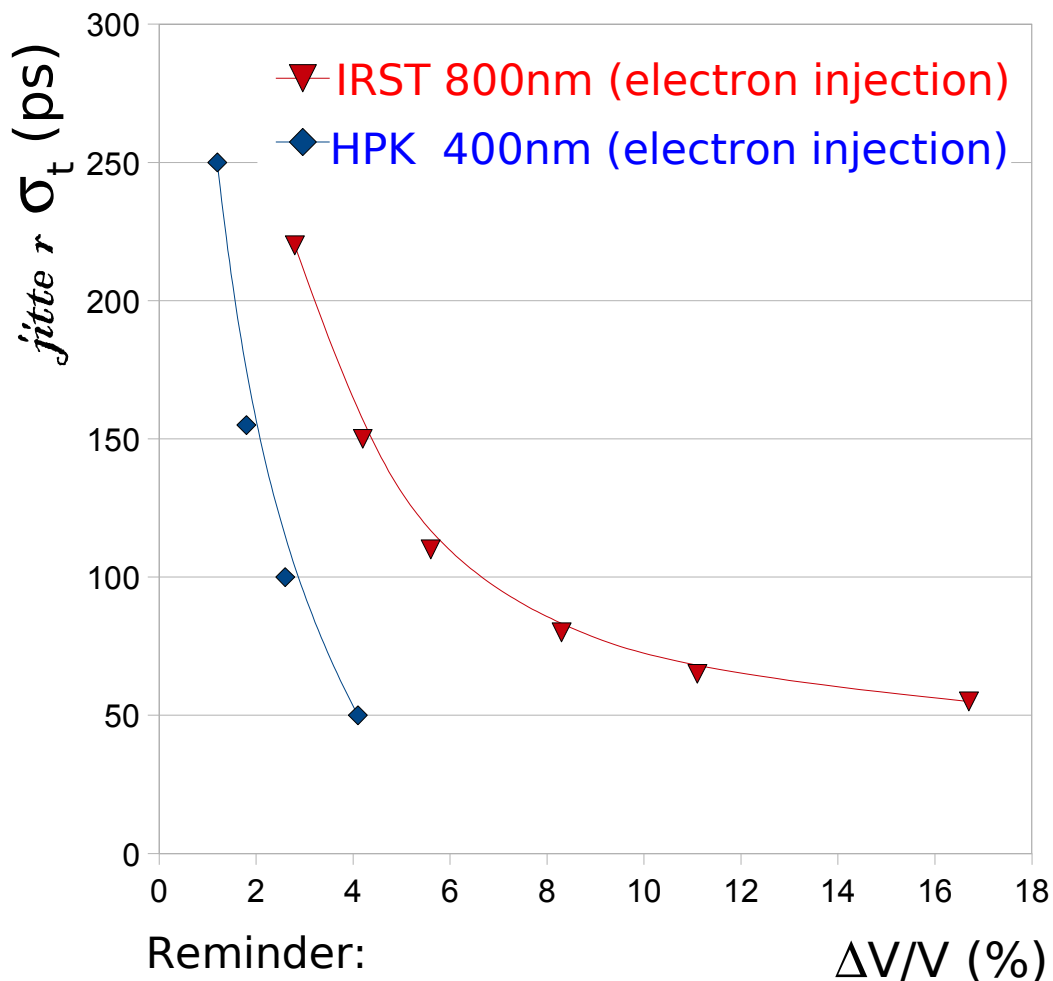
Comparison with data ... not yet

Example of RPL simulation of pure electron injection in Si SPAD

Courtesy of C.H.Tan



DATA
(DASIPM)



Reminder:

IRST structure is n on p

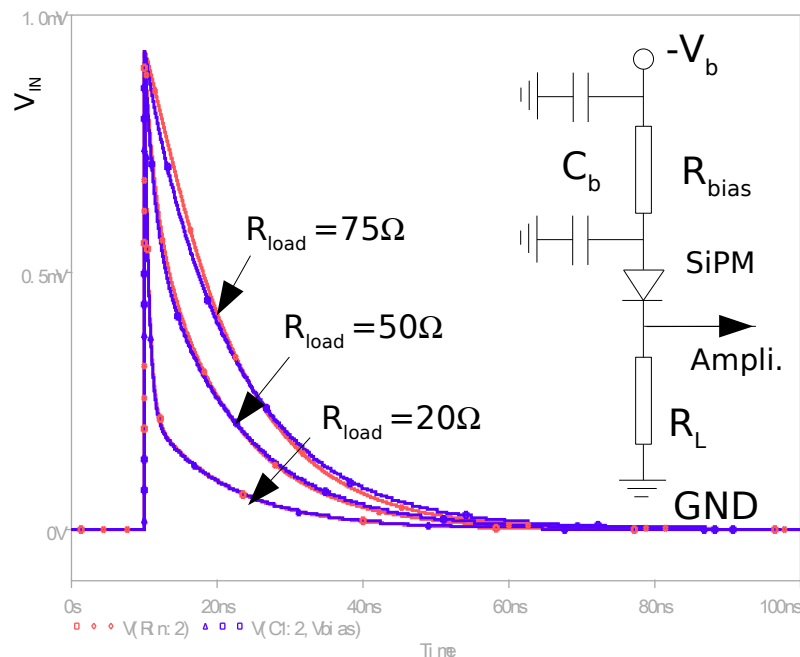
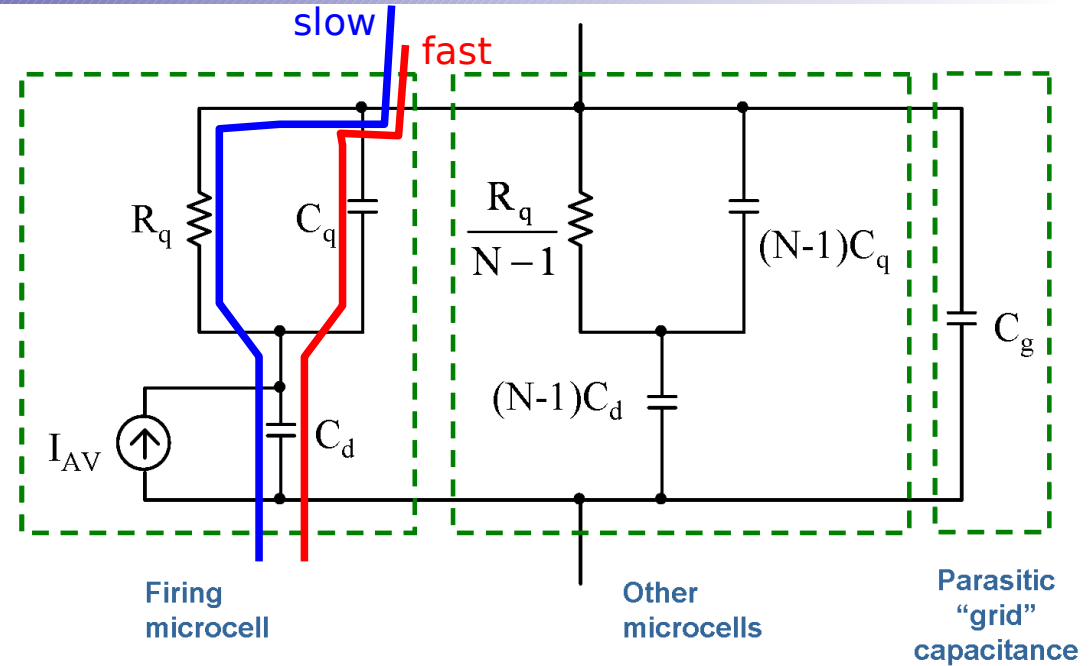
HPK structure is p on n



Electronics for timing applications

Electrical model of a SiPM

- R_q : quenching resistor (hundreds of k Ω)
 C_d : junction capacitance (few tens of fF)
 C_q : **parasitic capacitance** in parallel to R_q (few tens of fF, $C_q < C_d$)
 I_{AV} : **SiPM ~ ideal current source** current source modeling the total charge delivered by a cell during the avalanche $Q = \Delta V(C_d + C_q)$
 C_g : parasitic capacitance due to the routing of V_{bias} to the cells (metal grid, few tens of pF)



1) the peak of V_{IN} is independent of R_s

A constant fraction Q_{IN} of the charge Q delivered during the avalanche is instantly collected on $C_{tot} = C_g + C_{eq}$.

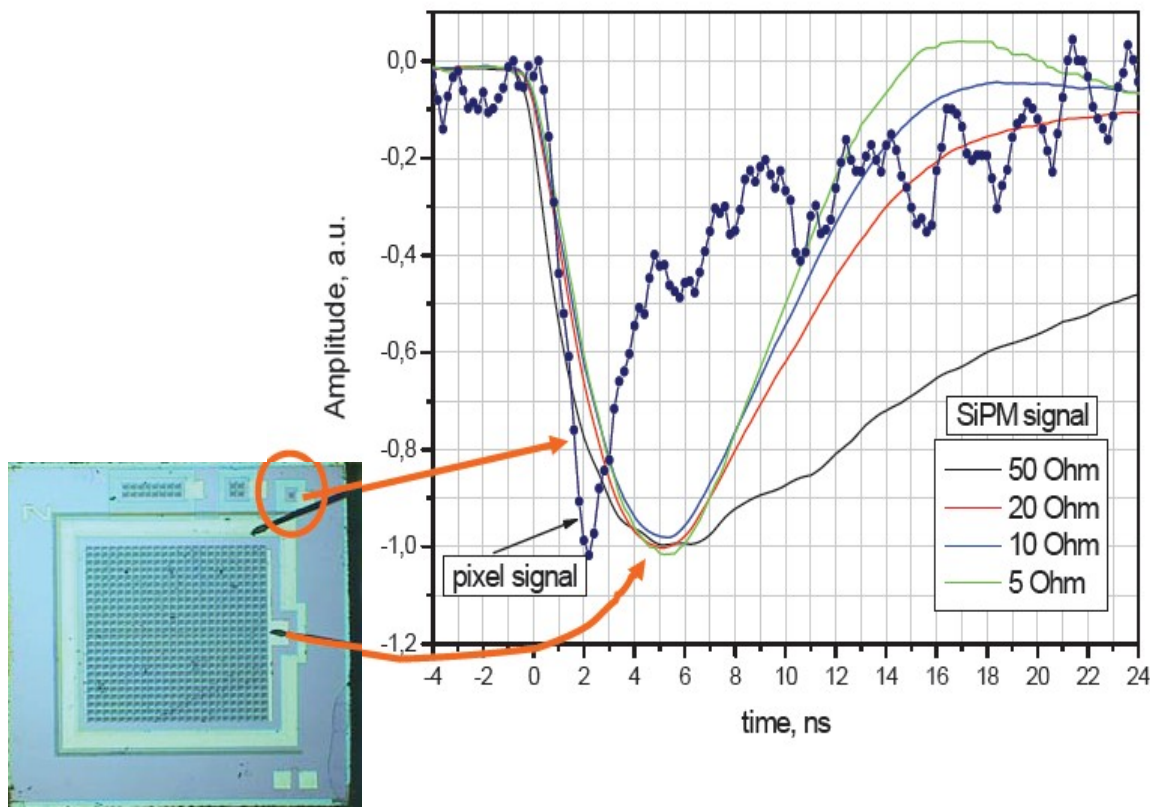
2) **The circuit has two time constants:**

- $\tau_{IN} = R_L C_{tot}$ (fast)
- $\tau_r = R_q (C_d + C_q)$ (slow)

Decreasing R_s , the time constant τ_{IN} decreases, the current on R_s increases and the collection of Q is faster

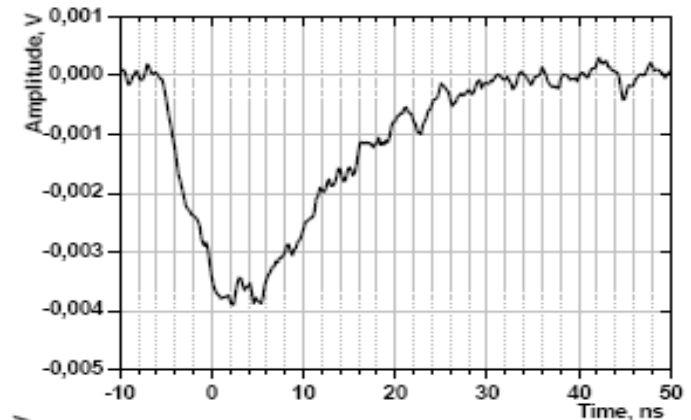
SiPM signal: effect of C_{tot} and Z_{load}

SiPM – MePhI/Pulsar:
1600 cells ($100 \times 100 \mu\text{m}^2$)
Area = $5 \times 5 \text{ mm}^2$
 $C_{tot} \sim 160 \text{ pF}$

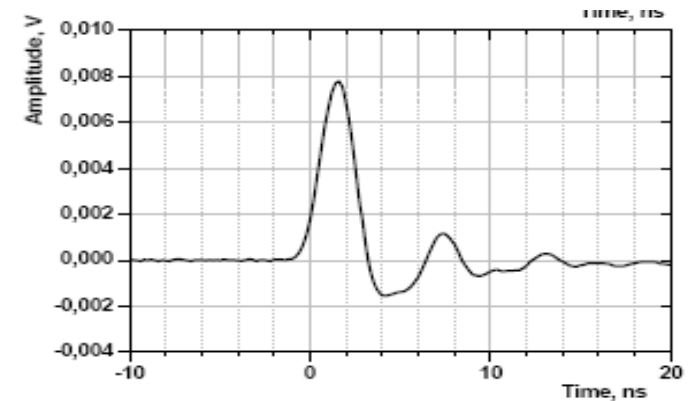


B. Dolgoshein and E. Popova
ICFHE-07

$Z_{in} \sim 50 \Omega$
 $FWHM \sim 15 \text{ ns}$



$Z_{in} \sim 7 \Omega + \text{shaper}$
 $FWHM \sim 2.5 \text{ ns}$



Trans-impedance amplifier

Ideal FE Electronics for timing (and high rate)

1) current amplifier or I-V converter:

- exploit detector fast component \rightarrow smallest Z_{in} (and smallest $C_{parasitic}$)
- detector need low external Gain $\sim x20 \rightarrow$ fast amplifier
- detector rise time $\sim 100ps \rightarrow$ match with 3GHz amplifier BW

2) RC shaper

- \rightarrow minimize signal occupancy (pile-up) per channel
- \rightarrow maximize the double pulse resolution (DPR)

3) sampling with FADC

- \rightarrow sampling at 1GHz time resolution better than 20 ps rms and DPR better than 5ps are easy to obtain
- \rightarrow very robust to noise
- \rightarrow cost/channel $\sim O(100 \$)$

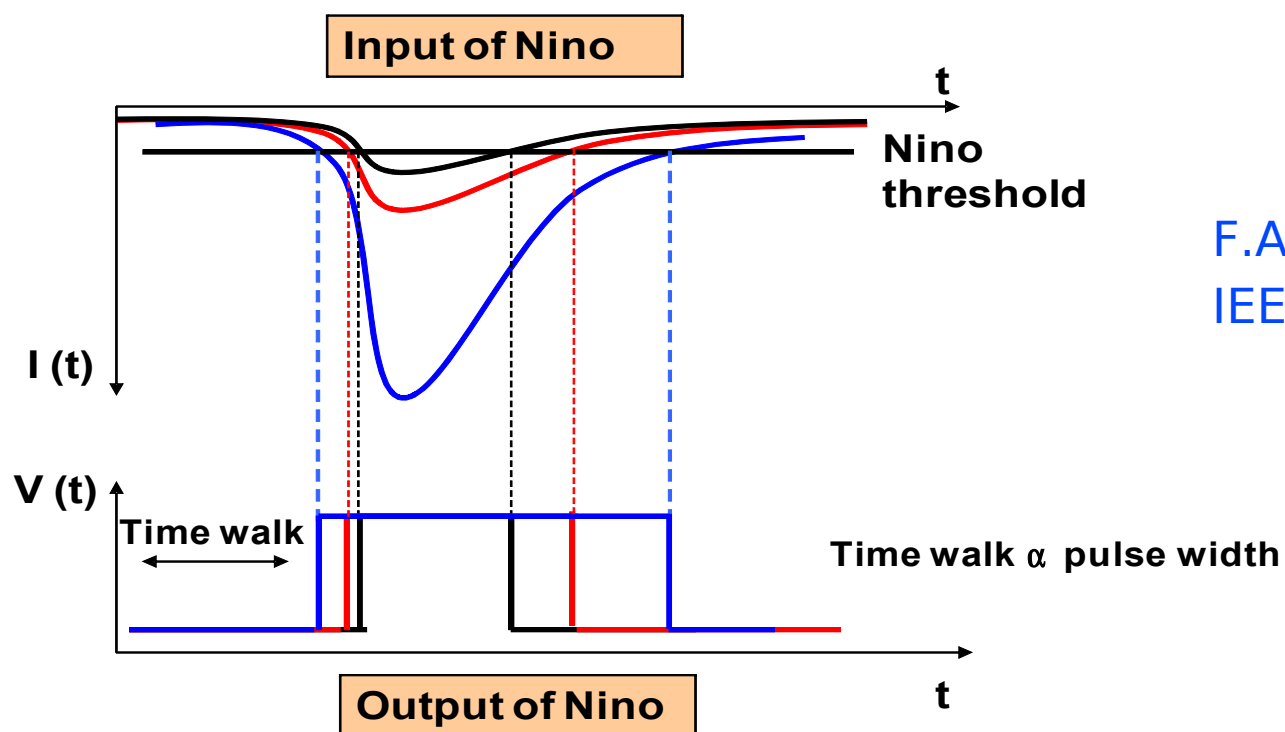
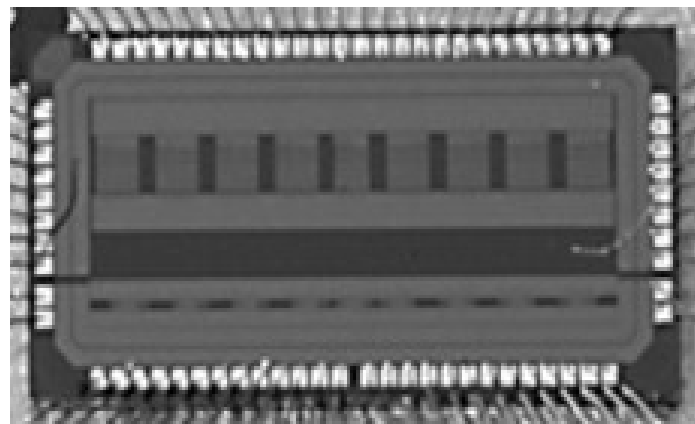
3') Time over Threshold (ToT) Discriminator (Slew correction)

- \rightarrow time resolution better than 40 ps rms and DPR better than 10ps (depending on noise and signal shape)
- \rightarrow cost/channel $\sim O(10 \$)$

Time over Threshold technique (ToT)

NINO chip

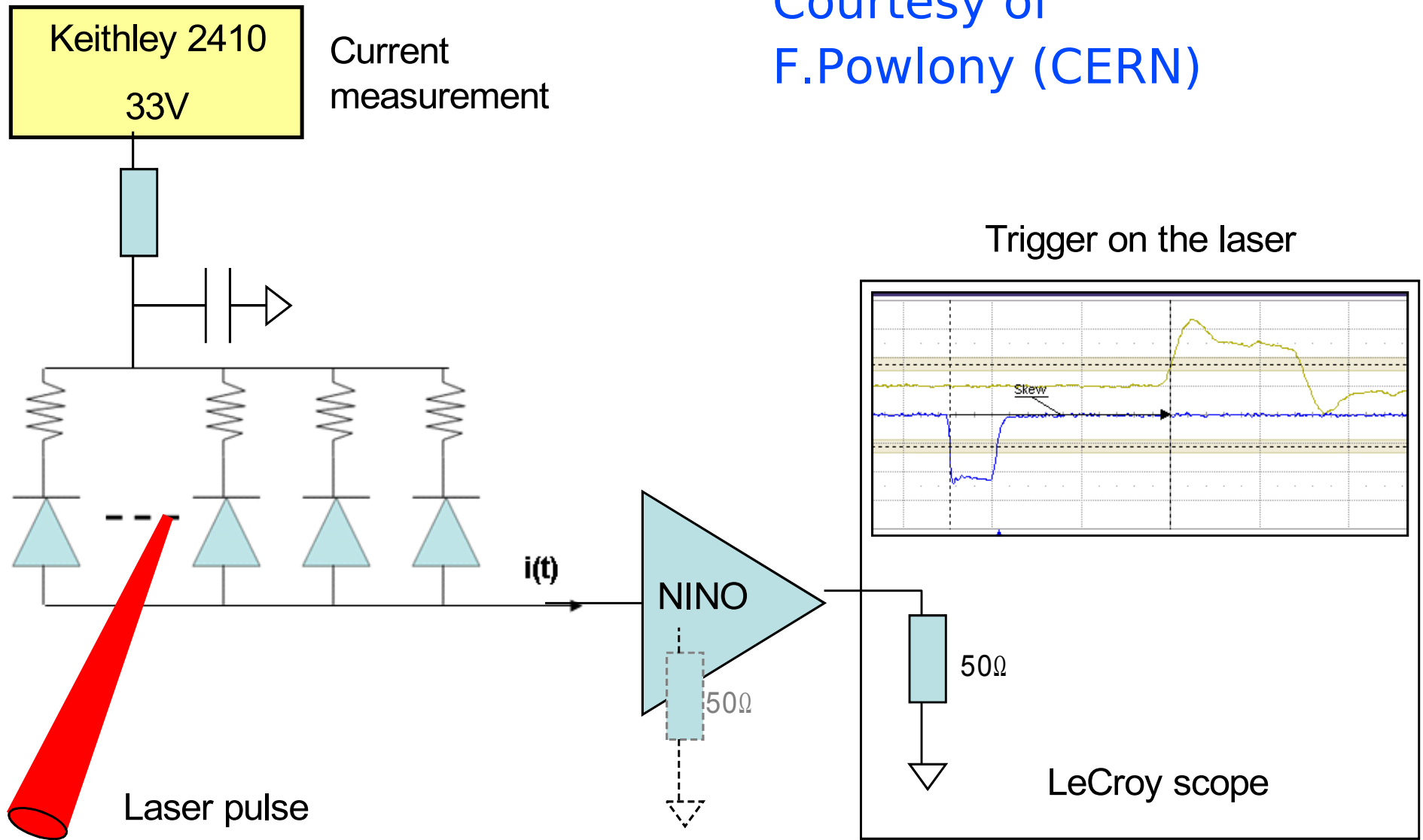
- developed for Alice TOF
- Ultra-fast low-power discriminator
- 8 channels (250 nm CMOS)
- 1 ns peaking time
- 25 ps rms time jitter
- Time over threshold technique



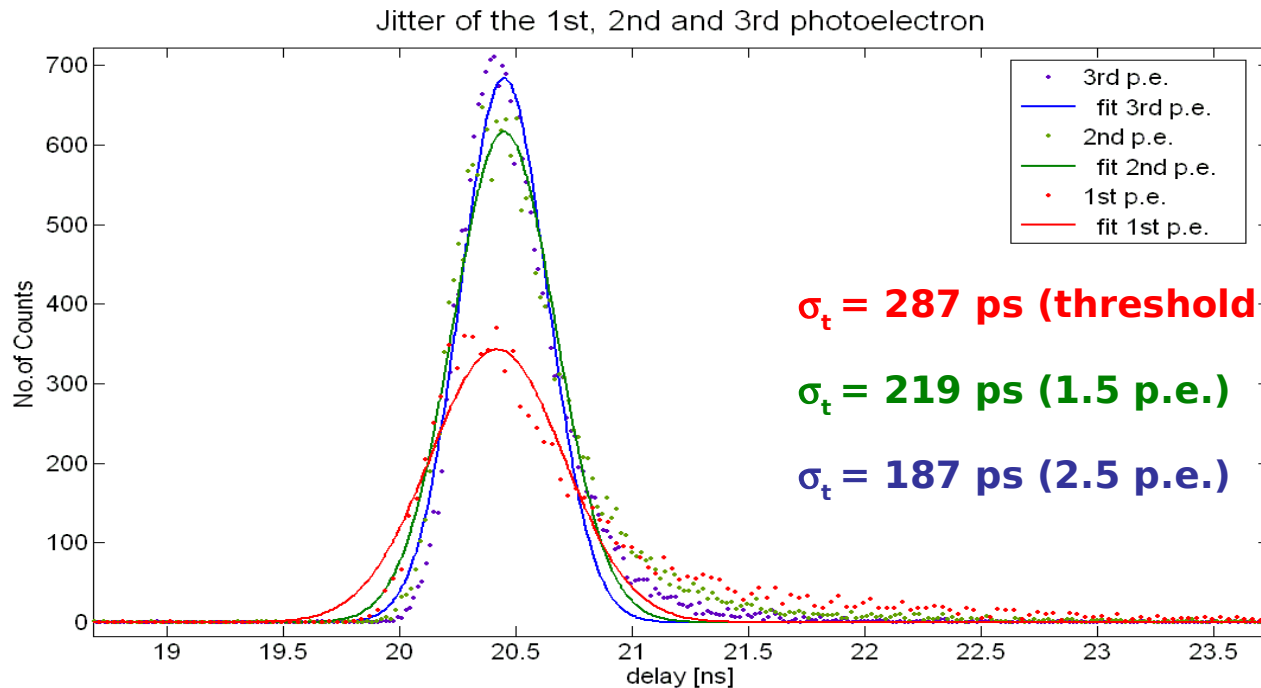
F.Aghinolfi et al
IEEE TNS 51 (2004) 1974

Time resolution with NINO

Courtesy of
F.Powlony (CERN)

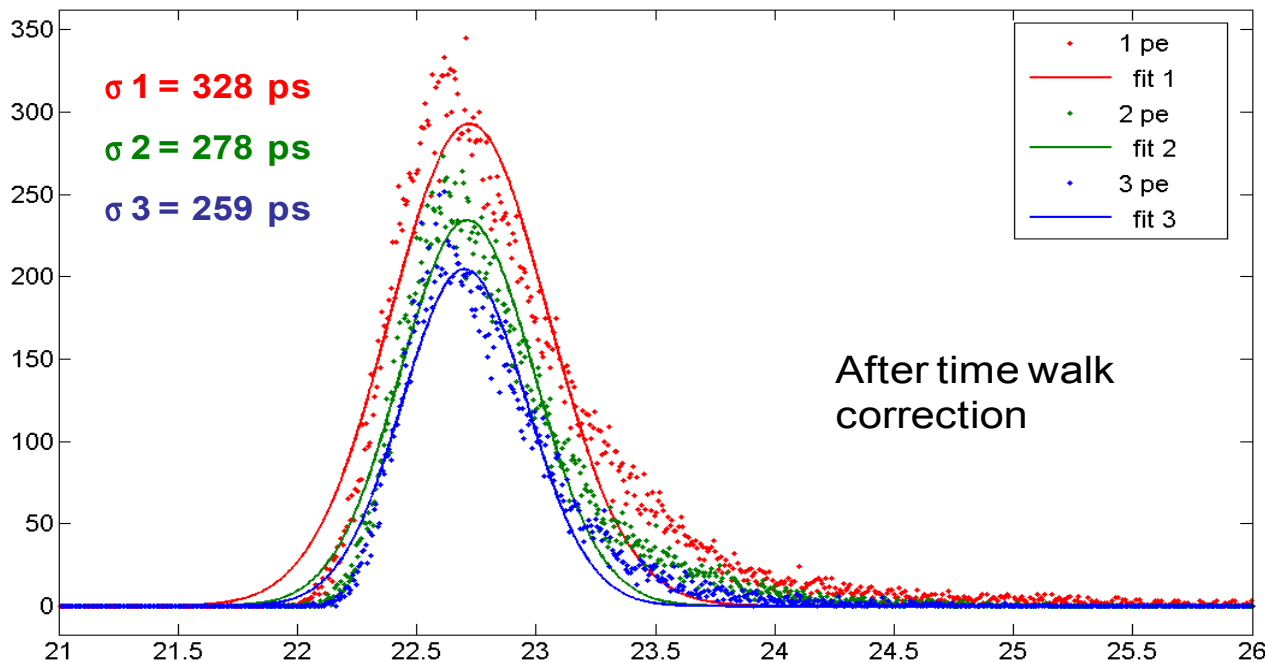


Time resolution with NINO



SiPM directly
to scope

Preliminary
results



SiPM + NINO

Courtesy of
F.Powlony
(CERN)



Examples of applications

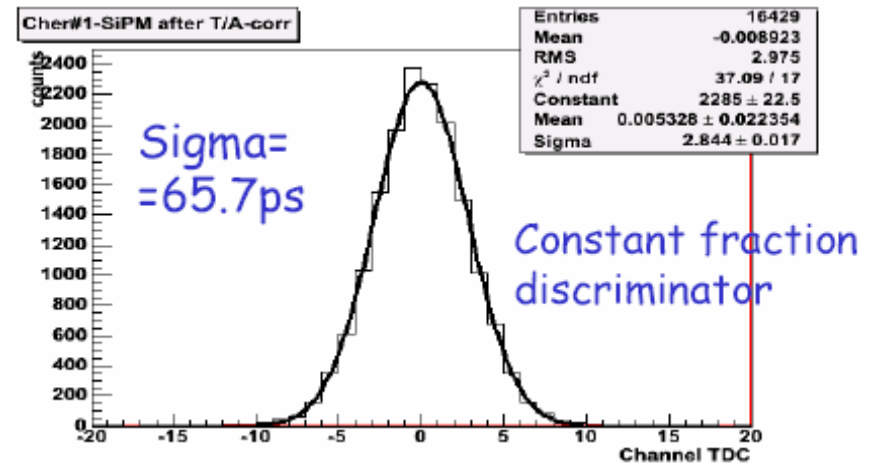
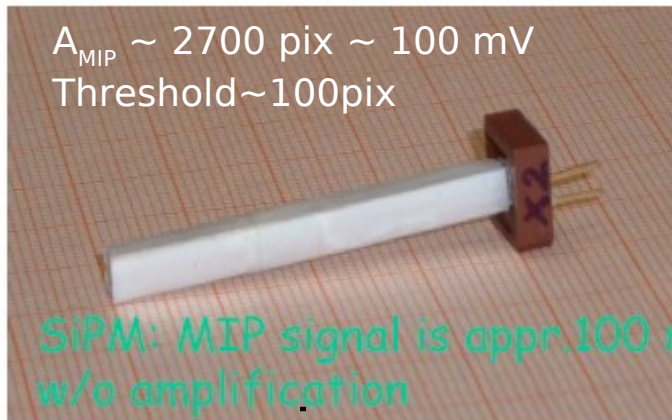
Timing with fast scintillator and SiPM

Dolgoshein
Beaune05

SiPM 3x3 mm² (5600 cells) **glued directly to BICRON-418 scintillator** 3x3x40 mm³
Signal is readout directly from SiPM **without any preamp and shaper** !

Timing between:

- PMT(FEU 187) + Cherenkov radiator
- SiPM + BC418

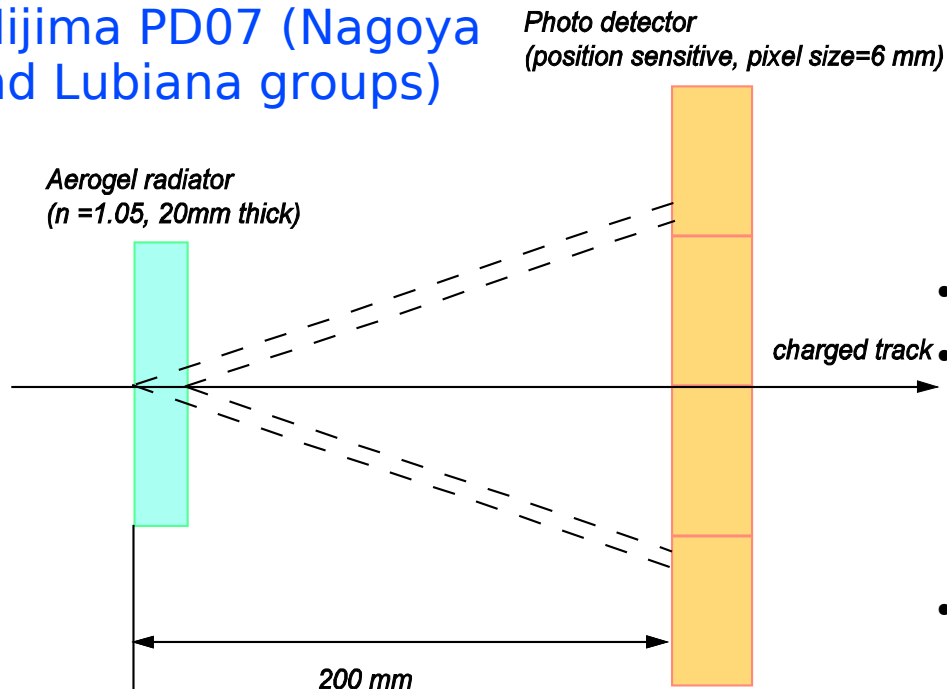


Results: $\sigma_{(\text{PMT}+\text{Ch.rad})} = 48.5 \text{ ps}$; $\sigma_{(\text{electronics})} = 31.7 \text{ ps}$

$\rightarrow \sigma_{(\text{SiPM}+\text{BC418})} = 33.4 \text{ ps}$

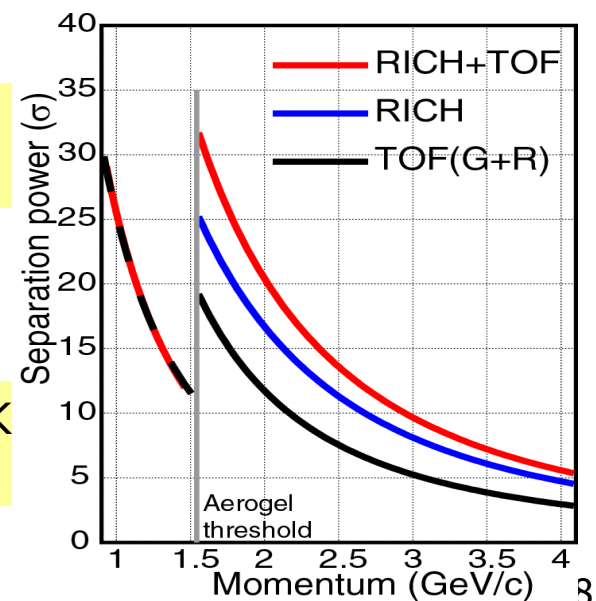
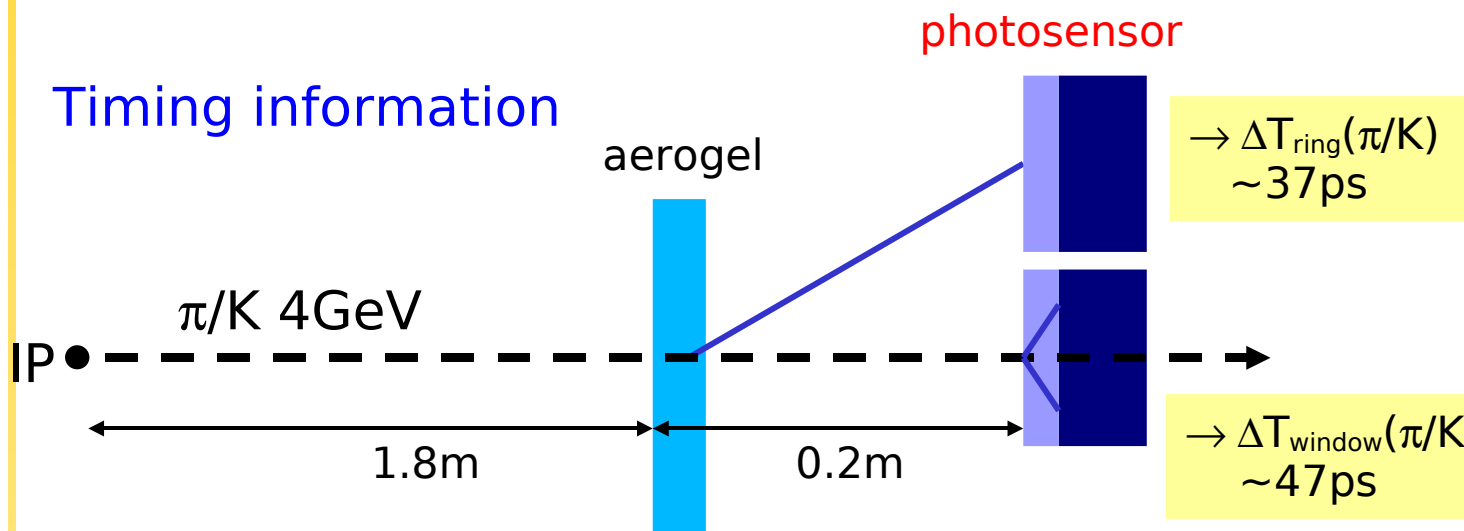
Proximity Focusing Aerogel RICH + TOF

T.Iijima PD07 (Nagoya and Lubiana groups)



- **Proximity focusing geometry**
 - aerogel radiator ($n \sim 1.05$, $\sim 2\text{cm}$)
 - no mirror complex.
 - suitable for collider and space experiments
- $>4\sigma$ K/ π for $0.7 < p < 4.5$ GeV/c
- **Rayleigh scattering** dominates in aerogel.
 - position measurement of single photons in the **visible wave length** region.
- **Timing measurement**
 - TOF and noise rejection by coincidences

Timing information

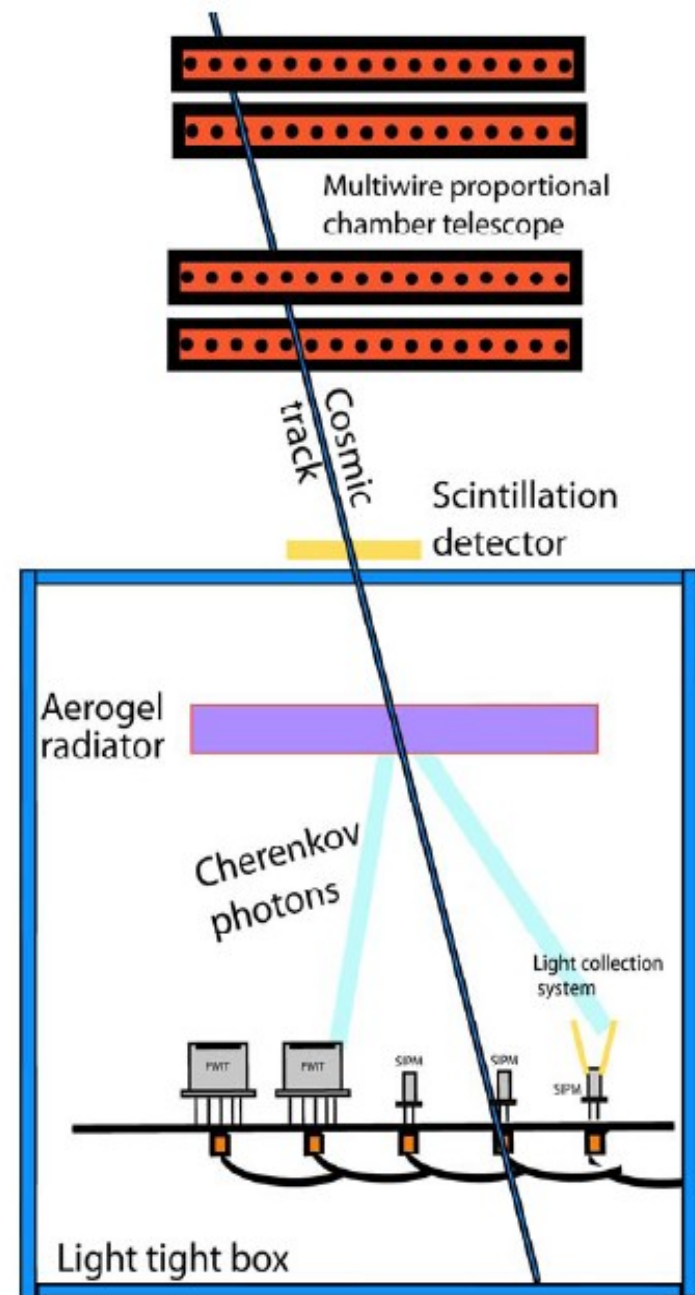


Cherenkov tests with cosmic rays

P.Krizan (Nagoya and
Lubiana groups)

Photon detector:

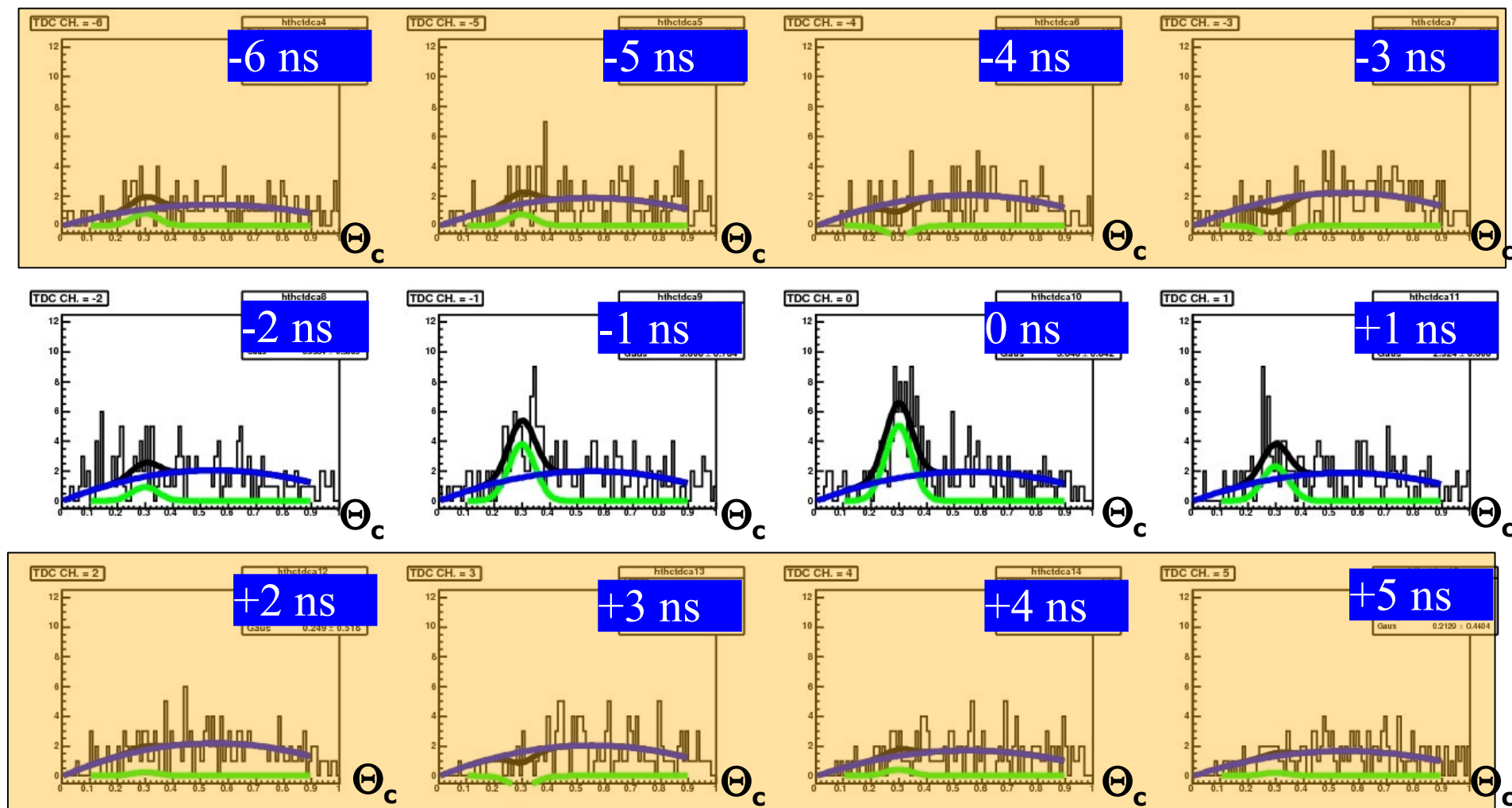
- Array of 6 SiPMs
- Array of 12 R5900-M16 PMTs as reference



Cherenkov tests with cosmic rays

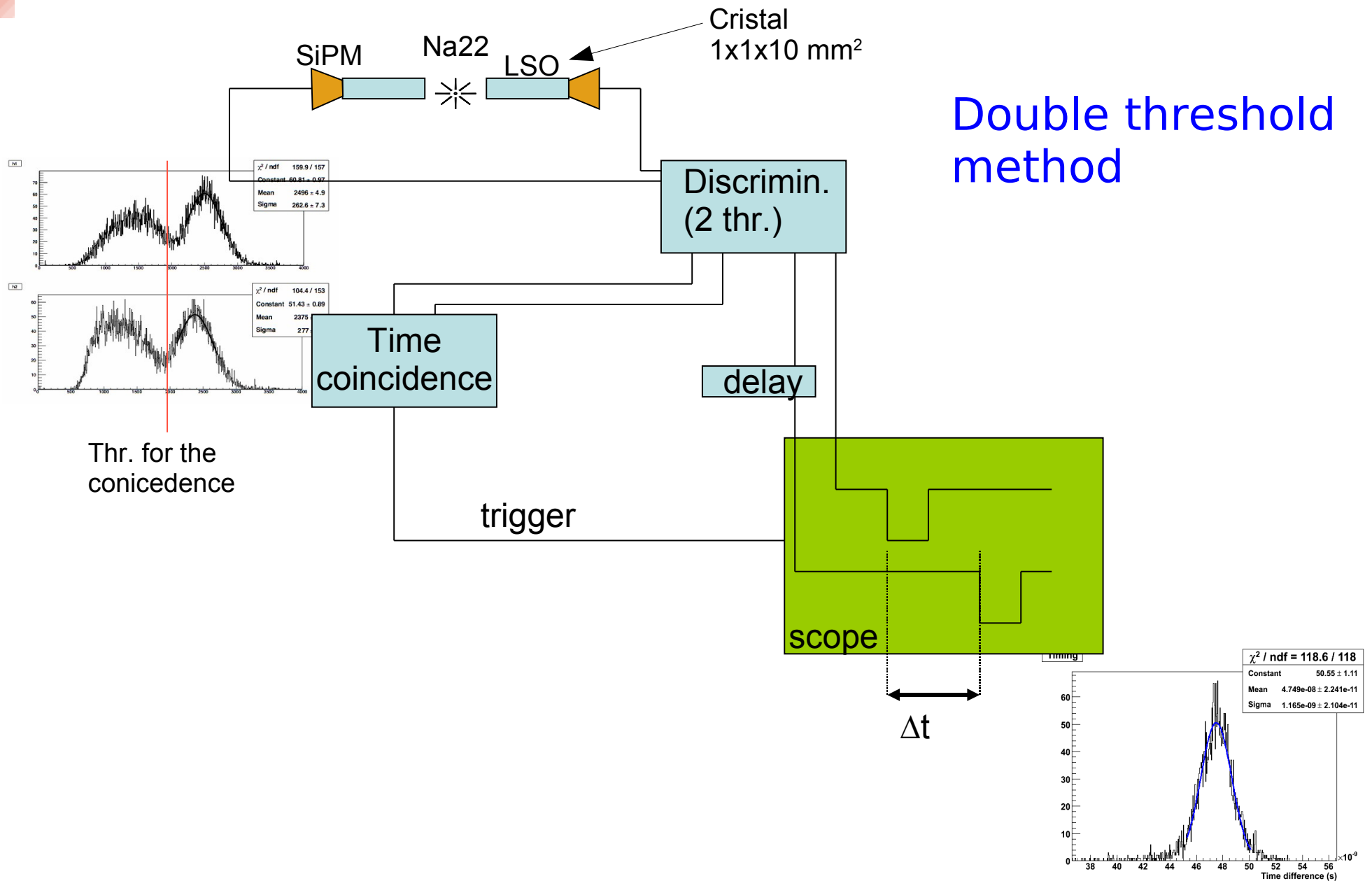
SiPM: Cherenkov angle distributions for 1ns time windows

P.Krizan (Novosibirsk 08)



Cherenkov photons appear in the expected time windows →
Cherenkov photons observed with SiPMs !

Timing with LSO



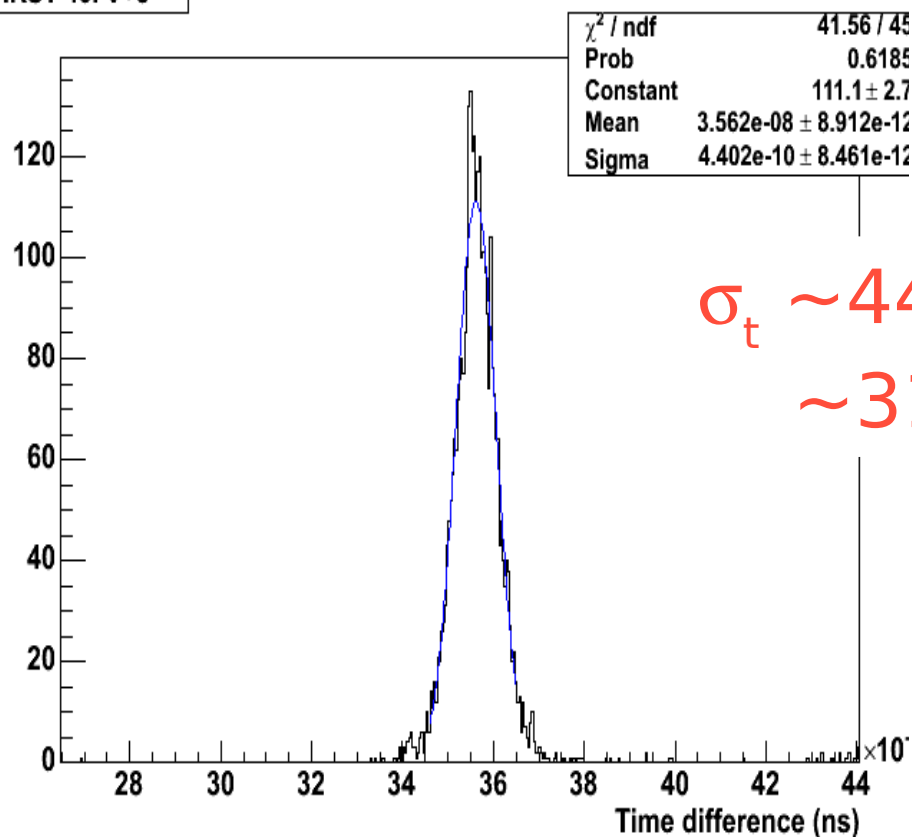
Timing with LSO

SiPM - IRST

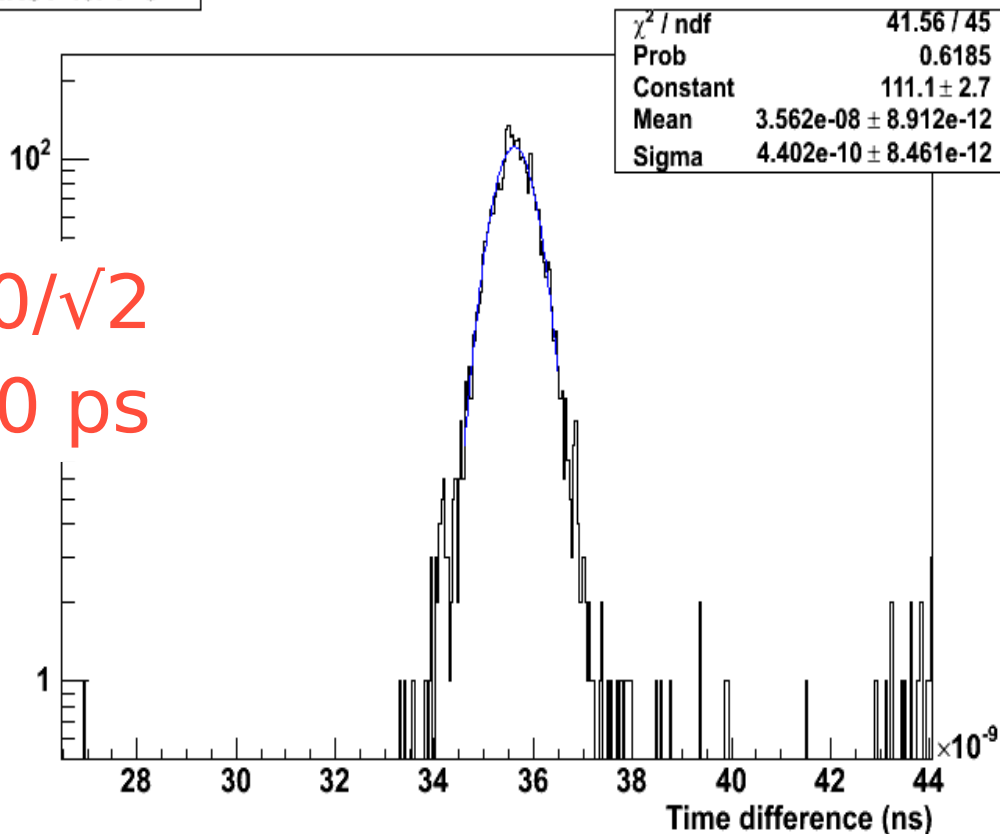
1x1 mm² (50x50μm²)

IRST 40. V+3

IRST 40. V+3



$$\sigma_t \sim 440/\sqrt{2} \\ \sim 310 \text{ ps}$$



Note:
$$\sigma_t \approx \frac{\sqrt{N_{\text{thr. [p.e.]}}}}{N_{\text{p.e.}}} \cdot \tau_{\text{decay}}$$

Post P.R. 80 (1950) 1113

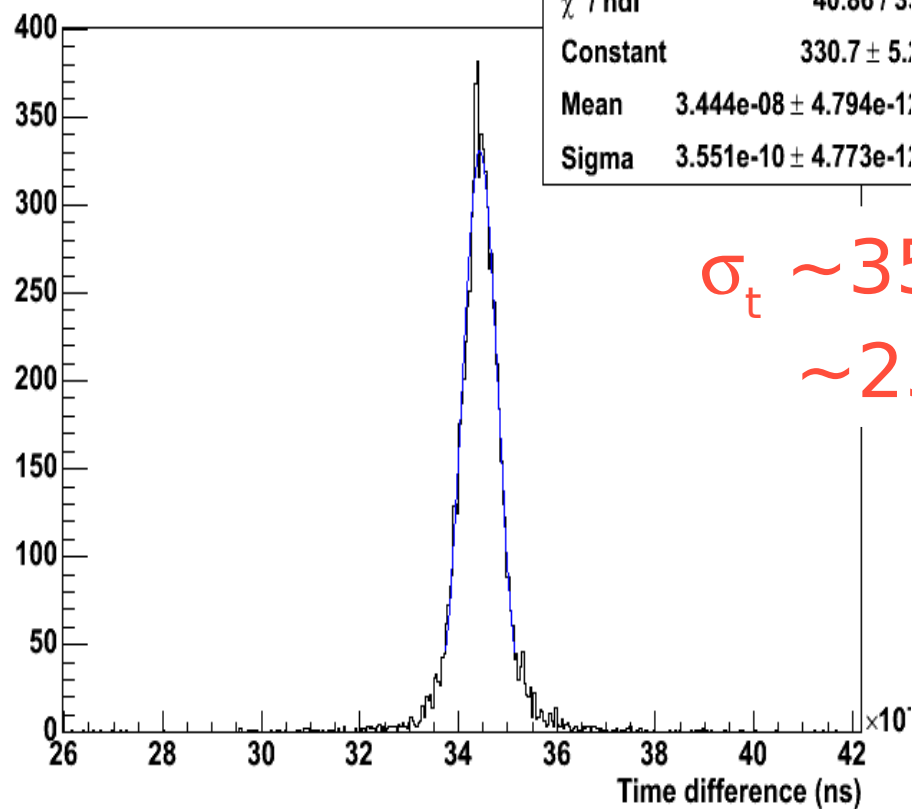
E.g.
$$\left. \begin{array}{l} \tau_{\text{decay}} \sim 40 \text{ ns (decay time for LSO)} \\ N_{\text{p.e.}} \sim 100 \text{ p.e. (photopeak)} \\ N_{\text{thr.}} \sim 1 \text{ p.e. (trigger on 1}^{\text{st}} \text{ p.e.)} \end{array} \right\}$$

Expected: $\sigma_t \sim 400 \text{ ps}$

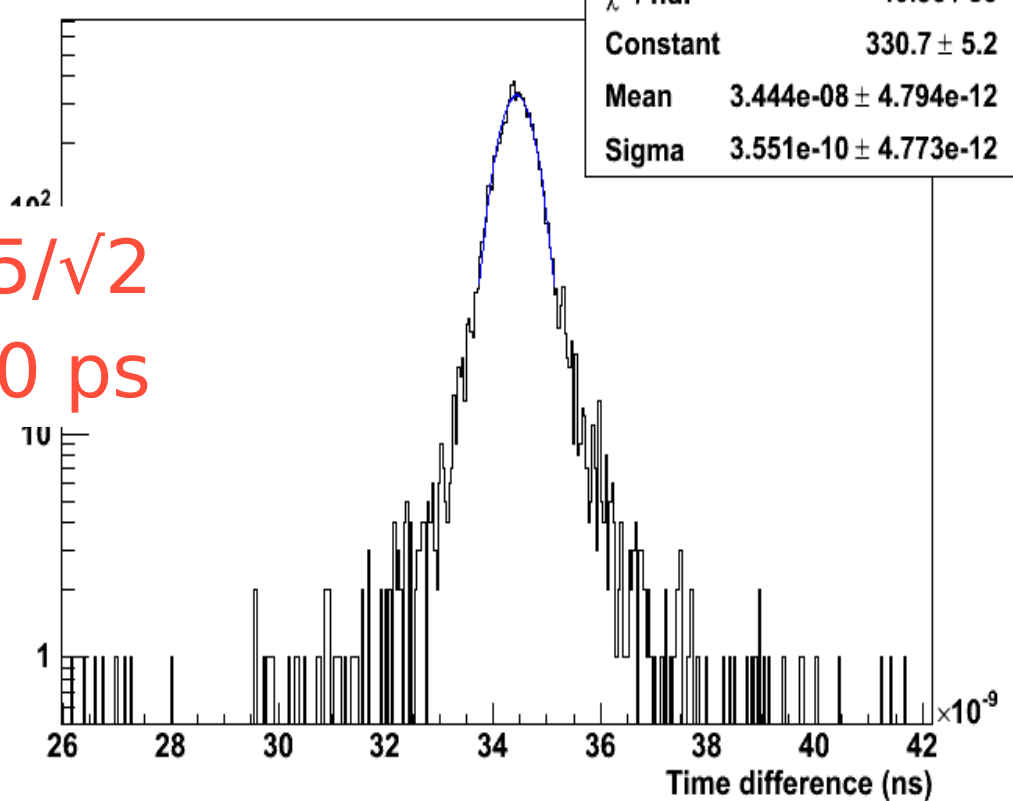
Timing with LSO

SiPM - HPK
1x1 mm² (50x50μm²)

Hamamatsu 50. Vop +1V



Hamamatsu 50. Vop +1V



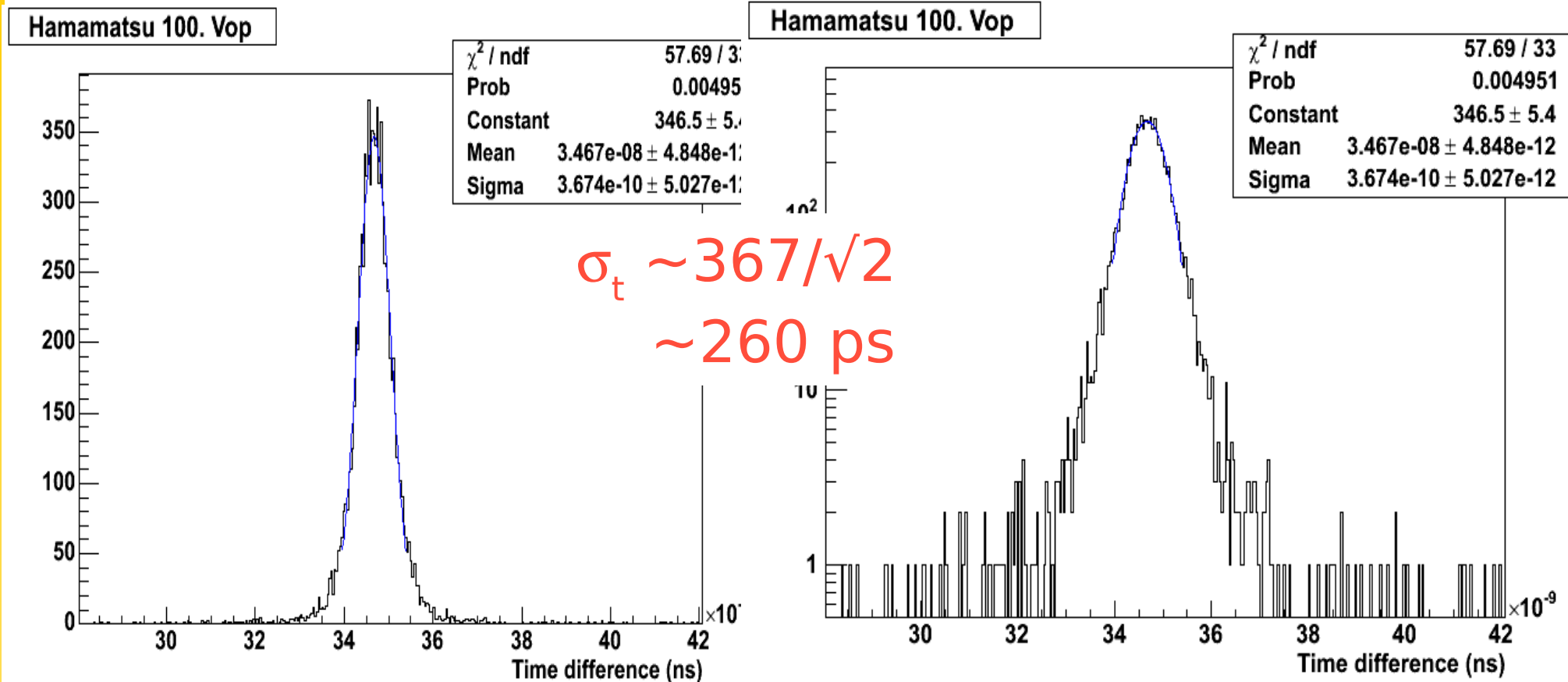
More photoelectrons
(higher PDE)

G.Llosa, DASIPM (unpublished)

Timing with LSO

SiPM - HPK

1x1 mm² (100x100μm²)

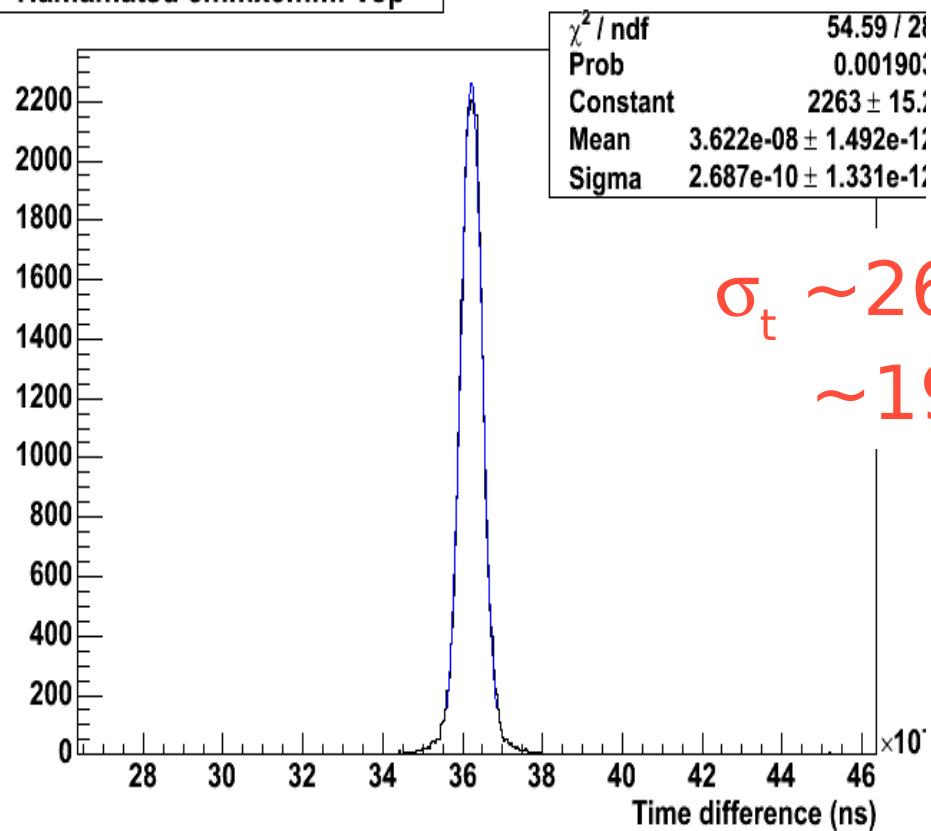


G.Llosa, DASIPM (unpublished)

Timing with LSO

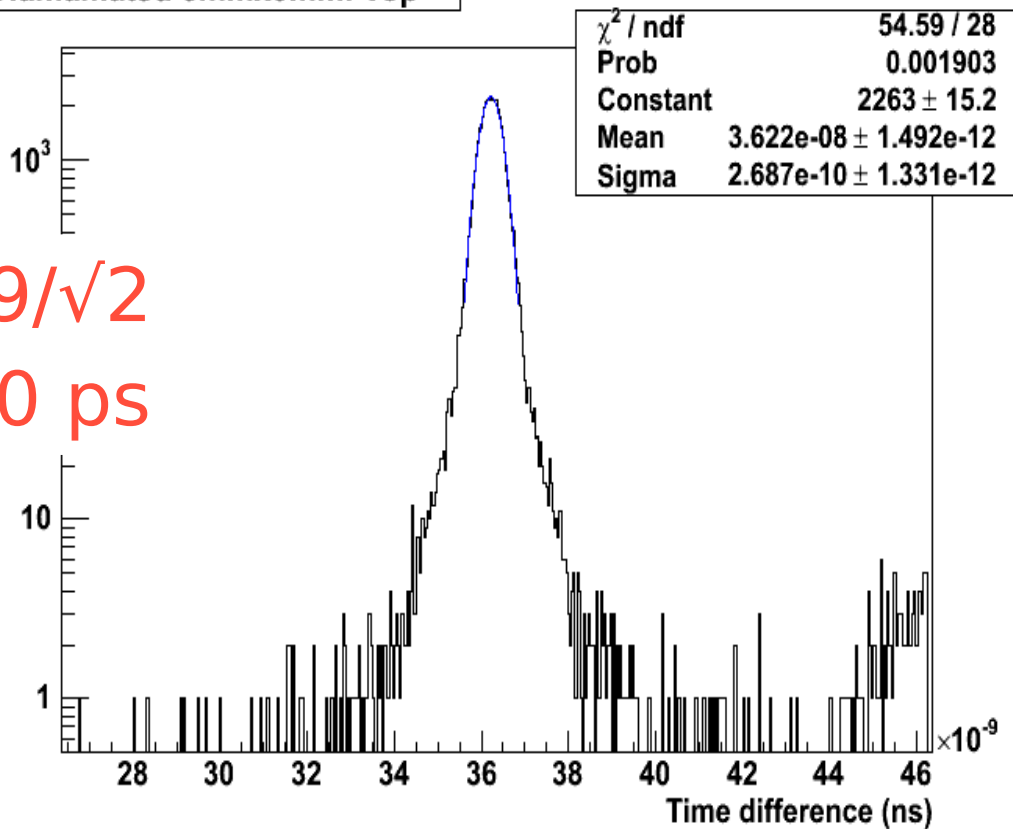
SiPM - HPK
3x3 mm² (50x50μm²)

Hamamatsu 3mmx3mm. Vop



$$\sigma_t \sim 269/\sqrt{2} \\ \sim 190 \text{ ps}$$

Hamamatsu 3mmx3mm. Vop



G.Llosa, DASIPM (unpublished)

Conclusions

SiPM are intrinsically very fast:

- core (gaussian) fluctuations below **100ps**, depending on ΔV
- **Non gaussian tails** up to **O(ns)**, depending on wavelength

The conditions to optimize the device **timing** (high impact ionization ratio β/α) are opposite of those to optimal (fast) **rise PDE vs ΔV**

High bandwidth current amplifier + fast sampling electronics
best choice for timing applications (robust against noise and pile-up)

Best (gaussian) resolutions in applications:

- **Cherenkov: O(10ps)**
- **Fast plastic scintillators O(20ps)**
- **Fast crystal scintillators O(150ps)**

Non-gaussian tails to be considered (for long wavelengths)



Appendix:

Recent measurements about
temperature dependence of SiPM
parameters

G. Collazuol - PIXEL 2008

[illegible]

48

T dependence: V_{BD} , τ_Q and Gain

V_{BD} breakdown voltage: V_{BD} increases with T:

At higher T carriers loose more to lattice
→ lower mobility, shorter mean free path (λ)
→ carriers need higher V to impact-ionize
(temp. coefficient $\Delta V_{BD}/\Delta T \sim 20\text{mV/K} - 80\text{mV/K}$
depending on doping concentration)

Recovery time: τ_Q decreases with T

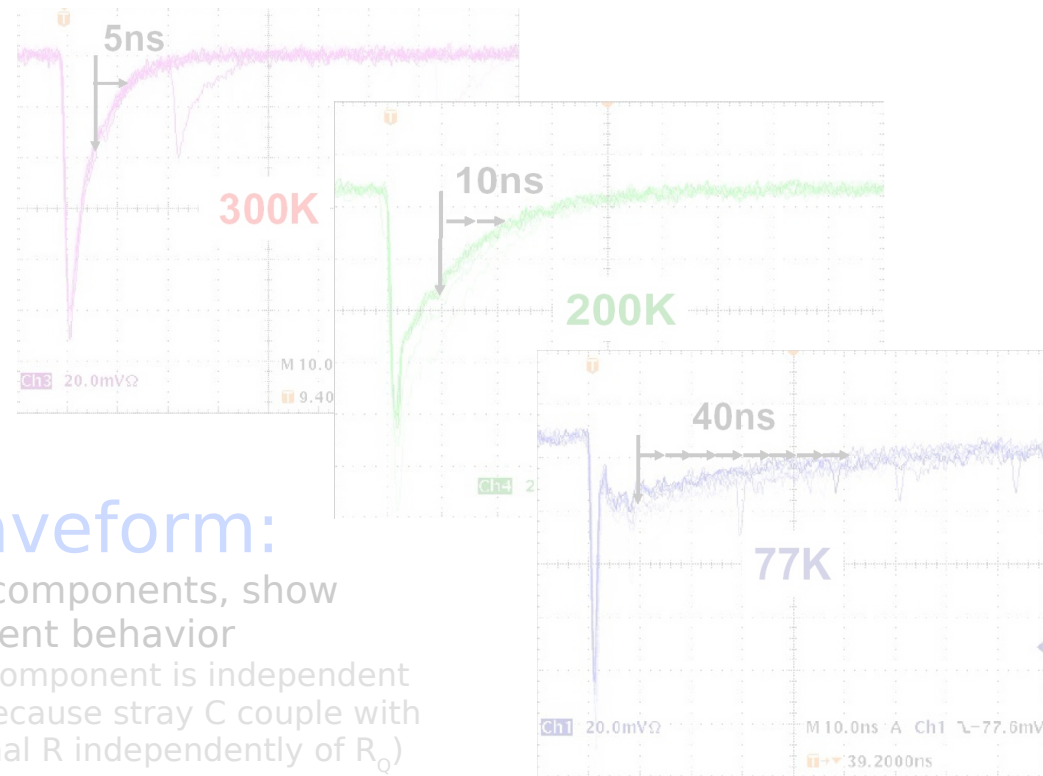
Due polysilicon R_Q properties

T (K)	R_Q (M Ω)
300	0,2
200	0,4
77	1,7

H.Otono - PD07
Characterization
of SiPM by HKP at low T

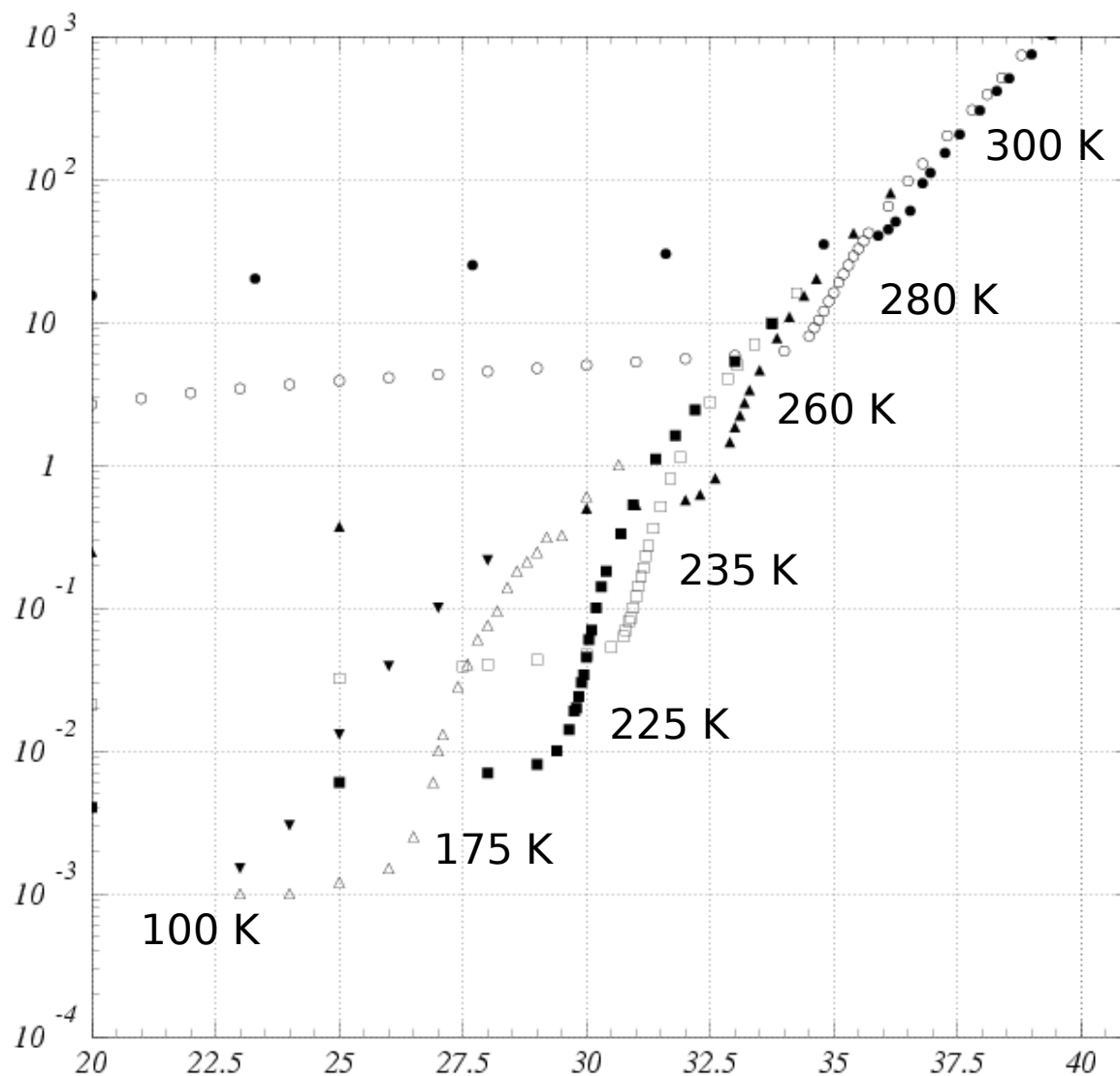
Cell Capacity does not vary with T

Gain independent of T
at fixed Over-Voltage



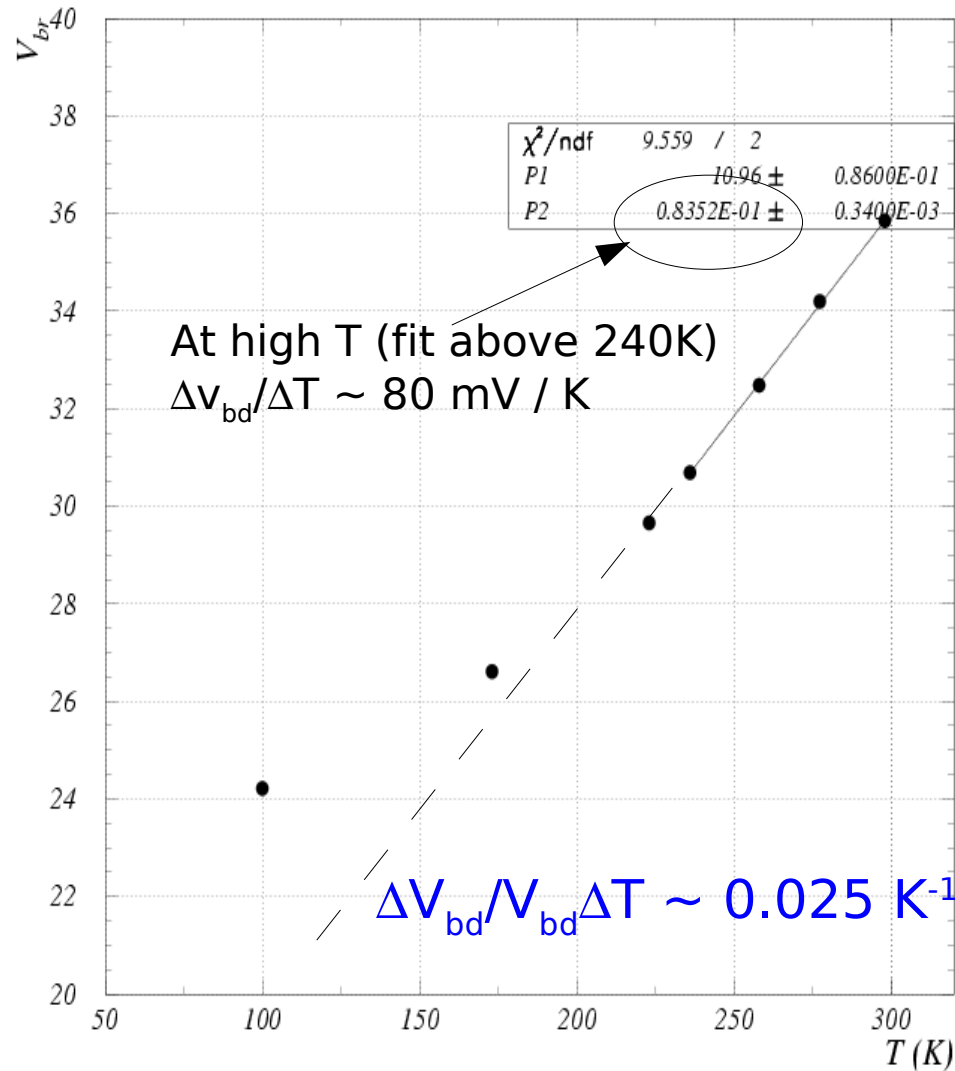
I-V measurements at different T

SiPM - IRST (1x1mm², fill factor 50%)



V_{BD} Break-Down vs T

Data: IRST devices



Model: Baraff PR 128 (1962) 2507

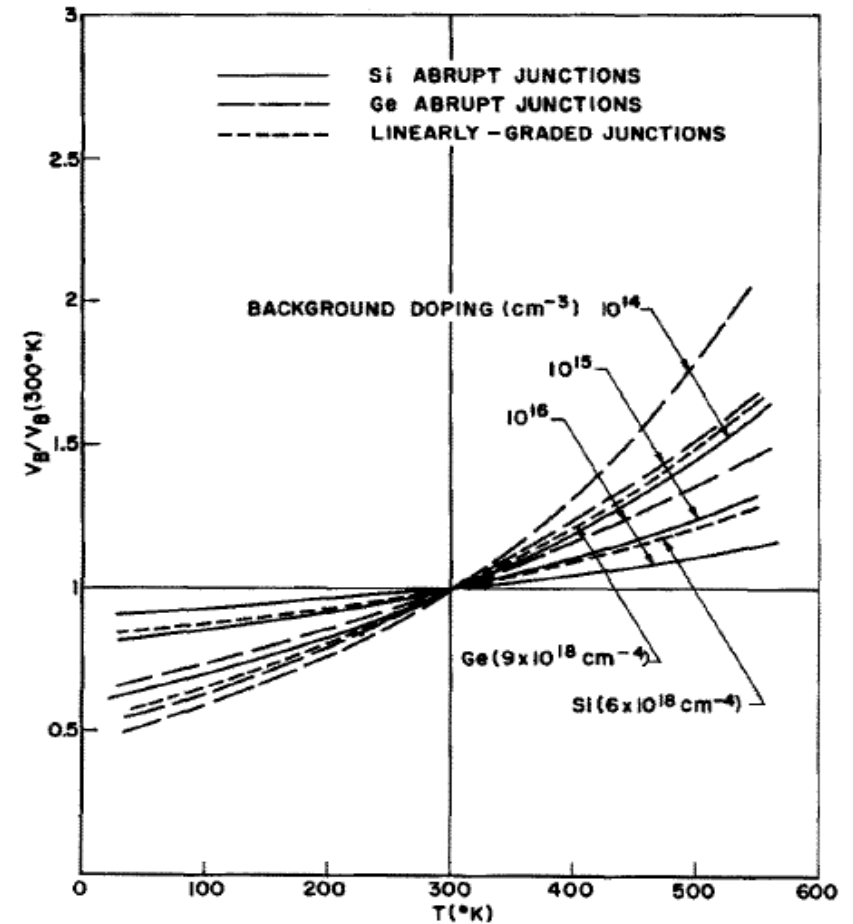


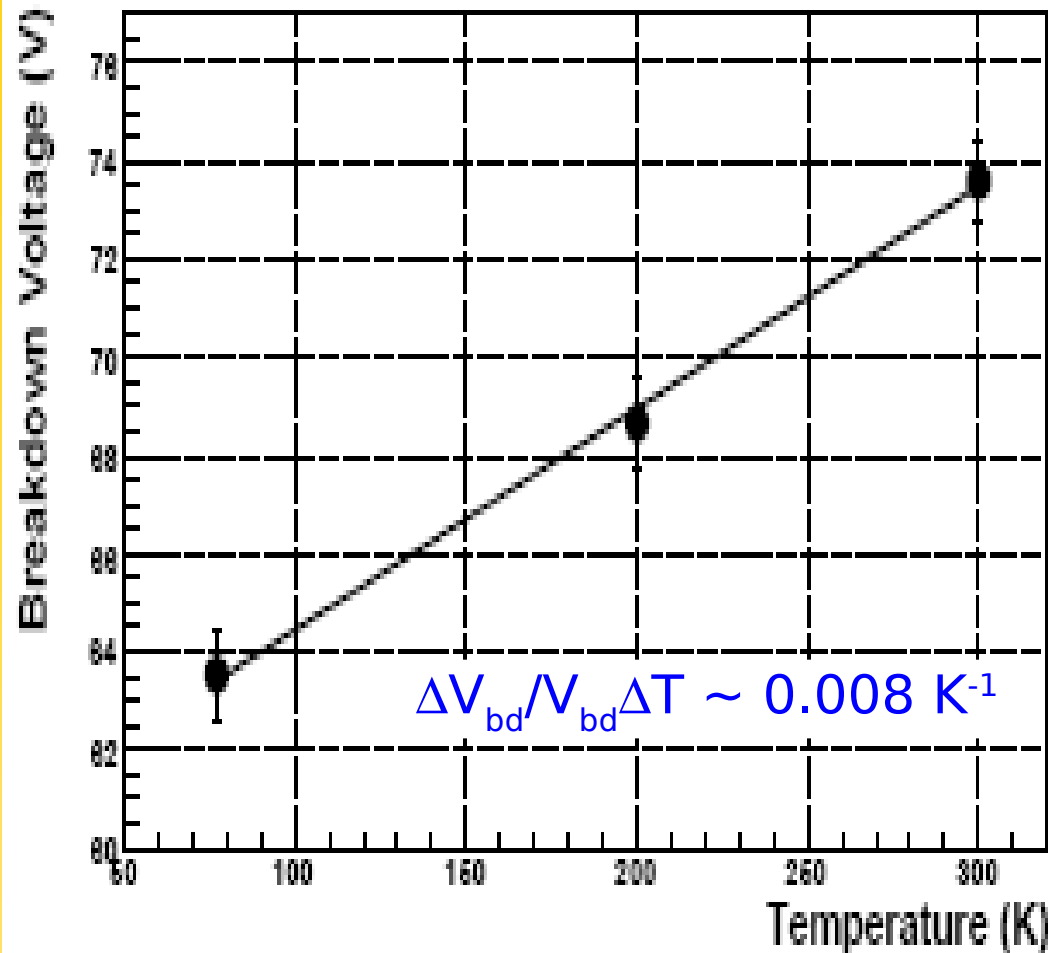
Fig. 4. Breakdown voltage vs temperature for Si and Ge p - n junctions. $V_B(300^\circ\text{K})$ is 2000, 330, and 60 V for Si and 950, 150, and 25 V for Ge for dopings of 10^{14} , 10^{15} , and 10^{16} cm^{-3} respectively. The linear-graded junctions have $V_B(300^\circ\text{K})$ the same as those for doping of 10^{13} cm^{-3} .

G.Collazuol (unpublished)

Crowell and Sze, APL 9 (1966) 242

V_{BD} Break-Down vs T

Data: HPK devices



Otono et al - PD07

Model: Baraff PR 128 (1962) 2507

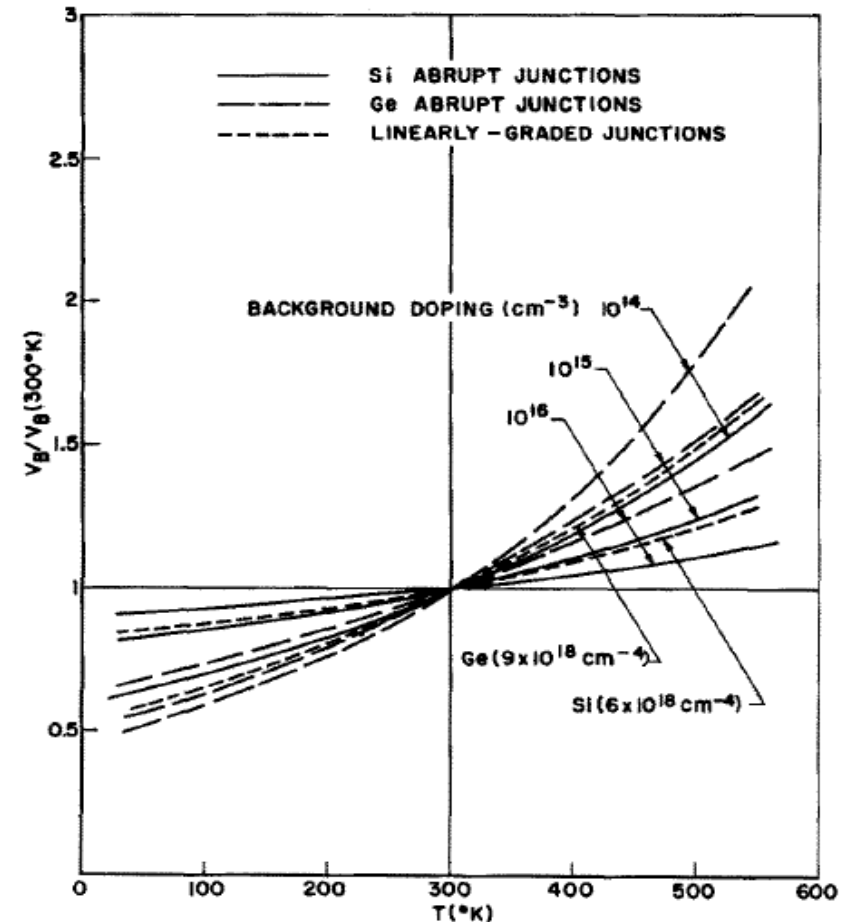


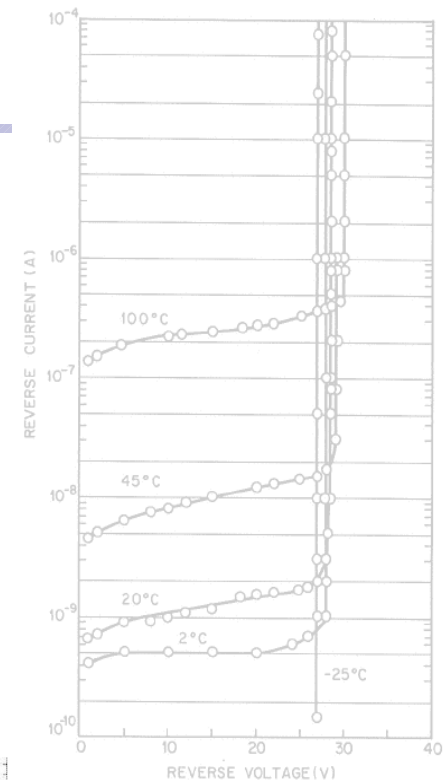
Fig. 4. Breakdown voltage vs temperature for Si and Ge p - n junctions. $V_B(300^\circ\text{K})$ is 2000, 330, and 60 V for Si and 950, 150, and 25 V for Ge for dopings of 10^{14} , 10^{15} , and 10^{16} cm^{-3} respectively. The linear-graded junctions have $V_B(300^\circ\text{K})$ the same as those for doping of 10^{15} cm^{-3} .

Crowell and Sze, APL 9 (1966) 242

T dependence: V_{BD} , τ_Q and Gain

V_{BD} breakdown voltage: V_{BD} increases with T:

At higher T carriers loose more to lattice
 → lower mobility, shorter mean free path (λ)
 → carriers need higher V to impact-ionize
 (temp. coefficient $\Delta V_{BD}/\Delta T \sim 20\text{mV/K} - 80\text{mV/K}$
 depending on doping concentration)



Haitz JAP 34 (1963)

Recovery time: τ_Q decreases with T

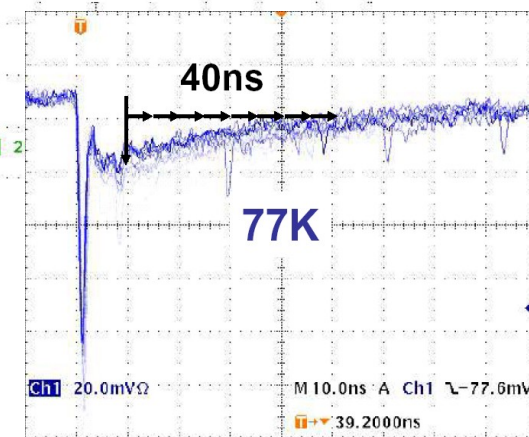
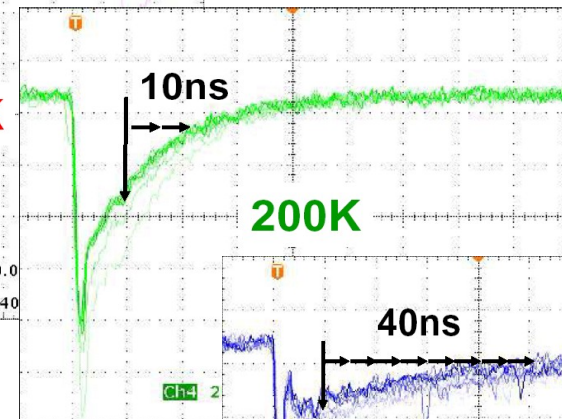
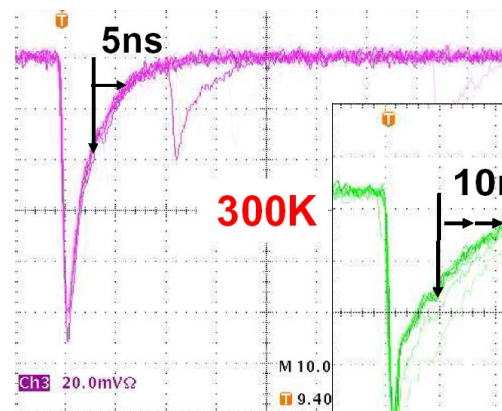
Due polysilicon R_Q properties

T (K)	R_Q (M Ω)
300	0.2
200	0.4
77	1.7

H.Otono - PD07
 Characterization
 of SiPM by HKP at low T

Cell Capacity does not vary with T

Gain independent of T
 at fixed Over-Voltage

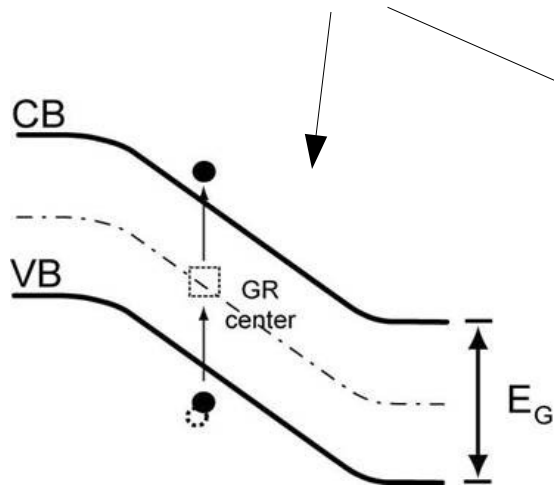


Waveform:

Two components, show
 different behavior
 (fast component is independent
 of T because stray C couple with
 external R independently of R_Q)

Dark count rate: free carrier generation

Two main mechanisms

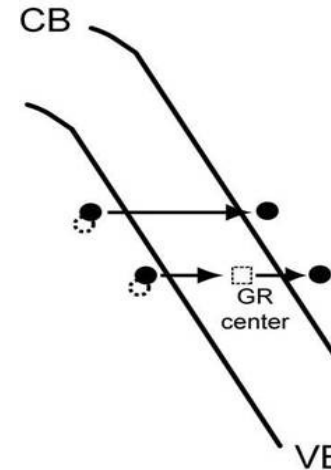


(1) Generation - Recombination Centers
SHR generation (Field Enhanced)
in the depletion region

$$\frac{dN_{\text{emiss}}}{dt} \equiv \frac{n_i}{2\tau_g}$$

n_i [1/cm³s] → intrinsic carrier concentration
 τ_g → minority carrier lifetime
 $\sim 1/N_{\text{generation centers}}$

(2) Field-Assisted Generation: **tunneling**
(trap-assisted and band to band)



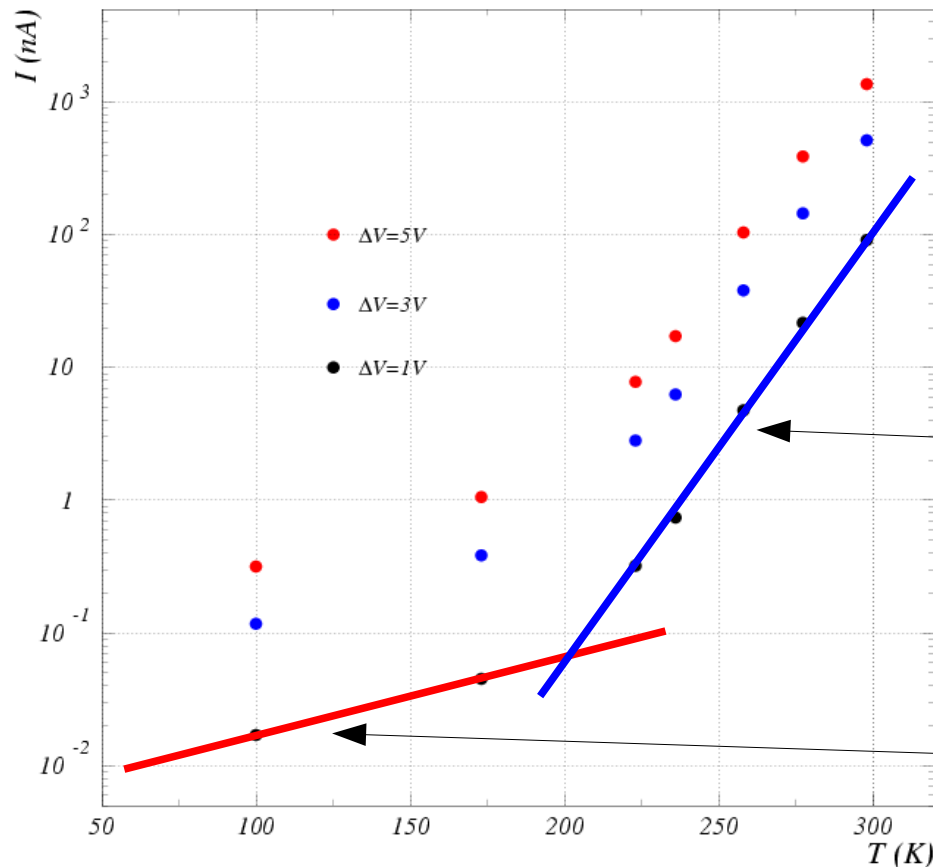
Example:

- effective volume $V_{\text{eff}} = A_{\text{eff}} \cdot W_{\text{depletion}}$
 $V_{\text{eff}} \sim 1\text{mm}^2 \cdot 50\% \cdot 4\mu\text{m}$
- $\tau_g \sim 10\text{ms}$ (good quality technology)
- Prob. to trigger avalanche P_{01}
 $P_{01}^e \sim 100\%$ for electrons
 $P_{01}^h \sim 1/2$ $P_{01}^e \sim 50\%$ for holes

→ Dark rate $\sim V_{\text{eff}} P_{01} / \tau_g \sim 2\text{MHz}$ (n+/p: **e trigger** the avalanche in depl. region)
 $\sim 1\text{MHz}$ (p+/n: h trigger the avalanche in depl. region)

T dependence: Dark Current

Data (IRST devices)
(fixed over-voltage)



Dark rate sources:

1. Diffusion

I_{reverse} by minority carriers: negligible at room T

2. SHR (Field Enhanced)

Rule of thumb: factor $\times 2/8k$ (at fixed Over-voltage)
Dominates at room T

$$I_{\text{reverse}} \propto T^2 \exp \frac{-E_g}{2K_B T}$$

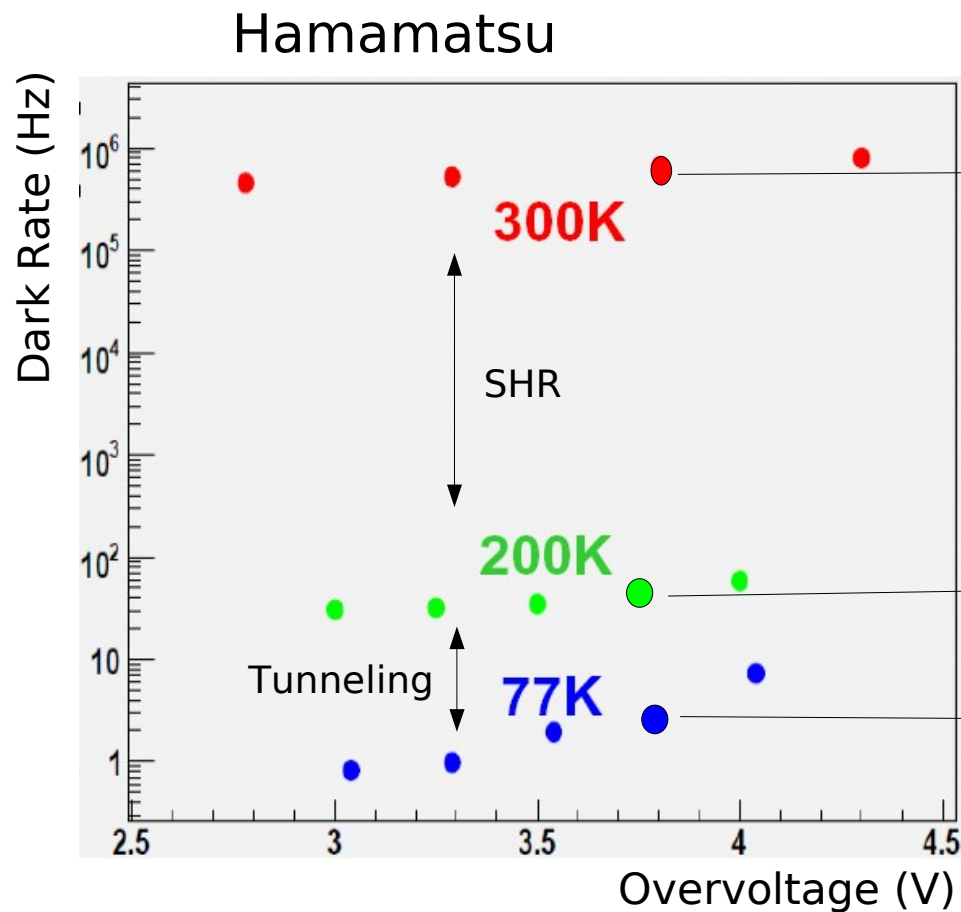
3. Band to band Tunnel

Strong dependence on the Electric field profile
May dominate at low T

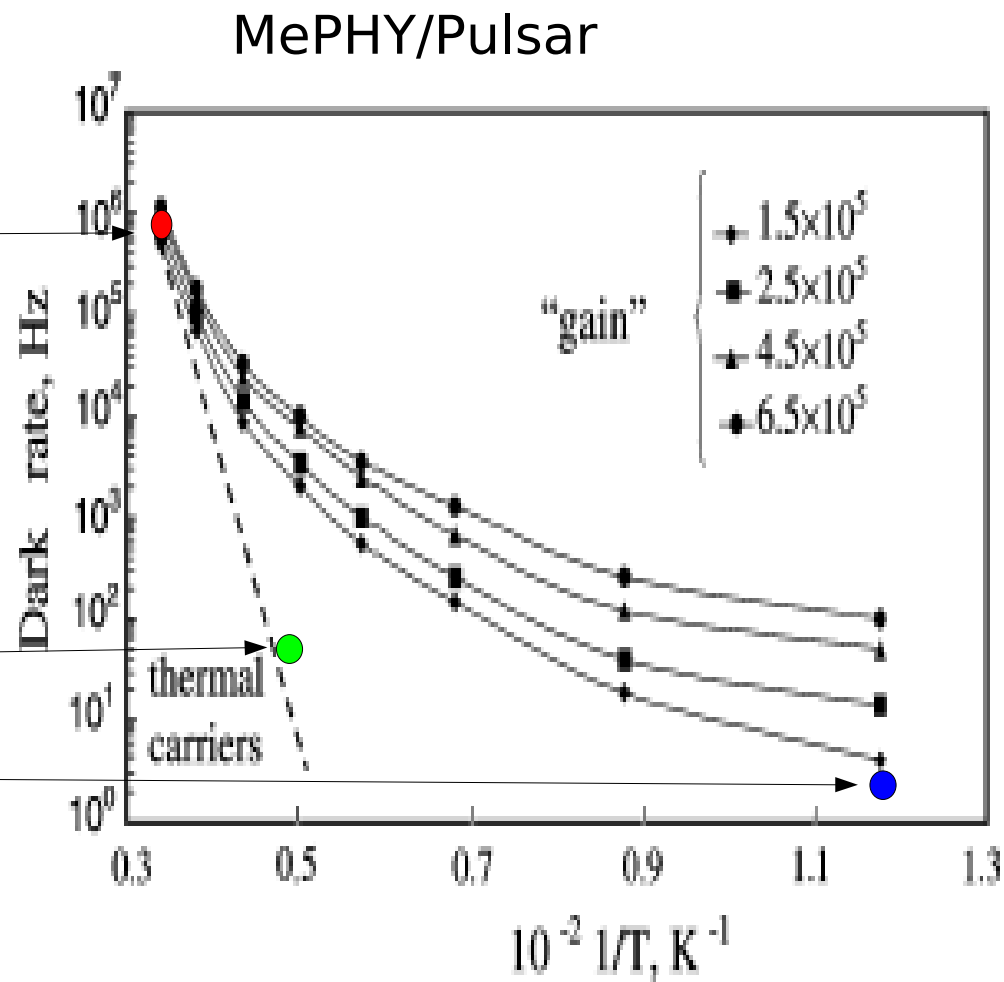
G.Collazuol (unpublished)

Acknowledgments: A.Baldini, A.Brez – INFN Pisa

T dependence: Dark Rate



H.Otono - PD07

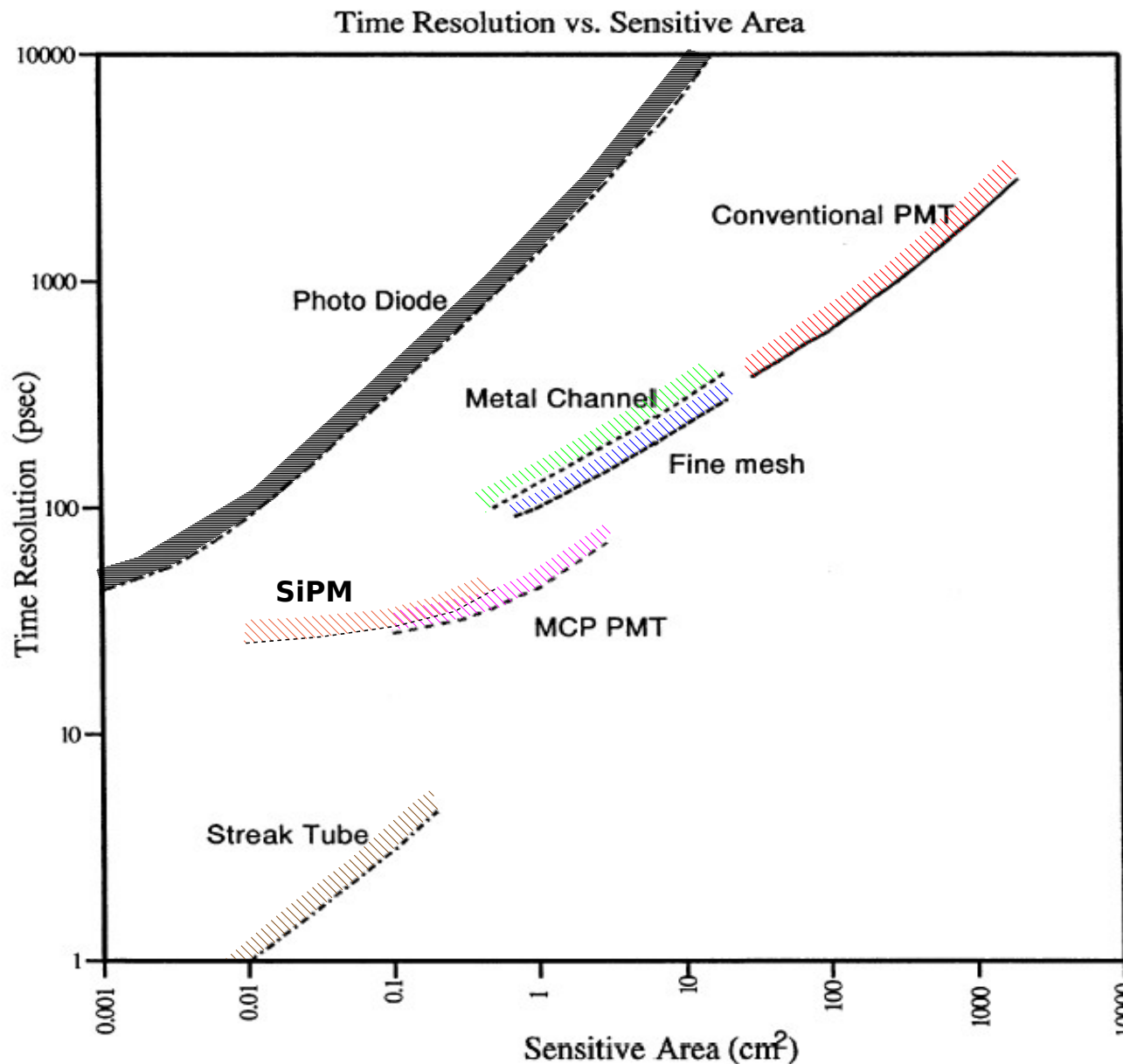


Dolgoshein et al, NIM A 442 (2000)

Electric field engineering and silicon quality
make huge differences in dark noise as a function of T

Spares

Timing resolution of photo-detectors



Note **resolution** improves:

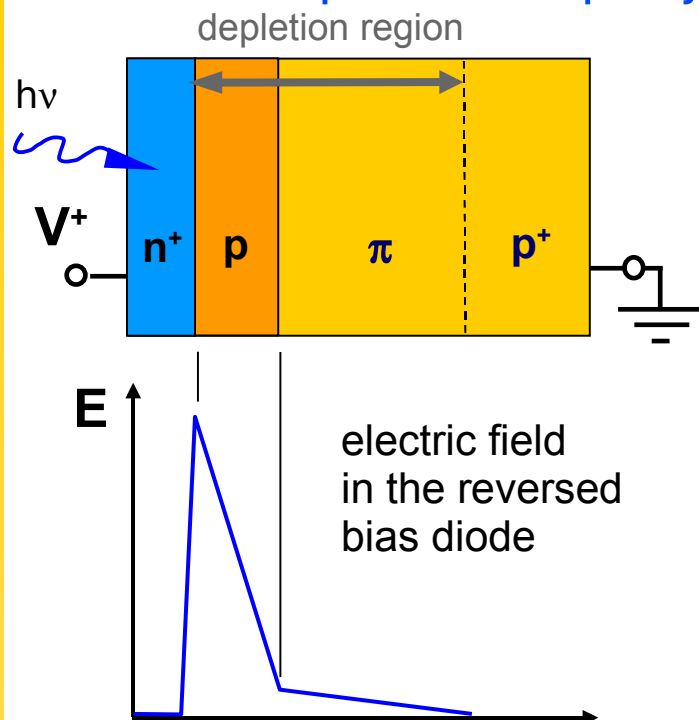
- by decreasing **active area**
- by decreasing the intrinsic
- **detector capacitance**
- as $\sigma_t/t \sim 1/\sqrt{Npe} \sim 1/\sqrt{QE}$

Note **tails** matter:

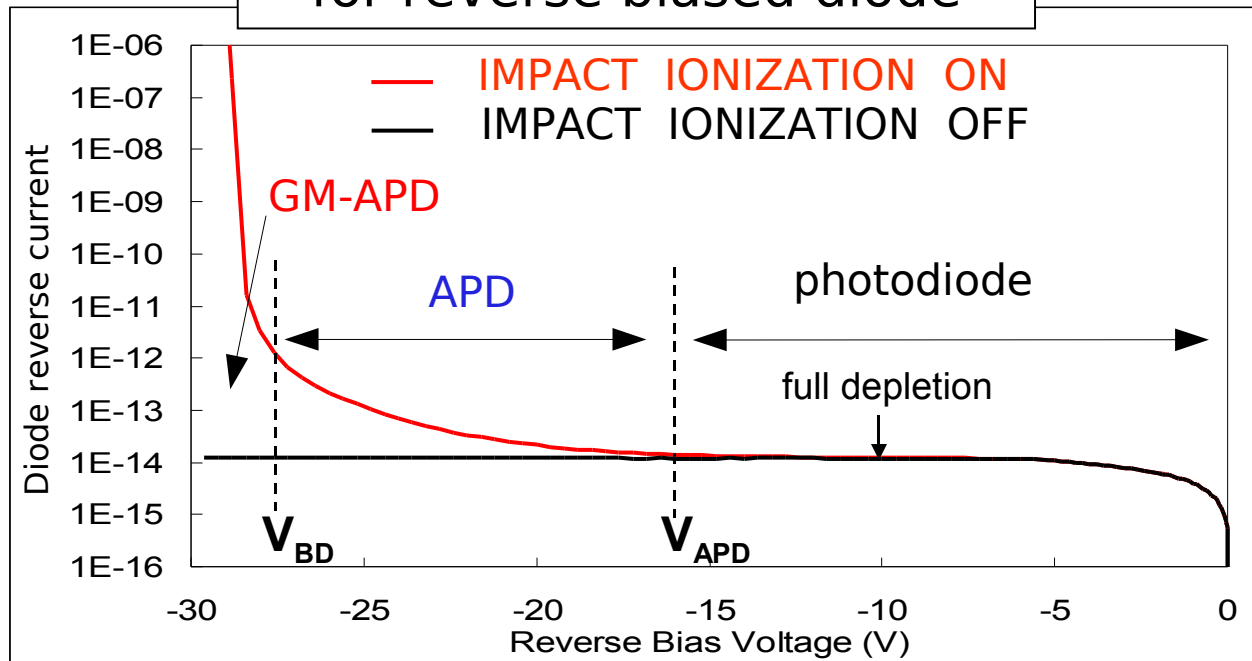
- MCP
- APD < 2ns at $1/10^5$ (best)
- SiPM < 1ns at $1/10^2$ (only large λ)

The building block of a SiPM: GM-APD

Reverse polarized p-n junction



Different working regimes for reverse biased diode



APD: Linear-Proportional Mode

- Bias **BELOW** V_{BD} ($V_{APD} < V < V_{BD}$)
- It's an **AMPLIFIER**
- Gain: limited < 1000 due to fluctuations
- Strong dependence on T and V_{bias}
- No single photo-electron resolution

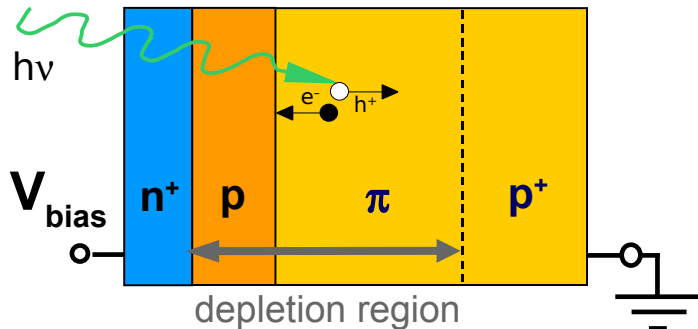
GM-APD: Geiger Mode

- Bias **ABOVE** V_{BD} ($V - V_{BD} \sim$ a few volts)
- It's a **TRIGGER** (BINARY) device
- Gain: $\rightarrow \infty$
- Limited by dark count rate
- Single photo-electron resolution

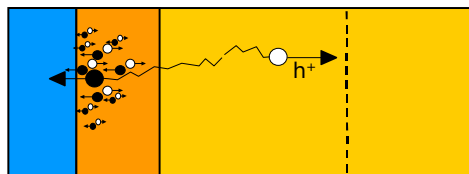
Operation principle of a GM-APD

Diode Biased ABOVE V_{BD}

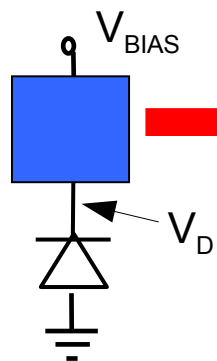
- $t=0$: carrier initiate the avalanche



- $0 < t < t_1$: avalanche spreading



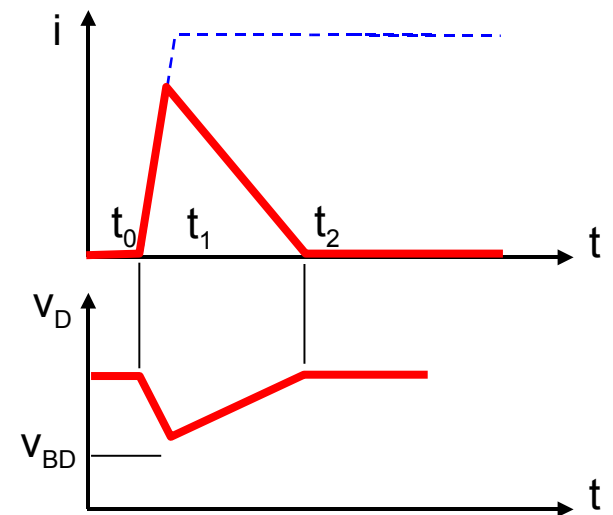
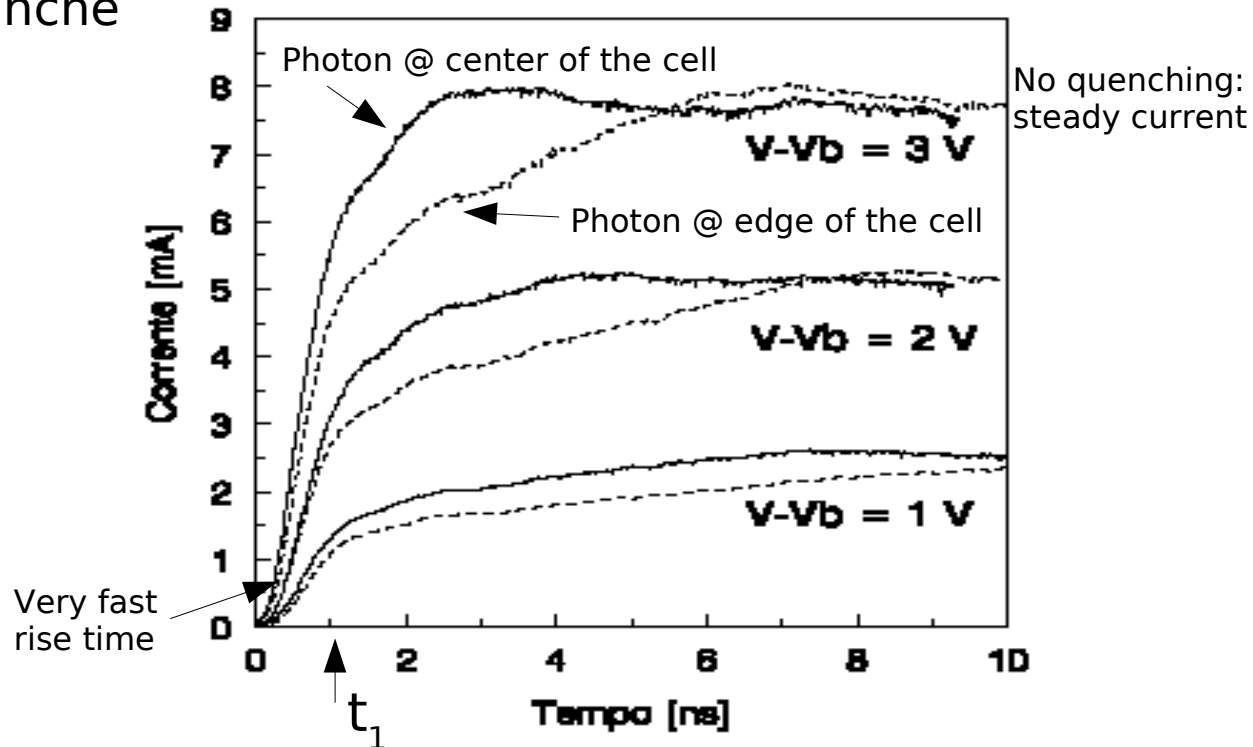
- $t_1 < t$: self-sustaining current (limited by series resistances)



To detect another photon need a **quenching mechanism**. Two solutions:

- large resistance: **passive quenching**
- analog circuit: **active quenching**

A. Spinelli Ph.D thesis (1996)



Electrical model of a GM-APD

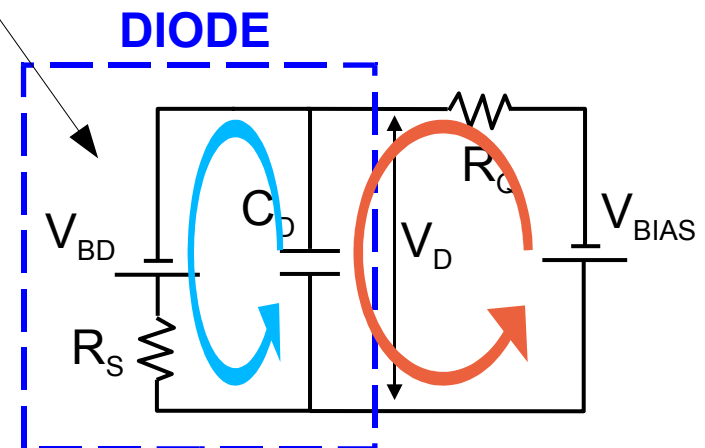
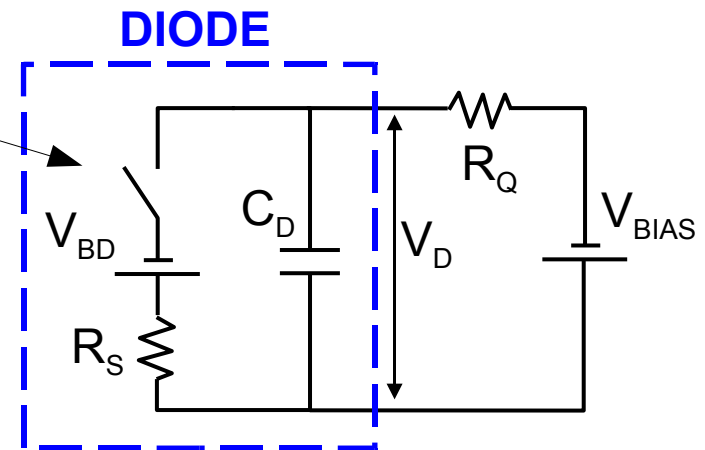
Passive quenching studied in detail in the '60 to model micro-plasma instabilities [McIntyre JAP 32 \(1961\)](#), [Haitz JAP 35 \(1964\)](#)

The Geiger-Mode APD can be modeled with an electrical circuit and two probabilities:

- Switch OFF = micro-plasma non-conducting
- Switch ON = micro-plasma conducting

- C_d diode capacitance (some 10fF)
- R_s series resistance ($\sim 1k\Omega$)
- R_q quenching resistance ($> 300k\Omega$)
- $V_{bd} < V_{bias}$ (few % relative)

- P_{01} turn-ON
Probability that a carrier traversing the high field region **trigger an avalanche**
- P_{10} turn-OFF
Probability that number of carriers in the high field region fluctuates to 0



Internal/external currents

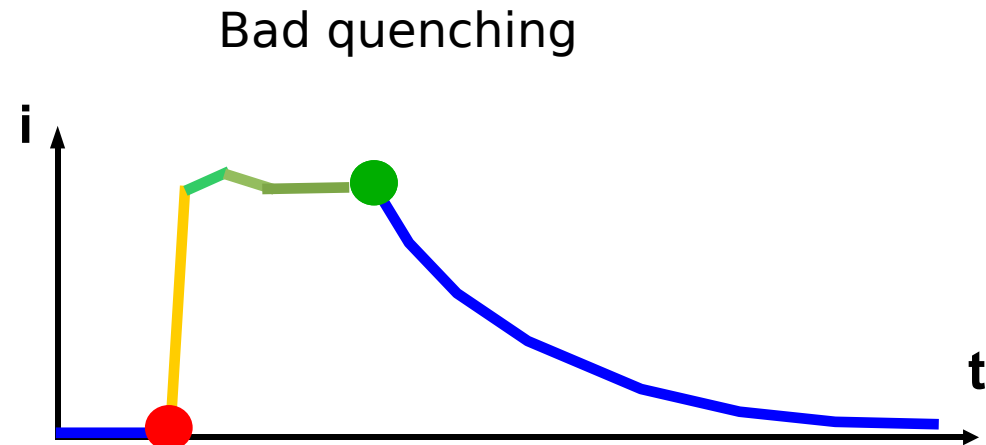
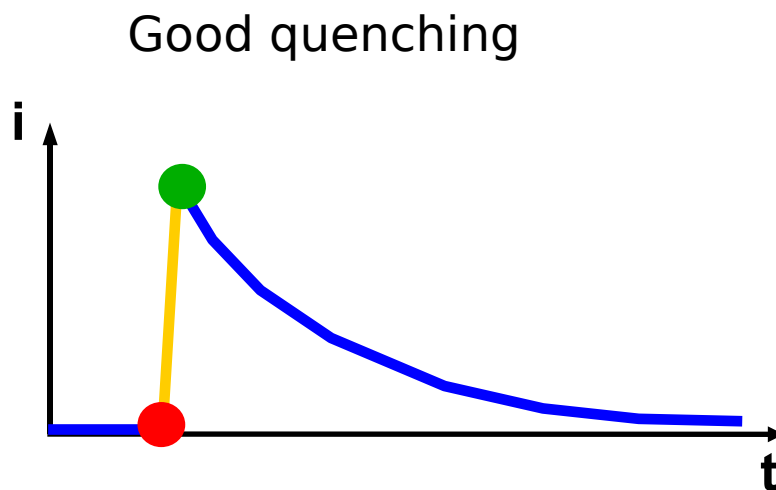
Operation principle of a GM-APD

In GM-APD the detection of a photon essentially triggers the full **discharge of a condenser** !

Gain = charge on the condenser / electron charge.

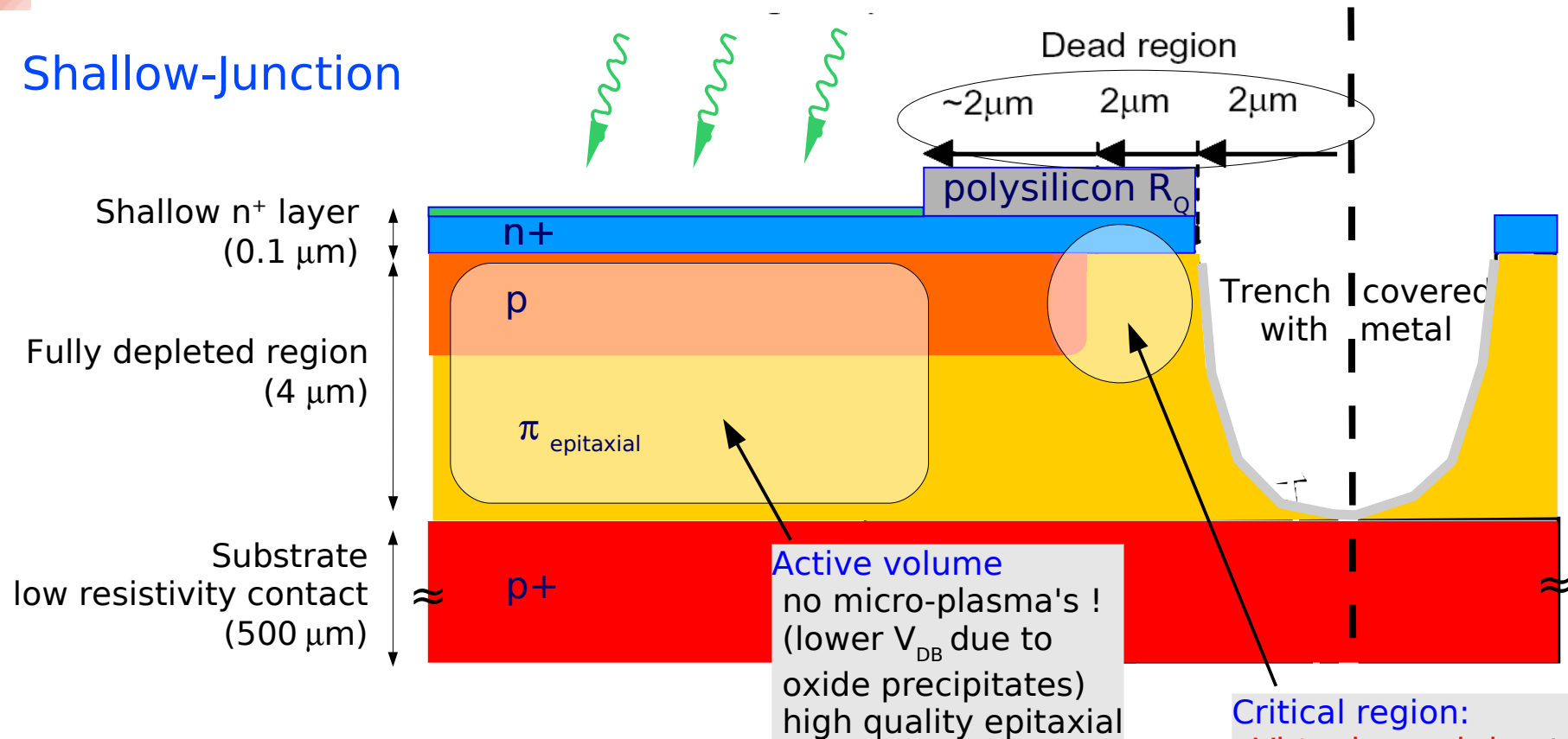
The **Gain fluctuations in GM-APD are very small** and different in nature compared to APD where the statistical process of internal amplification shows peculiar fluctuations (multiplication noise)

Note: effective quenching (R_Q) is crucial to have a well defined gain



Close up of a cell (IRST technology)

Shallow-Junction



Optimization for the blue light (420nm)

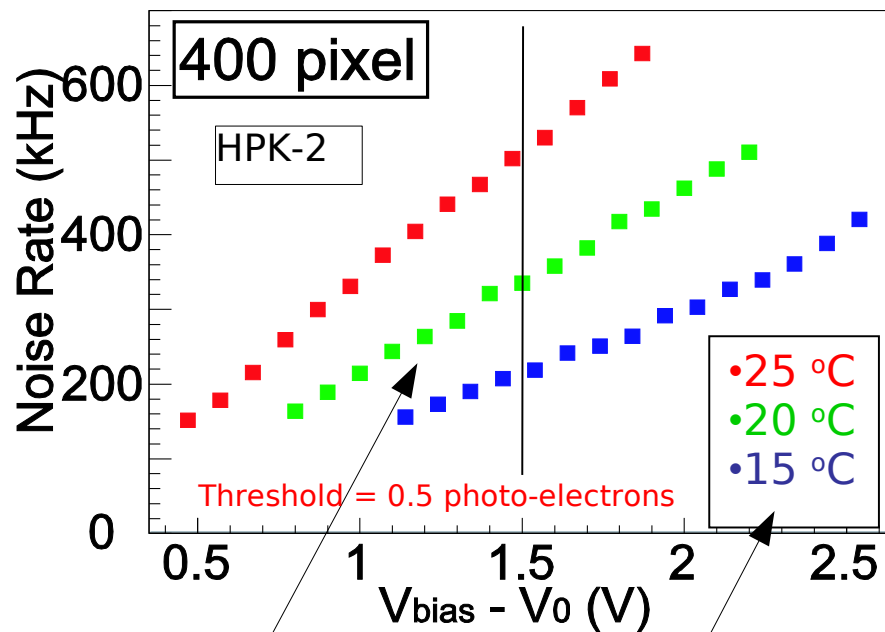
- n^+ on p abrupt junction structure
- Anti-reflective coating (ARC) optimized for $\lambda \sim 420\text{nm}$
- Very thin (100nm) n^+ layer: "low" doping n^+ layer
→ minimize Auger and SHR recombination
- Thin high-field region: "high" doping p layer (limited by tunneling breakdown)
→ fixes V_{BD} junction well below V_{BD} at edge
- R_Q by doped polysilicon
- Trenches for optical insulation (low cross-talk)
- Fill factor: 20% - 80%

Dark count rate

Critical issues: • quality of epitaxial layer
• gettering techniques

Hamamatsu device (1mm²)

S.Uozumi - Vienna VCI 2007



NOTE:
T dependence

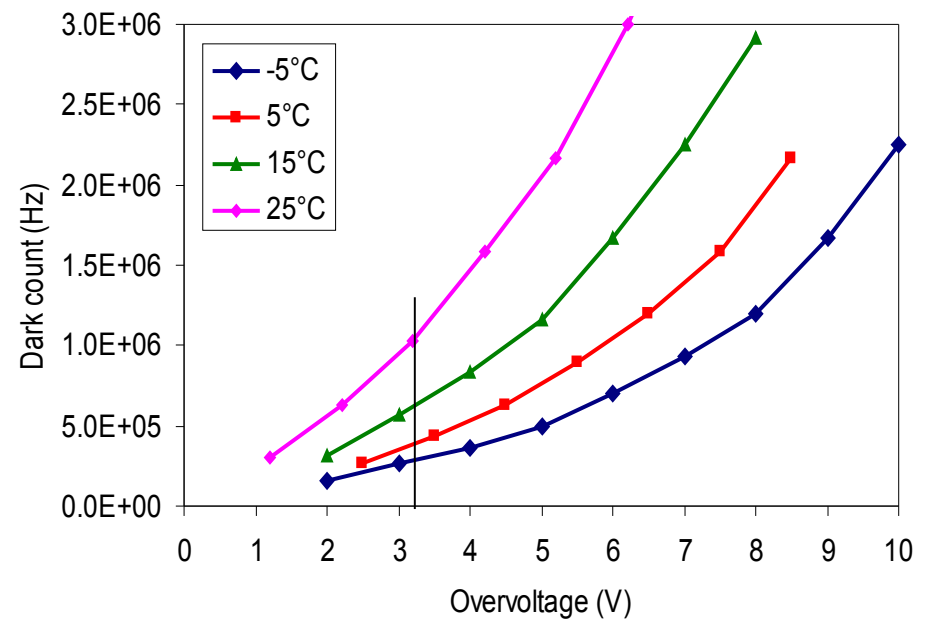
NOTE:

~ linear dependence due to $P_{01} \propto \Delta V$

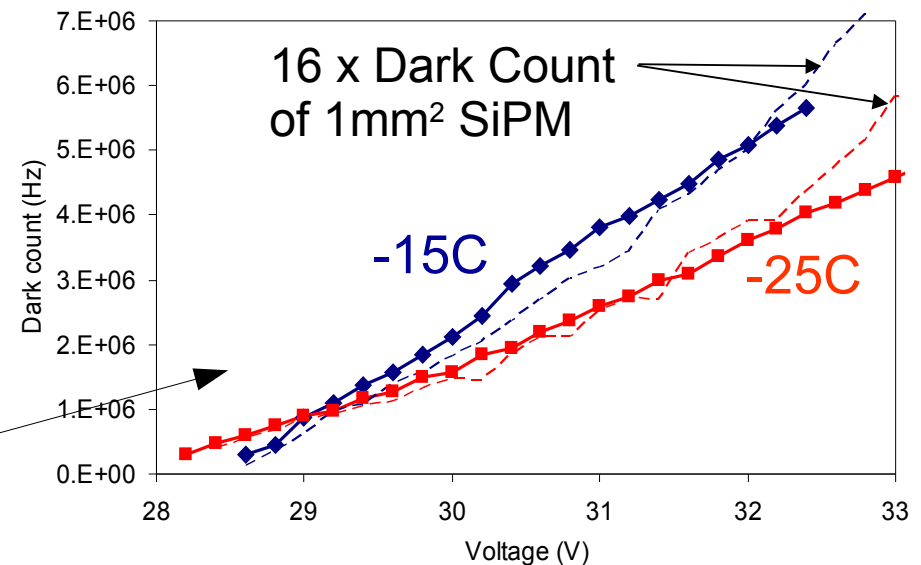
~ scales with active surface

~ non-linear at high ΔV due to additional rate from cross-talk ($\propto \Delta V^2$)

IRST device (1x1 mm²)



IRST device (4x4 mm²)



Detector performances

related to the recharge of the diode capacitance from V_{BD} to V_{bias} during the avalanche quenching time after I_{latch} is reached.

$$G = (V_{BIAS} - V_{BD}) * C_D / q$$

valid for few volts above V_{BD}

Gain

pulses triggered by non-photogenerated carriers (thermal / tunneling generation in the bulk or in the surface depleted region around the junction)

carriers can be trapped during an avalanche and then released triggering another avalanche

Noise: dark count
afterpulse
optical cross-talk

photo-generation during the avalanche discharge. Some of the photons can be absorbed in the adjacent cell possibly triggering new discharges

$$PDE = QE * P_{01} * \epsilon$$

QE = quantum efficiency
 P_{01} = avalanche triggering prob.
 ϵ = geometrical fill factor

Photo-detection efficiency

Related to the density of cells and recovery time

Dynamic Range

Related to the photogeneration and to the avalanche propagation

Time resolution

Photo-detection efficiency (PDE)

$$\text{PDE} = N_{\text{pulses}} / N_{\text{photons}} = \text{QE} \cdot P_{01} \cdot \varepsilon_{\text{geom}}$$

Carrier Photo-generation

(QE = probability for a photon to generate a carrier that reaches the high field region)

*

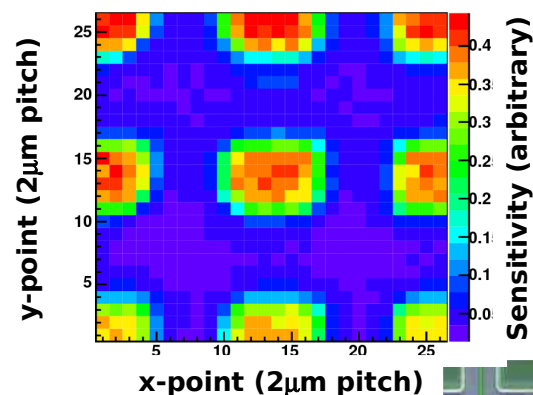
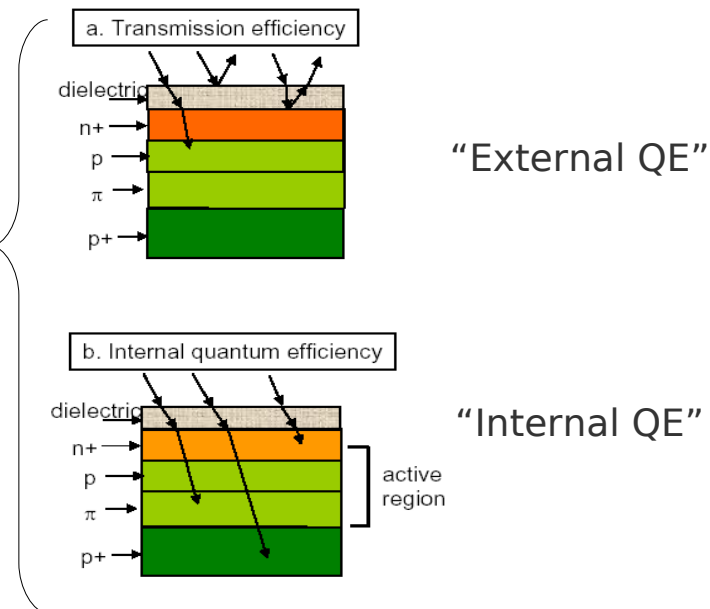
Avalanche triggering

(P_{01} = probability for a carrier traversing the high-field to generate the avalanche)

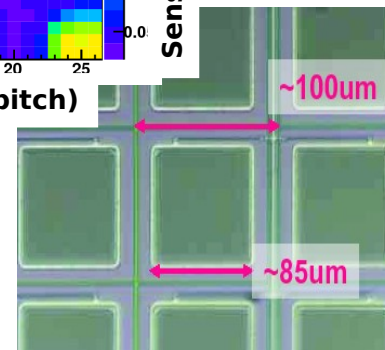
*

Geometrical fill factor

(ε = fraction of dead area due to structures between the cells, eg. guard rings, trenches)



Hamamatsu
SiPM close up



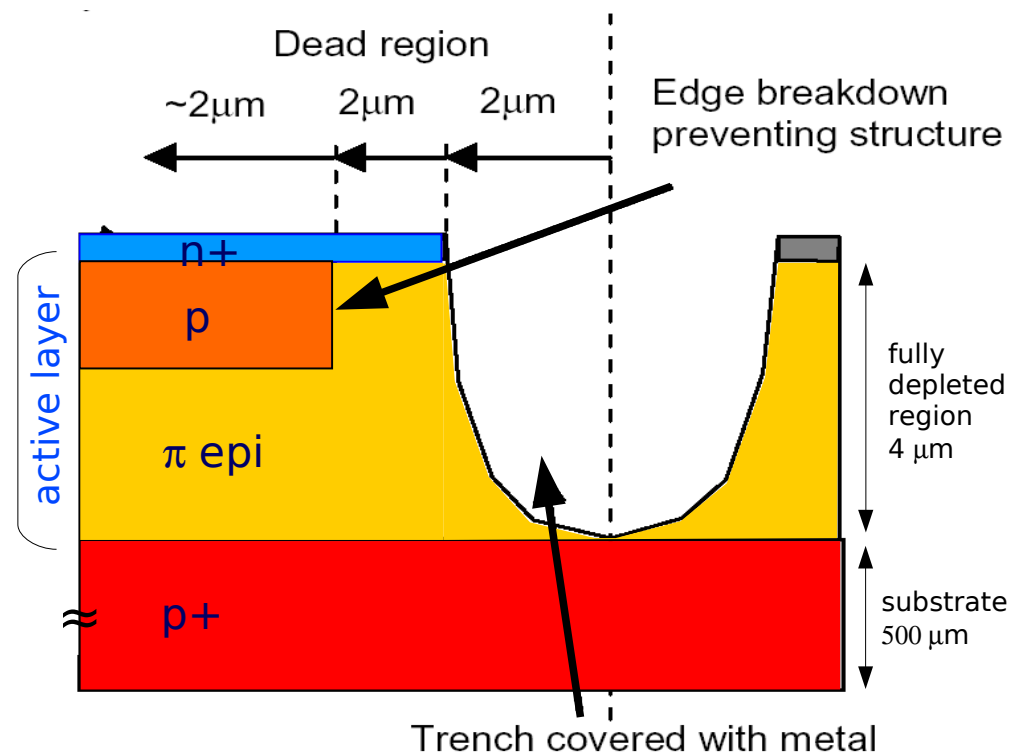
QE: Efficiency of a single cell

Two factors in QE:

- (1) **transmittance** of the entrance window (dielectric on top of silicon surface)
- (2) probability of a photon inside to generate a e-h pair in the **active layer** (internal quantum efficiency)

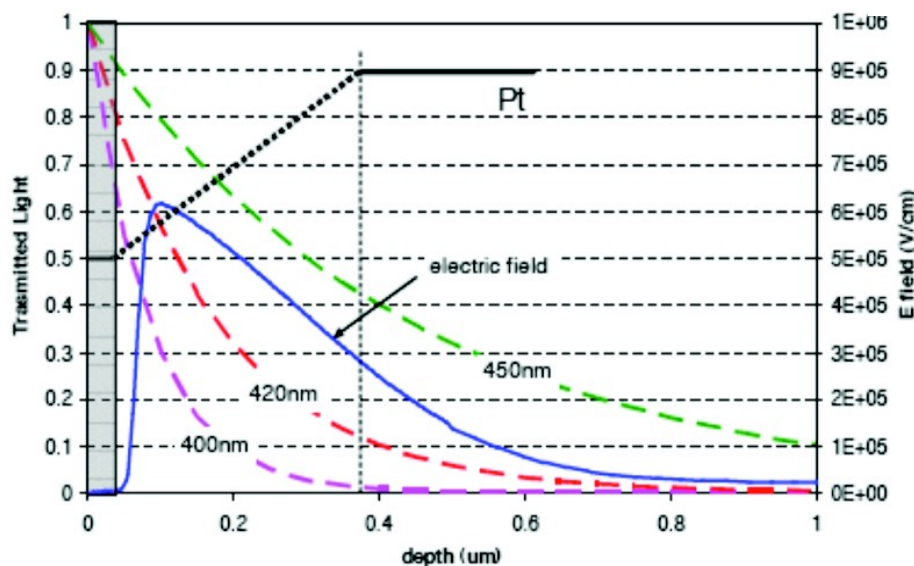
Only the depleted region is fully active to efficiently photo-generate because of high recombination probability in the un-depleted regions.

Only a small layer ($\lambda_{\text{diffusion}} \sim \sqrt{D\tau_{\text{recomb}}}$) at the edge of un-depleted regions contributes to the photo-generation (critical for UV light)



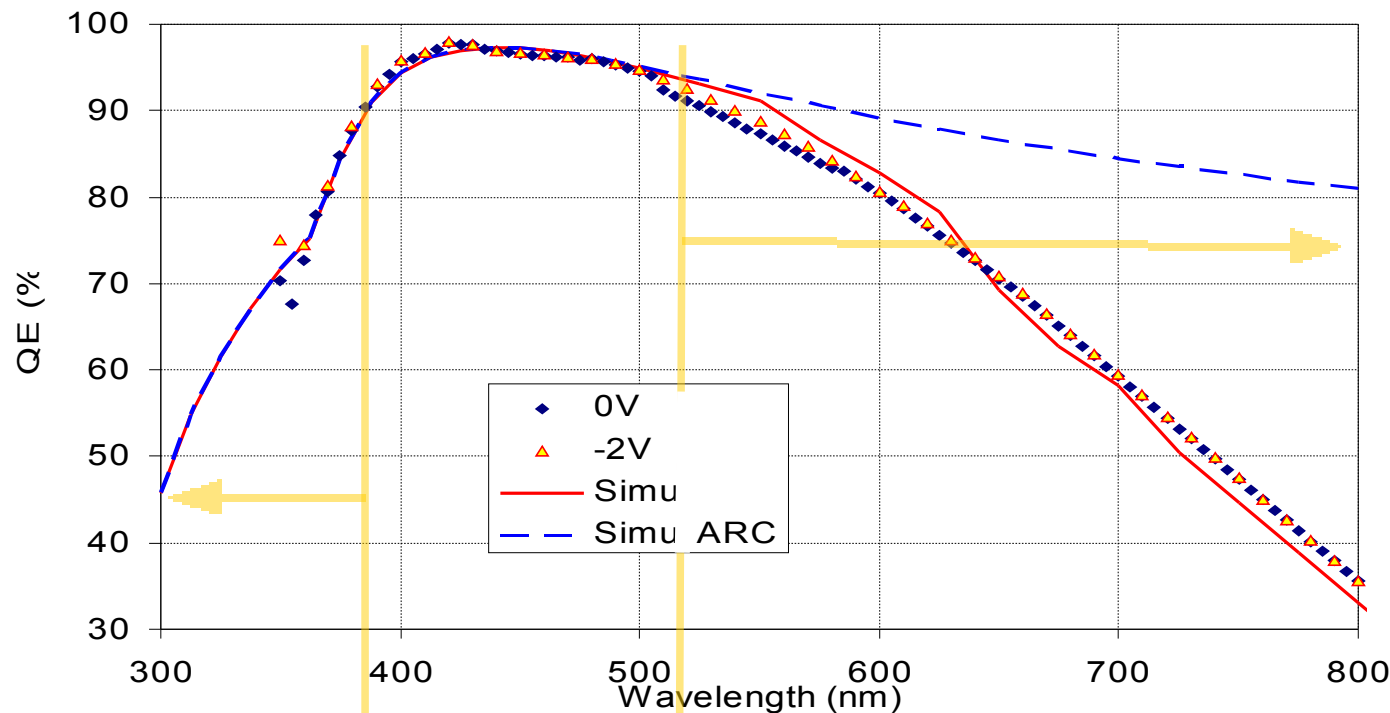
QE optimization

- Anti-reflective coating (ARC)
- Shallow junctions for short λ
- Thick epi layers for long λ



QE: Efficiency of a single cell

Direct access to **internal QE** and **transmittance through ARC** by measuring photo-voltaic regime ($V_{\text{bias}} \sim 0 \text{ V}$)
the photon detection efficiency of a
diode with the same n^+/p junction structure and same ARC

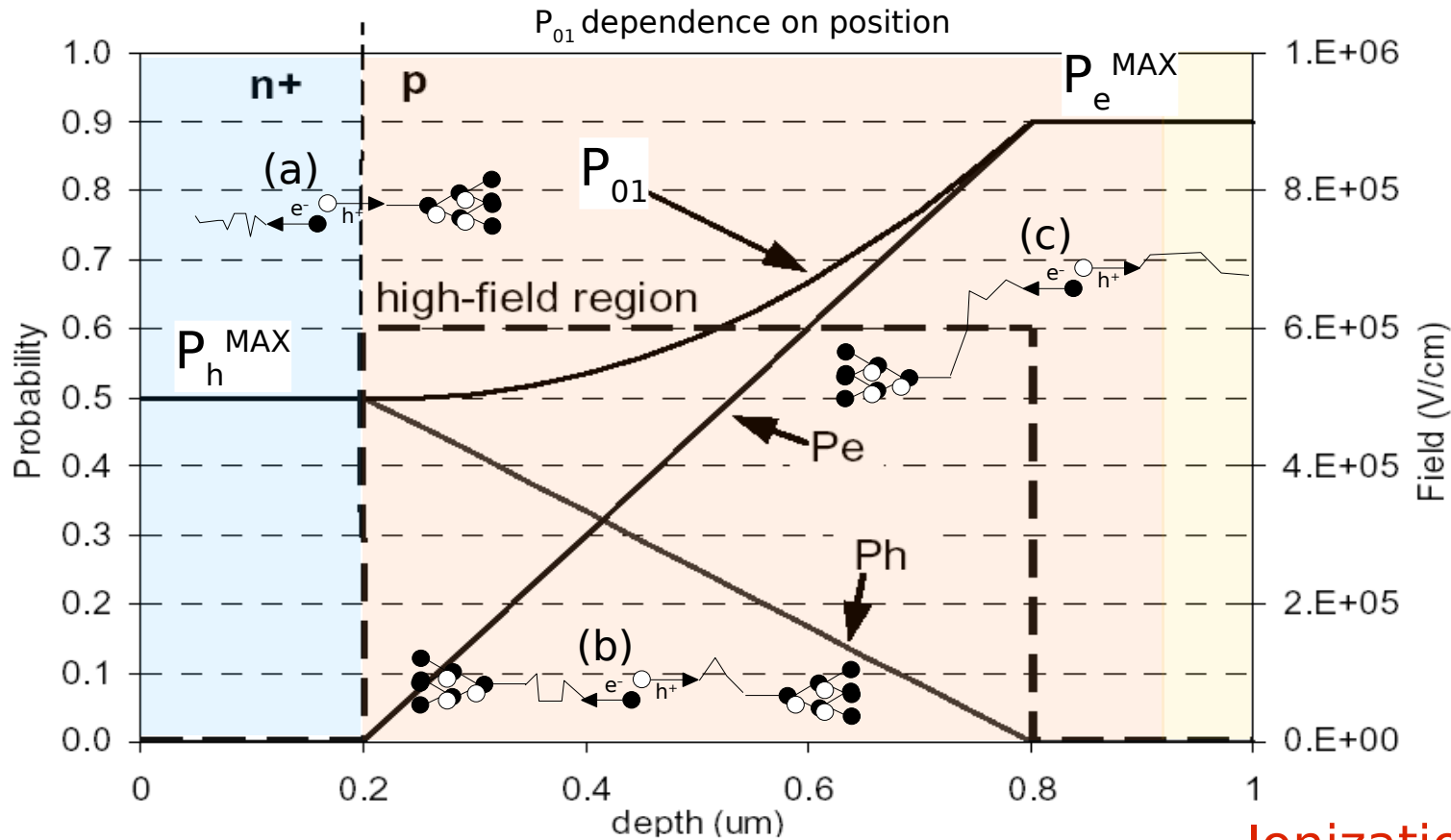


Reduced by
ARC Transmittance

Reduced by the
small π layer thickness

Avalanche trigger probability (P_{01})

C. Piemonte
NIM A 568
(2006) 224

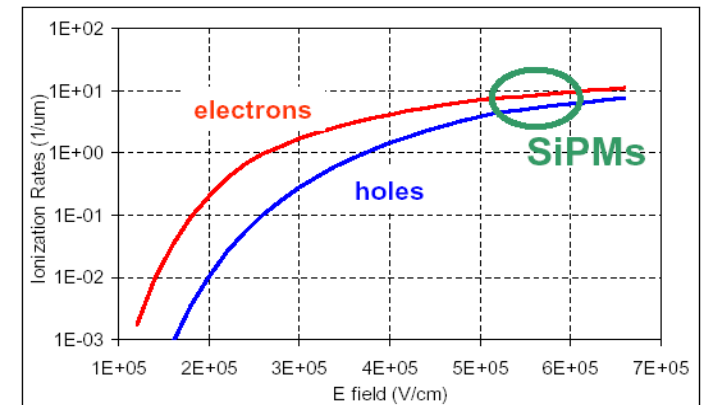


Example with constant high-field:

- (a) **only holes** may trigger the avalanche
- (b) **both electrons and holes** may trigger (but in a fraction of the high-field region)
- (c) **only electrons** may trigger

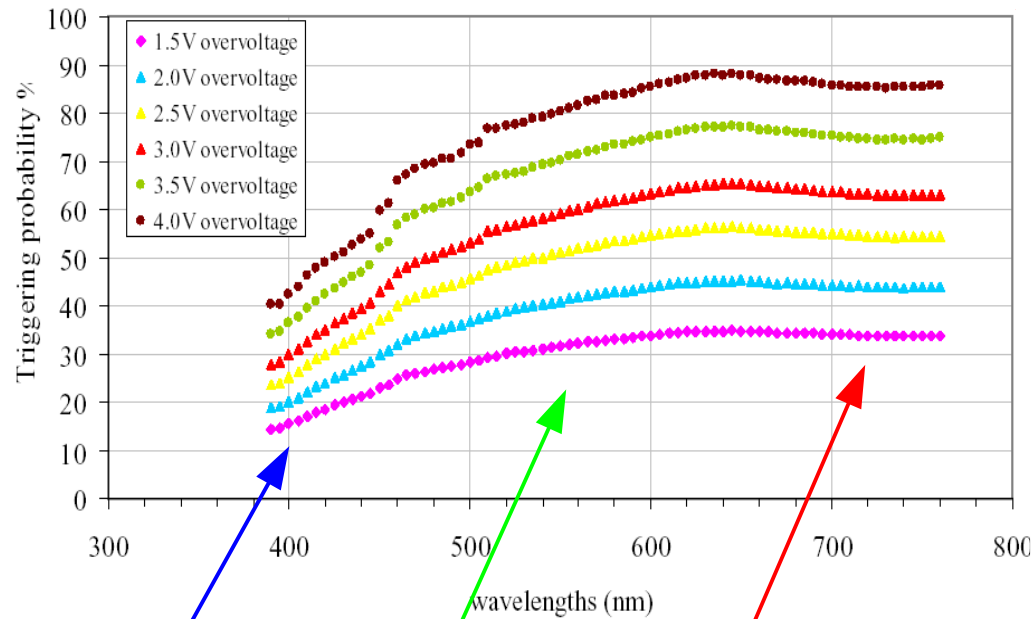
- high over-voltage
 - photo-generation in the p-side of the junction
- P_{01} optimization ←

Ionization rate in Silicon



Avalanche trigger probability (P_{01})

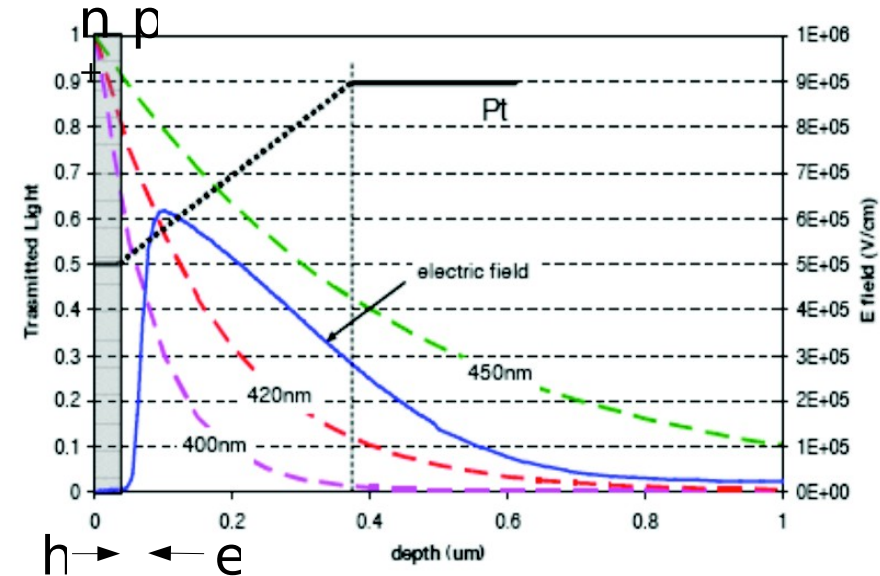
$$P_{01} = \text{PDE} / \text{QE} / \epsilon_{\text{geom.}}$$



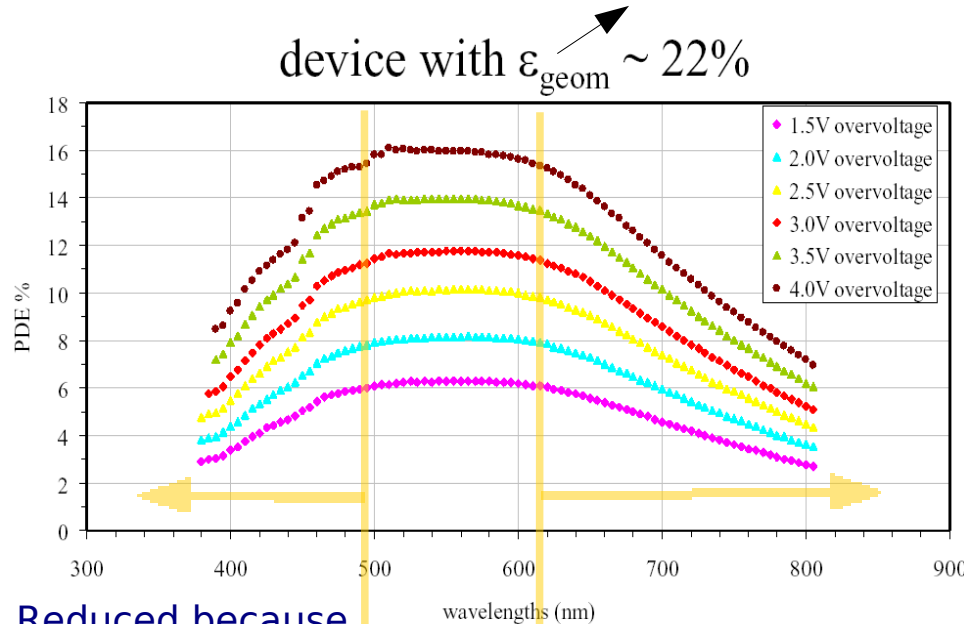
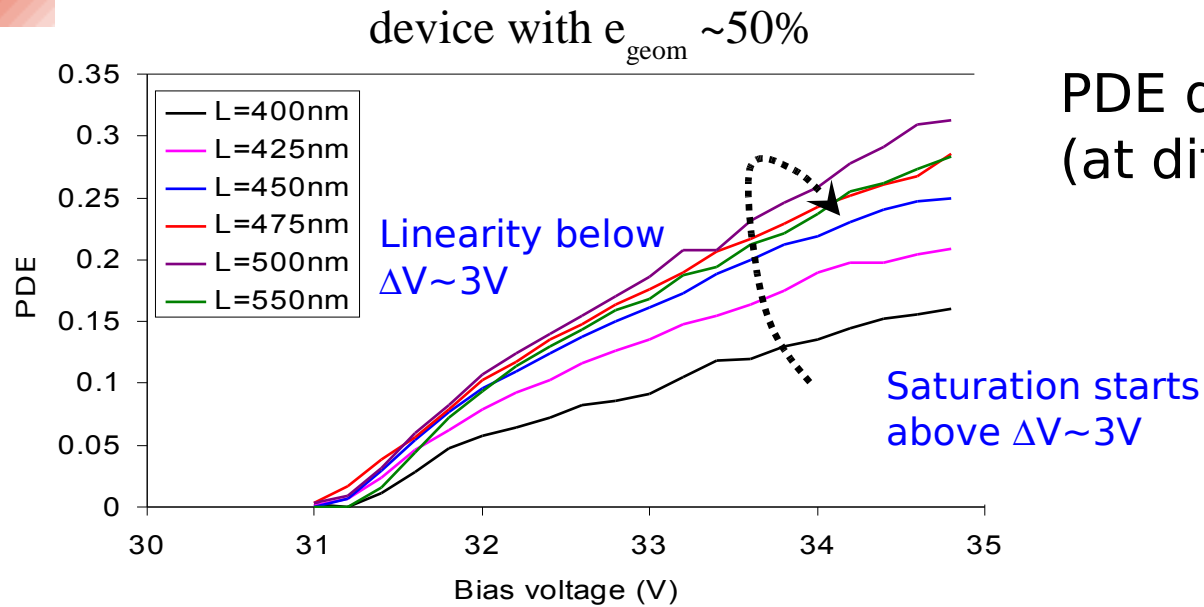
Only e^- cross the high E field region and trigger the avalanche

Both h^+ and e^- might trigger the avalanche (but cross only a fraction of high field region)

Only h^+ cross the high E field trigger the avalanche



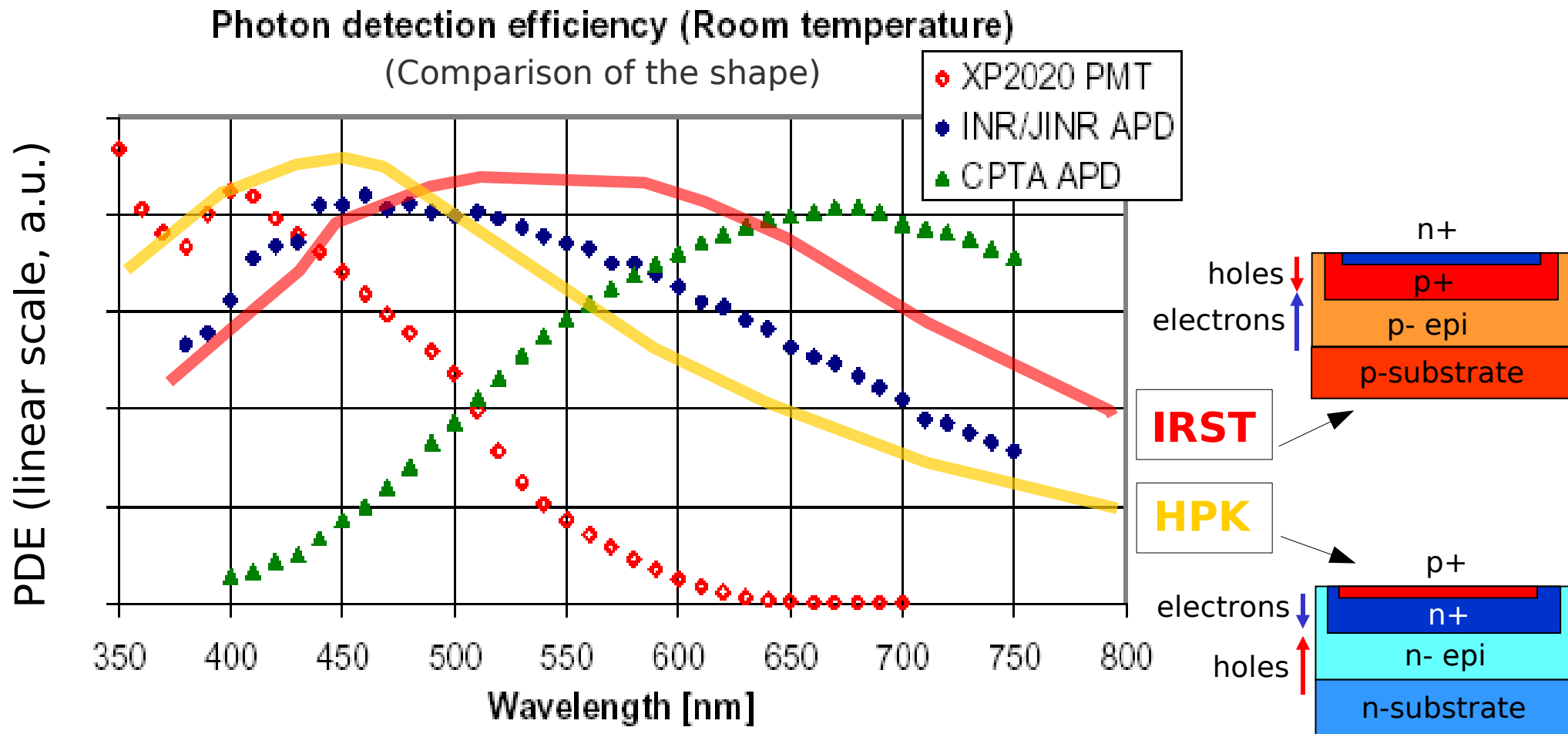
IRST devices – PDE vs over-voltage and λ



Reduced because
avalanche triggered
by holes (and ARC)

Reduced because
low QE

PDE VS wavelength shape: comparison



NOTE:

- The absolute scale (peak value) is set by fill factor (up to 70%) and over-voltage
- Obviously PDE shape is extremely dependent of the structure:
p-on-n (where essentially electrons trigger avalanches for short wavelengths) is naturally more blue sensitive than n-on-p (holes trigger avalanches for short wavelengths)
- The use of WLS on the surface (enhance PDE to short wl) degrades the timing resolution

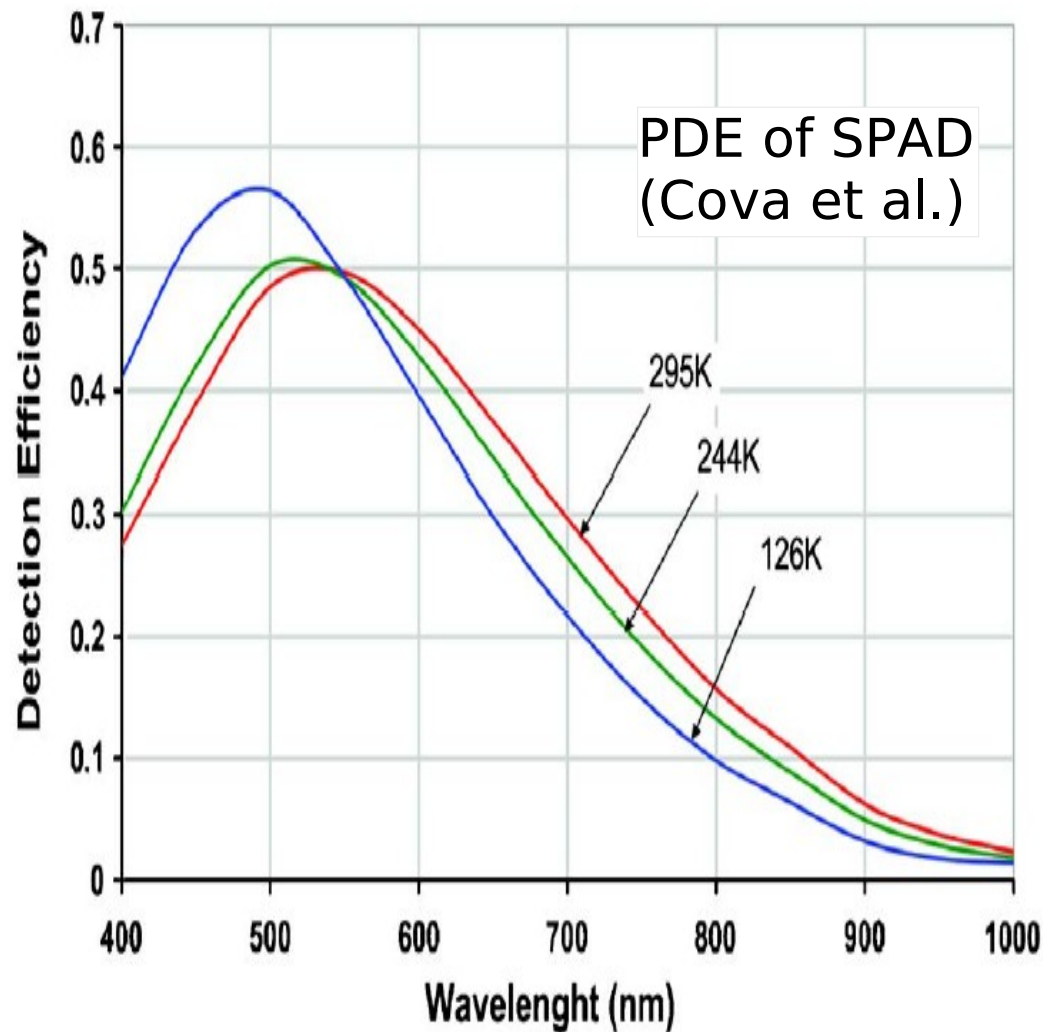
T dependence: PDE (SPAD devices)

PDE dependence on T (Over-voltage fixed)

Combination of two effects:

- P_{01} increases at low T
because of increased impact ioniz.
- Energy gap increases at low T

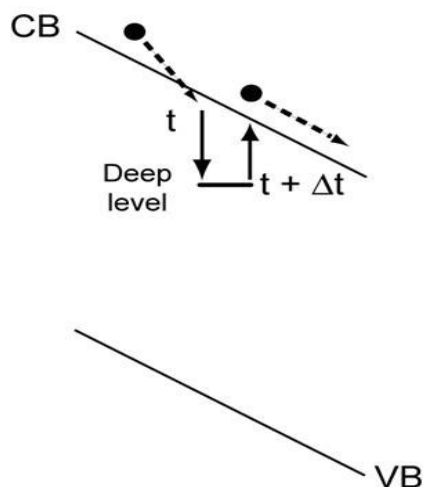
Similar effect expected also for SiPM



I.Rech et al, Rev.Sci.Instr. 78 (2007)

After-pulsing (delayed noise)

i.e. Carrier trapping and delayed release



$$P_{\text{after-pulse}}(t) = P_c \cdot \frac{\exp(-t/\tau)}{\tau} \cdot P_{01} \propto \Delta V^2$$

P_{01} : trigger probability

$\propto \Delta V(t)$ (over-voltage, recovery)

τ : trap lifetime

depends on trap level position

quadratic dependence on ΔV

P_c : trap capture probability

\propto carrier flux (current) during avalanche $\propto \Delta V$ (over-voltage)

$\propto N$ traps

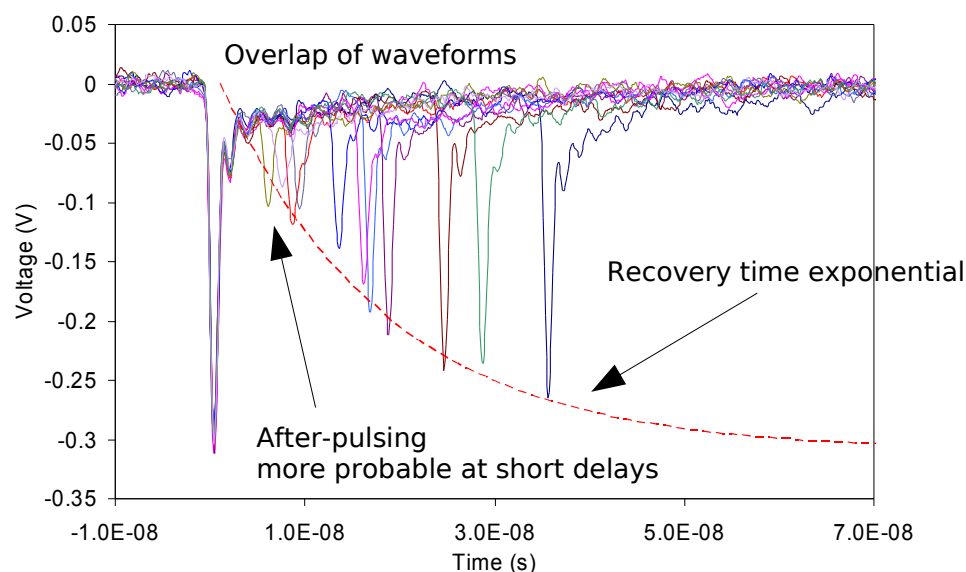
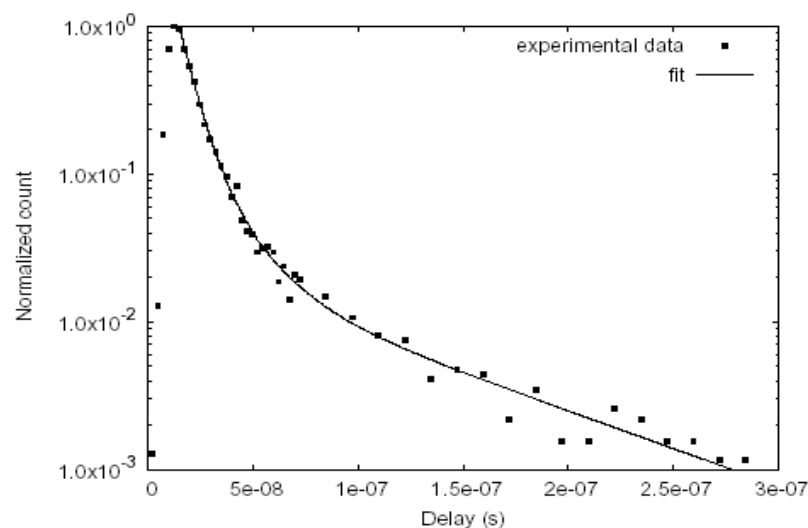


Fig. 10. Spectrum of the delay time from the primary pulse to the after-pulse.
C.Piemonte et al. IEEE TNS 54 (1) (2007) 236

It can be reduced to % in a wide ΔV range

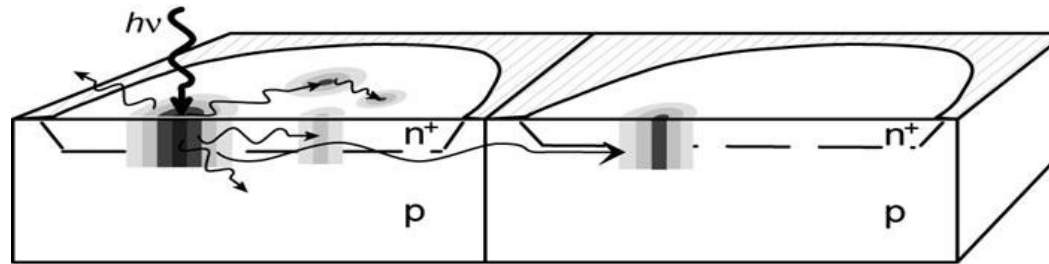
Optical cross-talk (excess noise)

Carrier luminescence (spontaneous direct relaxation in the conduction band) during the avalanche: probability $3 \cdot 10^{-5}$ per carrier (crossing the junction) to emit photons with $E > 1.14$ eV

A.Lacaita et al. IEEE TED (1993)

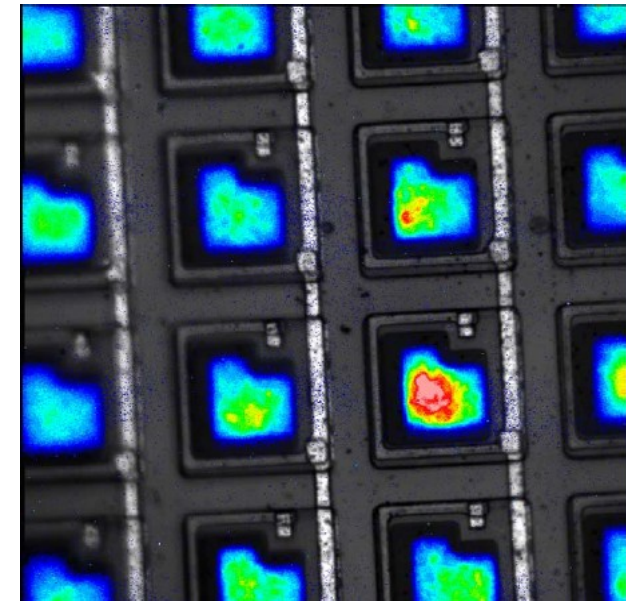
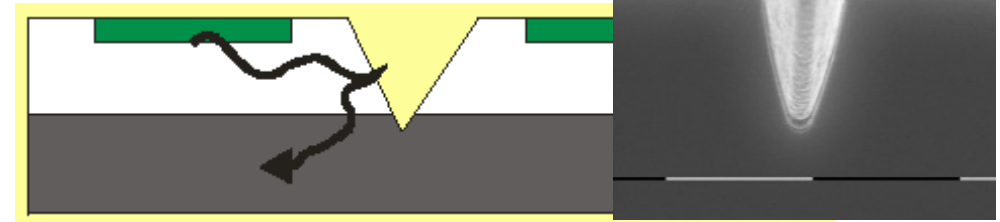
Photons can induce avalanches in neighboring cells.
Depends on distance between high-field regions
Quadratic dependence on over-voltage:

- carrier flux (current) during avalanche $\propto \Delta V$
- gain $\propto \Delta V$



Counteract:

- **optical isolation** between cells by trenches filled with opaque material
- low over-voltage operation helps



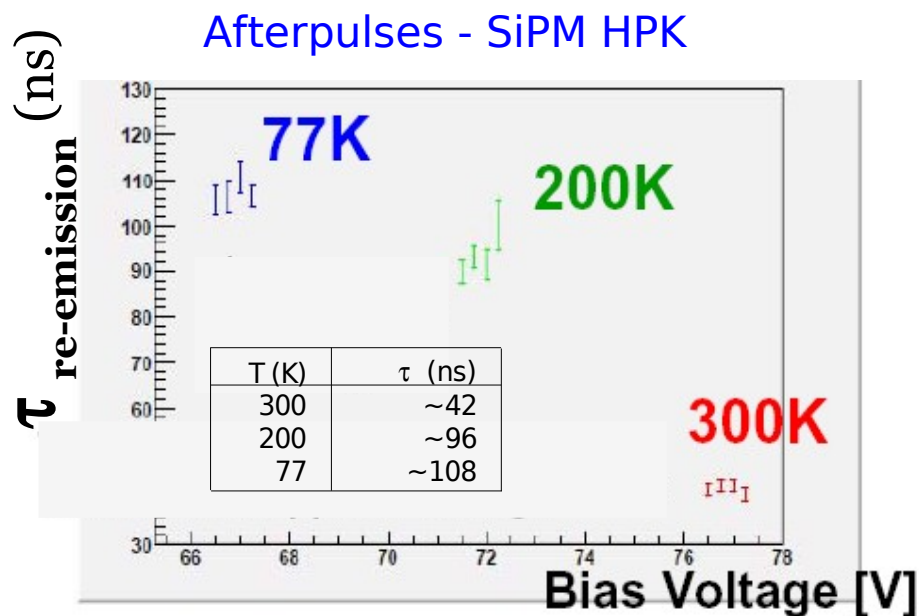
N.Otte, SNIC 2006

It can be reduced below % in a wide ΔV range

T dependence: after-pulsing, cross-talk

After-pulses: increases at low T

Trap lifetime decreases as T increases

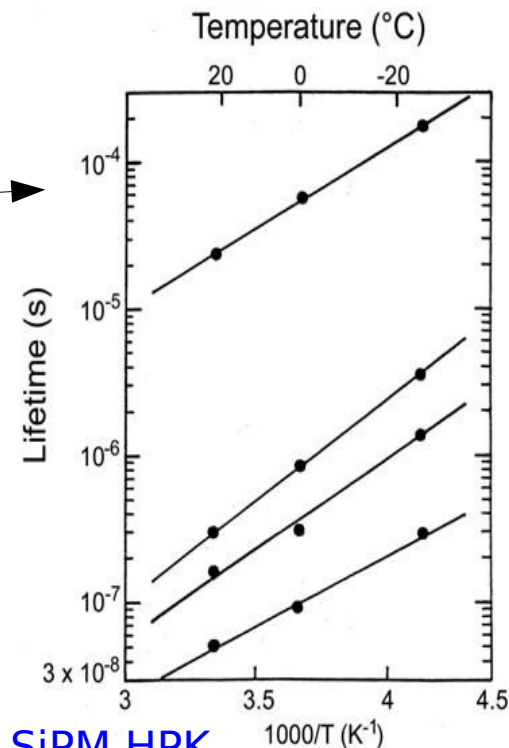


H.Otono - PD07 28 June 2007

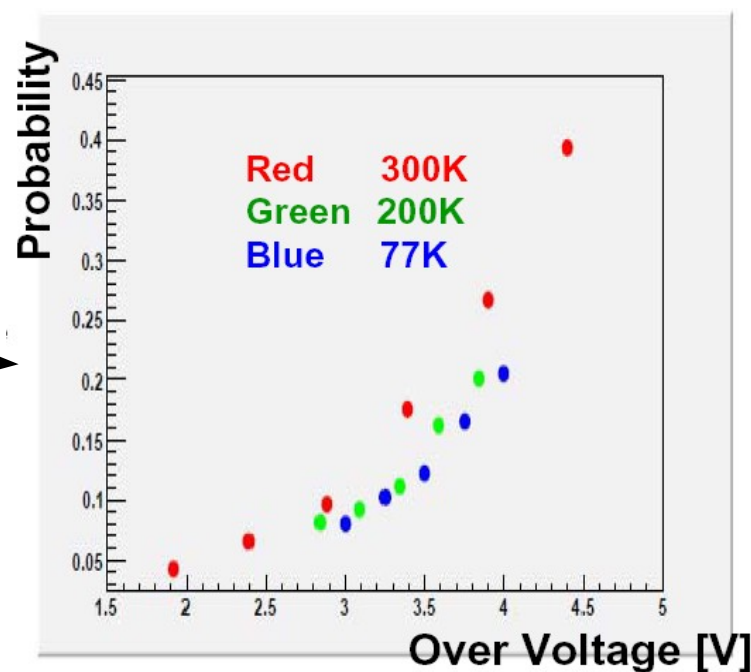
Cross-talk: decreases at low T

Observed slight reduction at low T

(due to lower PDE for long wavelength photons which dominate the carrier luminescence spectrum)

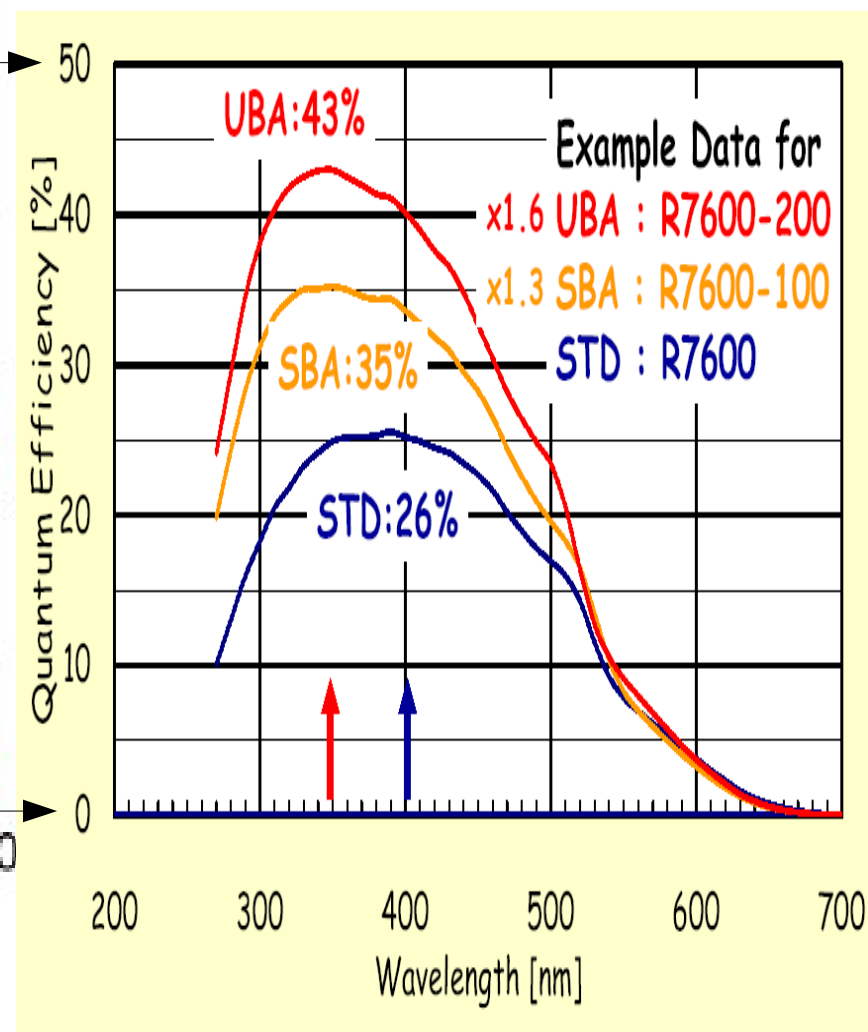
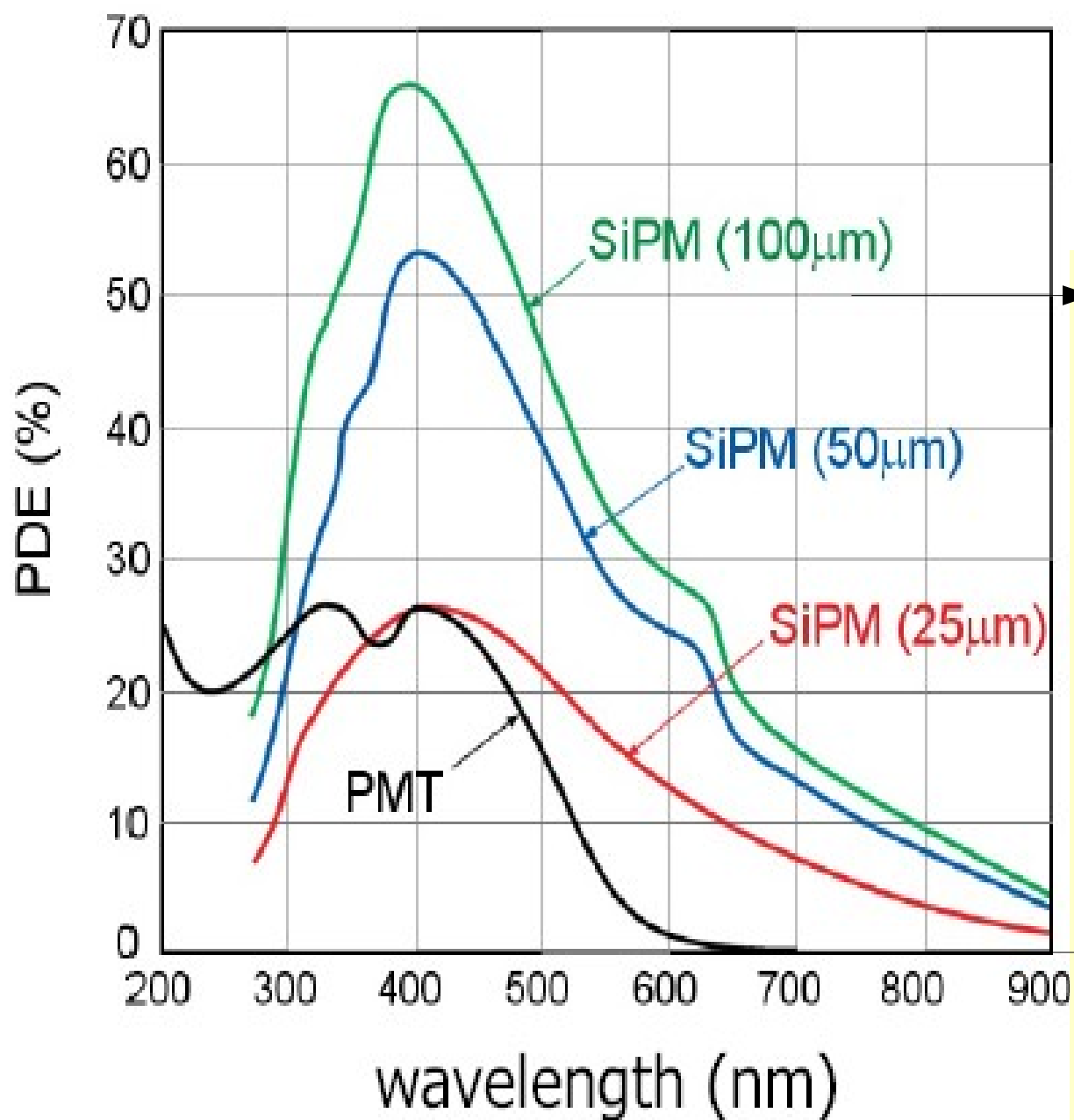


Crosstalk - SiPM HPK

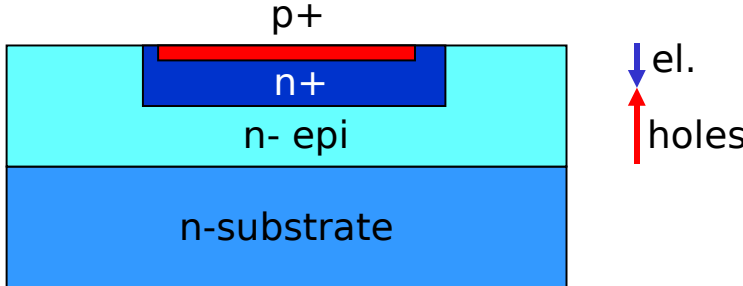
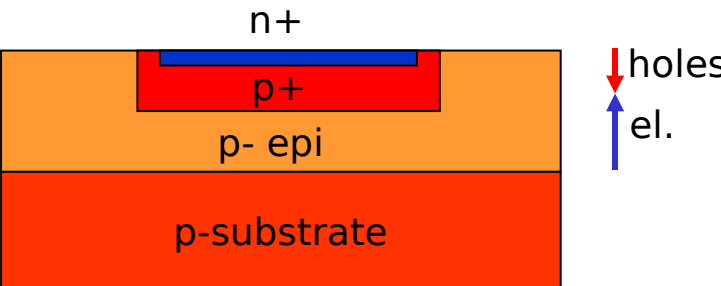


S.Cova, A.Lacaita,
G.Ripamonti, IEEE EDL (1991)

Hamamatsu: PDE of SiPM vs QE of PMT



Comparison HPK-IRST

Product.	Hamamatsu	IRST
Type		
Gain	$10^5 - 10^6$	$10^5 - 10^6$
PDE	30-70% (UV)-blue-green	30-70% (blue)-green-IR
Noise	200kHz - 1MHz	~ HPK x 2
After-pulse	~ 10%	~ 1%
Cross-talk	~ 10%	~ 1%
Timing	~ 100 ps	~ 60 ps

NOTE: in the standard working V_{bias} range

Fast detectors, fast signals

Detector Signals:

Moving charges (in an electric field):

$$i(t) = n(t) q v(t)$$

Rise-time $i'(t) = q [n(t) v'(t) + n'(t) v(t)]$

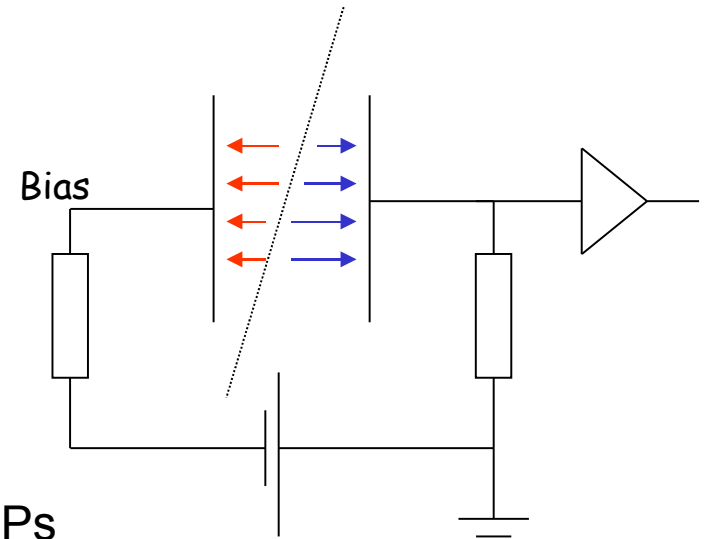
Maximize

n electron multiplication PMTs, MCPs

dv/dt qE/m electric field (in vacuum)

dn/dt primary ionisation, multiplication

v $t \cdot qE / m$ electric field



- Vacuum devices
- Electron multiplication
- Low capacitance
- High electric fields

Fast detectors

Sub-nanosecond: 10-100 ps rise-time

Fast

	Signals	Rise-time	Time resolution
Solid state			
• APDs	10^2	300 ps	50 ps
• Silicon PMs	10^7	100 ps	50 ps
• 3D Silicon	10^4	500ps	?

Very fast

• Multi-anode/mesh PMTs	10^7	200ps	50 ps
• MCP PMTs	10^6	150 ps	20-30 ps
• Multi anodes MCP PMTs		30 ps ?	1 ps ?

Pulse sampling

Digitize samples over pedestal and signal

Fast analog sampler + ADC: [E. Delagnes, Saclay, this workshop]

Assuming the signal waveform is known from the detector and electronics properties:

Least square fit yields:

- 
- Amplitude
 - Time

Iterate with new values until convergence

LSQF: [W.E. Cleland and E.G. Stern. NIM A 338 pp 467-497]

- **All samples contribute to timing estimation**
- **Very robust to noise**